PROTECTED QUANTUM BITS AND JOSEPHSON JUNCTION ARRAYS

BY RUSLAN USMANOV

A dissertation submitted to the

Graduate School—New Brunswick

Rutgers, The State University of New Jersey

in partial fulfillment of the requirements

for the degree of

Doctor of Philosophy

Graduate Program in Physics and Astronomy

Written under the direction of

Professor Lev Ioffe

and approved by

_____

_____

_____

_____

_____

_____

New Brunswick, New Jersey

October, 2010

ABSTRACT OF THE DISSERTATION

Protected quantum bits and Josephson junction arrays

by Ruslan Usmanov

Dissertation Director: Professor Lev Ioffe

In this thesis we consider a Josephson junction device whose symmetry is described by the point group T_d. It can be visualized as a tetrahedron that contains two Josephson junctions on each edge. We find the conditions under which the ground state of the system is degenerate or almost degenerate. In this case, the low-energy degrees of freedom can be mapped to the Hilbert space of a quantum spin 1/2. We evaluate effects of different physical perturbations on the degenerate ground state and find that they are small for most perturbations. We argue that this system can be considered as a very promising candidate for a protected quantum bit with built-in error correction.

We propose and discuss an experimental method that allows to test validity of some of the theoretical results obtained for the tetrahedral Josephson junction array and other similar symmetric circuits. We have chosen a simpler pyramidal array to demonstrate the main ideas of our method. Even though the noise resistance and theoretical decoherence time of the pyramidal array are worse than those of the more complex tetrahedral systems, it is much easier to realize the pyramid experimentally. The proposed design can be used with any symmetric Josephson junction circuit.

We explore a natural generalization of the tetrahedral quantum bit and consider devices whose symmetry can be described by one of the higher-order permutation groups S_n. We

study the level structure and the associated built-in protection of some conceptually simple circuits and show that these circuits have many interesting properties. In particular, their ground state can be highly degenerate and stable with respect to perturbations violating the symmetry. Unfortunately, these highly symmetric systems consist of a large number of identical Josephson junctions. This makes them too complicated for experimental realization.

Acknowledgements

I would like to thank my advisor, Lev Ioffe, for sharing his ideas and his time with me. I am very grateful to him for his patience and help. It has been a great pleasure for me to work with Lev, from whom I have learned much. I also want to thank Lev for suggesting the projects: all this thesis is based on our joint work.

It is a pleasure to thank Mikhail Feigelman for collaboration on a project on protected quantum bits with tetrahedral symmetry. In fact, a huge part of the second chapter originated in our joint work.

I would like to thank Alexander Dyugaev and Mikhail Lashkevich for very helpful discussions. Their advises and comments were extremely useful.

I would like to thank members of my research committee: Frank Zimmermann, Michael Gershenson, Emil Yuzbashyan, and a graduate program director, Ronald Ransome, for their time, advice and comments on my reports and this thesis.

I want to thank Sergey Frolov, who agreed to become an outside member of the defence committee. His valuable advices were also very helpful on the early stages of my graduate studies.

And, of course, it is the time to thank Ronald Ransome, Jolie Cizewski, Theodore Williams, Frances DeLucia, and Kathy DiMeo for their help and efficiency in every administrative task.

Ruslan Usmanov

Rutgers University

May 2010

Dedication

To my family.

Table of Contents

Chapter 1

Introduction

This thesis consists of four chapters. The first chapter can be considered as an introduction into the subject. In the first section of the introduction we give a brief description of the idea of a quantum computer. The section tells why quantum computers can be so powerful and describes two main classes of physical systems that can be used to perform quantum calculations.

In the second section of the introduction we describe the main obstacle to creating working devices that arose when people had tried to realize the idea of a quantum computer in practice. The problem is relevant for all quantum bits made of superconducting materials and caused by decoherence processes in qubits due to interaction with their environment.

The third section of the introduction tells briefly about the most recent experiments that tried to resolve the problem of decoherence described in the previous section. These experiments are extremely important since they demonstrate that macroscopic quantum bits are not just interesting theoretical toys but something that can be made and studied in practice. The byproducts of these studies were some experimental techniques that can be very useful not only for scientists working on quantum computers but also for all people studying macroscopic quantum systems.

The second chapter is devoted to a specific representative of one very interesting and important class of superconducting devices: all systems that belong to this class can be characterized by one or another *nonabelian* symmetry. In particular, we consider a Josephson junction device whose symmetry is described by the point group T_d. It can be visualized as a tetrahedron that contains two Josephson junctions on each edge. We find the conditions under which the ground state of the system is degenerate or almost degenerate. In this

case, the low-energy degrees of freedom can be mapped to the Hilbert space of a quantum spin 1/2. We evaluate effects of different physical perturbations on the degenerate ground state and find that they are small for most perturbations. We argue that this system can be considered as a very promising candidate for a protected quantum bit with built-in error correction.

The third chapter proposes an experimental method that allows to test validity of some theoretical results obtained in the second chapter. We generalize the ideas developed in [1, 2, 3, 4, 5]. We have chosen a simpler pyramidal array to demonstrate the main ideas of our method. Even though the noise resistance and theoretical decoherence time of the pyramidal array are worse than those of the more complex tetrahedral systems, it is much easier to realize the pyramid experimentally.

Any symmetric Josephson junction array can be considered as a set of a few superconducting islands connected with each other and with the environment through Josephson junctions. Since the size of these islands is very small, the Coulomb blockade effects become very important. If we use gate voltages to control the potentials of the islands, we can consider the array as a generalized version of the Single-Electron Transistor (SET). We can draw the current-voltage curve of the system and extract the information about the spectrum and decoherence rates. The proposed design can be used with any symmetric Josephson junction circuit.

In the fourth chapter we explore a natural generalization of the tetrahedral quantum bit and consider devices whose symmetry can be described by one of the higher-order permutation groups S_n. We study the level structure and the associated built-in protection of some conceptually simple circuits and show that these circuits have many interesting properties. In particular, their ground state can be highly degenerate and stable with respect to perturbations violating the symmetry. Unfortunately, these highly symmetric systems consist of a large number of identical Josephson junctions. This makes them too complicated for experimental realization.

The fifth chapter evaluates the results of the previous three chapters and concludes the

thesis by identifying the future work that should be done.

The appendices provide a brief discussion of the three terms widely used in physics of quantum computers: the RSA algorithm, Shor's algorithm, and the quantum error correction scheme[1].

1.1 Background

The idea of a quantum computer dates back to 1982 when Richard Feynman tried to model quantum processes numerically. He has quickly realized that even the most powerful traditional computers do not allow researchers to simulate dynamics of complicated quantum systems. Feynman has proposed a very interesting solution: a new type of computers where such fundamental phenomena of quantum mechanics as quantum superposition and probabilistic character of quantum processes would play an important role. Computers of this new type are now known as "quantum computers".

To better understand Feynman's ideas, note that classical mechanics is a very special case of quantum mechanics and, therefore, the set of all classical trajectories is a subset of all quantum trajectories. We can expect that a computer using general quantum processes to perform calculations should be at least as much powerful as a computer that is only allowed to use classical processes. Furthermore, it is likely that the quantum computer will be in general *more* powerful.

In a traditional computer, information is encoded in a series of bits and these bits are manipulated via Boolean logic gates arranged in succession to produce a final result. Similarly, a quantum computer manipulates qubits by executing a series of quantum gates. Each gate produces a unitary transformation acting on a single qubit or a pair of qubits. Applying the gates in succession, a quantum computer can perform a complicated unitary transformation to a set of qubits in some initial state. The qubits's quantum state can then be found, with the final computational result being determined by the state's wave

[1]Even though the RSA and Shor's algorithms are not used in this thesis, their brief description is given because it is very common among physicists working on the theory of quantum computations and information to refer to the algorithms as scientific evidence that substantiates the need for quantum computers.

function. This similarity in calculation between classical and quantum computers leads to the fact that in theory, a classical computer can accurately simulate a quantum computer. However, if a quantum computer has N quantum bits, the corresponding classical computer will have to store a wave function of these N qubits, which implies dealing with 2^N complex variables. If $N \gg 100$, this number becomes too big even for supercomputers.

Thus, although a classical computer can theoretically simulate a quantum computer, it is incredibly inefficient. There are many computational problems that can hardly be solved using a classical computer because the total time required to finish computations is comparable to the age of the Universe while a quantum computer solves these problems with ease. The simulation of a quantum computer on a classical one is a computationally hard problem because the correlations among quantum bits are qualitatively different from correlations among classical bits. Take, for example, a system that contains only one thousand qubits. Its Hilbert space is of dimension $\sim 10^{330}$. Hence, a classical computer that is able to simulate it has to deal with exponentially large vectors, so that, we have to wait exponentially longer than we would in the case when we have even a primitive quantum computer.

Let us imagine that we have a system that contains 1000 qubits. Each quantum state of such a system can be represented as a quantum superposition of as many as 2^{1000} states:

$$|\psi\rangle = a_1|000...00\rangle + a_2|000...01\rangle + ... + a_{2^{1000}}|111...11\rangle.$$

When we perform a calculation, we rotate this quantum state in the 2^{1000}-dimensional Hilbert space. Doing this, we change all coefficients in the quantum superposition. Therefore, with one tick of the computer clock, a quantum operation could compute not just on one machine state, as serial computers do, but on 2^{1000} machine states at once. Even if one tick of a quantum computer takes very long time, its computing power will be exponentially better than that of a classical computer.

Scientists were naturally excited by the potential of such enormous computing power, and a few algorithms that allow to use it have been invented in the early 90s. These include the following well-known quantum algorithms: Deutsch–Jozsa algorithm [6, 7], Grover's

algorithm for searching an unsorted database [8, 9] and, of course, Shor's algorithm [10] (see Appendix B).

Shor's algorithm allows very fast factorization of a large number (its complexity is proportional to n^2, where n is the number of digits contained in a decimal record of the large number, while the complexity of the classical algorithm is proportional to $\exp(n)$). This algorithm is very useful for different encryption problems. One of the best encryption code RSA relies heavily on the difficulty of factoring very large composite numbers into their primes (see Appendix A). It is rather natural that all organizations and individuals that use RSA are interested in getting a quantum computer.

Encryption is not the only application of a quantum computer. Feynman asserted [11, 12] that a quantum computer could function as a simulator for quantum physics and especially for condensed matter physics, where the number of degrees of freedom is usually very large.

Taking all the above into account, it is rather natural that nowadays, one of the most important topics in condensed matter physics is implementation of quantum computations. In general, creation of a quantum computer seems to be an extremely difficult problem because two almost contradictory conditions must be satisfied [13]. First, the system in consideration should be tolerant to all environmental perturbations. This means that all interactions of the system with its environment should be very weak. Second, we want to be able to control its quantum state (when we do some quantum calculations) and also we want a final state to be readable (since we desire to know the result of our calculation) without loss of information. But any measurement process involves interaction of the system whose state we want to know with a macroscopic device which is a part of the environment [14]. Some compromise between these two requirements can still be found. The compromise means that one should be able to turn off the interaction with the environment while running quantum algorithms and turn it on while reading quantum information. In this case, the most important characteristic of the system is the so-called decoherence time which can be defined as typical decay time of a quantum state of the system[2].

[2] The decoherence time is infinite if the interaction of a qubit with its environment is completely suppressed. This means that all matrix elements of non-unitary noise operators projected to the Hilbert subspace

A variety of different approaches to the solution of the problem of a quantum computer have been developed. Strictly speaking, we can say that all the systems realized so far belong to two big classes. The first class consists of all systems in which each elementary cell called a quantum bit has microscopic size. These are examples of such systems: ions and atoms in magnetic traps [15, 16], nuclear spins [17, 18, 19], and photons in cavities [20, 21]. At the same time, all quantum computers that include macroscopic quantum bits belong to the second class. The most important representatives of this class are Josephson junction arrays [22, 23, 24, 25, 26, 27, 28, 29, 30, 31], transmons [32, 33, 34, 35] and quantum dot devices [36, 37].

Each of these two approaches has its own advantages and drawbacks. For example, decoherence processes in microscopic systems can be very slow[3], so that the decoherence time (introduced in the next section) is long enough to run quantum algorithms (all the microscopic systems listed in the previous paragraph are characterized by "long" decoherence time). However, it seems to be almost impossible to build a quantum computer that contains more than a few dozens of such microscopic bits. The main problems that arise here are due to impossibility to control many quantum bits simultaneously[4] and even produce a stable system that has so many qubits.

Probably, the most successful device using the microscopic approach was demonstrated in 2001 by a research group from IBM's Almaden Research Center [19, 38]. In this experiment a seven-qubit quantum computer has found the prime factors 3 and 5 of the number 15. The computer itself was represented by a molecule that had seven nuclear spins. These nuclear spins have been programmed by radio frequency pulses and detected by nuclear magnetic resonance devices. Unfortunately, as the scientists said, it would be

---

spanned by the vectors $|0\rangle$ and $|1\rangle$ are zero, that is, the subspace is invariant to the noise operators. Such a subspace is called a *decoherence free subspace (DFT)*. In some sense, qubits whose eigenstates $|0\rangle$ and $|1\rangle$ form a basis of DFT support a built-in quantum error correction scheme.

[3]By definition, decoherence processes lead to decay of a quantum state. This means that any quantum information that is stored in a quantum bit is being lost as time passes.

[4]One can easily control 10 individual ions but no modern technique allows to control 1000 (not saying about millions) individual ions. It is also very unlikely that such a technique will be developed in the foreseeable future.

extremely difficult (or even impossible) to synthesize similar molecules with thousands of nuclear spins.

In contrast to the microscopic case, systems of the second class do not suffer from this disadvantage, that is, quantum computers built using macroscopic elementary cells can contain any number of such cells. This allows us to consider them as very perspective candidates for being the material base of the future quantum computer. However, the macroscopic size also presents a challenge: is it possible to isolate qubits from outside parasitic noise while retaining efficient communication channels for the write, control and read operations? The outside parasitic noise leads to very short decoherence time and, therefore, to very severe restrictions on the typical time required to run quantum algorithms.

The main task for scientists who try to build a quantum computer using solid state systems is increasing the decoherence time without losing advantages of working with macroscopic quantum bits.

The first implementation of a quantum bit in a solid state device was achieved 11 years ago in a Cooper pair box, a circuit where a single superconducting island is coupled to a reservoir by a low capacitance tunnel junction [3]. In this circuit, the competition between the Coulomb blockade and the Josephson effect allows the coherent superposition and manipulation of charge states [39]. However, the processes leading to decoherence are more difficult to control than in microscopic systems. For this reason, it is important to understand both origin and effects of the interaction of qubits with other macroscopic degrees of freedom of the circuit. This interaction determines the decoherence time which is the main topic of the next section.

1.2 Decoherence time in superconducting qubits

In this section we will discuss decoherence in a simple Josephson junction circuit that can be considered as a quantum bit. We also introduce two very important phenomenological quantities: pure dephasing time and relaxation time. This will allow us to study more interesting "protected" devices whose internal symmetry suppresses some effects of decoherence

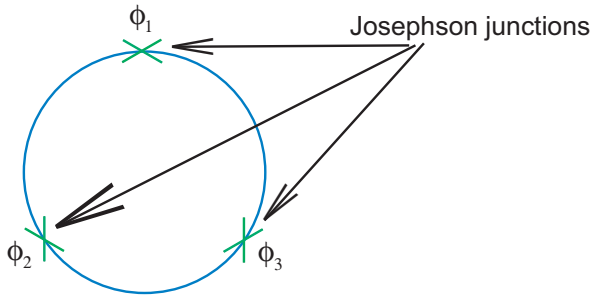

Figure 1.1: An example of a superconducting qubit.

processes.

Let us consider the system shown in Fig. 1.1. This system consists of three identical Josephson contacts and three superconducting wires. The contacts are characterized by the Josephson energy $E_J = (\hbar/2e)I_c$ and the charge energy $E_c = e^2/2C$. We will consider the case of E_J being much larger than E_c, $E_J \gg E_c$, that is, we will use the quasiclassical approximation. If the magnetic flow through the ring is equal to $\Phi_0/2$, then the following equation must be valid:

$$\phi_1 + \phi_2 + \phi_3 = \pi.$$

In this case, the potential energy of the system,

$$E_J = -E_J \cos(\phi_1) - E_J \cos(\phi_2) - E_J \cos(\phi_3), \tag{1.2.1}$$

has two classical minima:

$$E_L = E_R = -\frac{3}{2}E_J.$$

Here we denote the phase differences across the three contacts by ϕ_1, ϕ_2, and ϕ_3. The corresponding quasiclassical wave functions can be written in the form:

$$\begin{aligned} |L\rangle &= \left|\phi_1 = \frac{\pi}{3}, \phi_2 = \frac{\pi}{3}, \phi_3 = \frac{\pi}{3}\right\rangle, \\ |R\rangle &= \left|\phi_1 = -\frac{\pi}{3}, \phi_2 = -\frac{\pi}{3}, \phi_3 = \frac{5\pi}{3}\right\rangle. \end{aligned} \tag{1.2.2}$$

We can see that the minima are characterized by identical in magnitude but opposite directed currents through the junctions (see Fig. 1.2):

$$|I_L| = |I_R| = \frac{\sqrt{3}eE_J}{\hbar}.$$

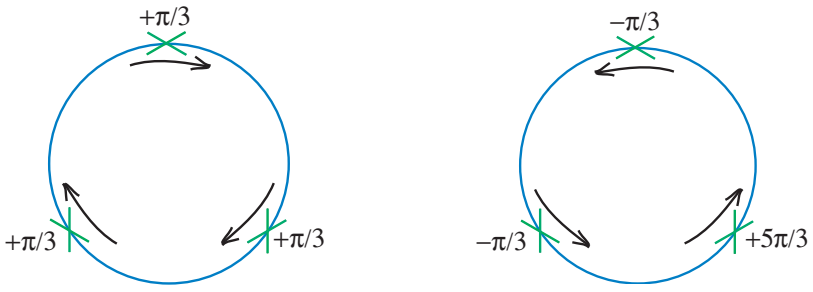

(a) $|L\rangle$ (b) $|R\rangle$

Figure 1.2: Two classical states corresponding to the minimum of the potential energy (1.2.1).

The effective Hamiltonian of the qubit has the following simple form:

$$\hat{H}_{eff} = \begin{bmatrix} E_{local} & t \\ t & E_{local} \end{bmatrix},$$

where E_{local} is the energy of a localized quantum state and t is the non-diagonal matrix element that describes tunneling between the quantum states $|L\rangle$ and $|R\rangle$.

If dissipation in the Josephson junctions is sufficiently weak[5], then tunneling from one minimum to the other becomes possible (with the tunneling amplitude between the two quasiclassical minima being equal to t) and the eigenstates of the system can be written in the form of the symmetric and the antisymmetric superpositions of the wave functions (1.2.2):

$$\begin{aligned} |0\rangle &= \frac{1}{\sqrt{2}}\left(|L\rangle + |R\rangle\right), \qquad E_0 = E_{local} - |t|, \\ |1\rangle &= \frac{1}{\sqrt{2}}\left(|L\rangle - |R\rangle\right), \qquad E_1 = E_{local} + |t|. \end{aligned} \tag{1.2.4}$$

[5] If we denote the widths of the two levels (1.2.4) by Γ_0, Γ_1, we will find that the described system can be considered as a quantum bit only if the following conditions are satisfied:

$$\begin{aligned} &\Gamma_0, \Gamma_1 \ll \Delta E = 2|t|, \\ &\Gamma_0, \Gamma_1 \ll \Delta E_{12}, \end{aligned} \tag{1.2.3}$$

where E_2 is the next energy level of the system, and $\Delta E_{12} = E_2 - E_1$. Otherwise, it does not make sense to speak about the energy levels $|0\rangle$ and $|1\rangle$.

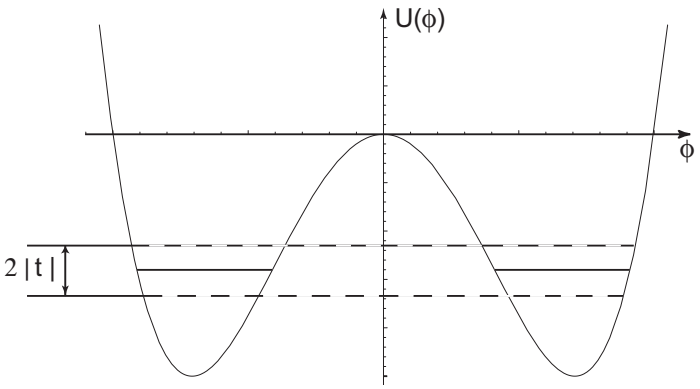

Figure 1.3: The potential energy of the qubit in the case when $\phi_1 = \phi_2 = \phi$, $\phi_3 = \pi - 2\phi$: $U(\phi) = -E_J(2\cos(\phi) - \cos(2\phi))$. Two classical minima correspond to two localized quantum states. If dissipation in the system is weak, the eigenstates of the qubit are symmetric and antisymmetric linear combinations of the localized quantum states.

The energies of the two eigeinstates are separated by the energy gap $\Delta E = \hbar\omega = 2|t|$ (see Fig. 1.3).

In those cases when the lifetime of any linear combination

$$|\psi\rangle = a|0\rangle + b|1\rangle, \qquad |a|^2 + |b|^2 = 1, \tag{1.2.5}$$

of these quantum eigenstates (that is, its decoherence time) is long enough, the system can be considered as a candidate for a quantum bit, with the two states $|0\rangle$, $|1\rangle$ being a basis in the two-dimensional Hilbert space of the qubit. The coefficients a and b of the linear combination carry quantum information.

Unfortunately, there are physical processes that lead to "dissipation" of the quantum information, that is, to finite lifetime of the quantum state $|\psi\rangle$. In reality, any measurement is performed by a device that is a physical system: the circuit used for readout and control is composed of some macroscopic impedances, inductances, and conductances. Each of these elements is a source of various noises, and, therefore, a source of decoherence. It is convenient to speak about five different sources of decoherence: 1) charge noise; 2) critical current noise; 3) flux noise; 4) quasiparticles; 5) phonon (photon) emission.

To understand the origin and effects of all these noises, we will need the Hamiltonian of

a general Josephson junction circuit:

$$\mathcal{H} = \mathcal{H}_{qubit} + \mathcal{H}_{control} + \mathcal{H}_{int}, \tag{1.2.6}$$

where $\mathcal{H}_{control}$ is the Hamiltonian of the readout and control circuit, $\mathcal{H}_{int}$ describes interaction of a qubit and a readout circuit, and $\mathcal{H}_{qubit}$ is the Hamiltonian of the quantum bit:

$$\mathcal{H}_{qubit} = \sum_i \frac{q_i^2}{2C_i} - \sum_j E_J \cos(\phi_j - a_j). \tag{1.2.7}$$

Here q_i are the charges of superconducting islands, ϕ_j are the phases across the corresponding Josephson junctions, and a_j are chosen to agree with the magnetic fluxes through all contours of the circuit.

The *charge noise* is explained by fluctuations of the charges q_i of superconducting islands. Physically these charges are induced by potentials produced by the electrostatic environment (for example, by dipoles in the insulating environment). The low frequency part of this noise ($f < 1$ kHz) is characterized by the spectral density

$$S_q(f) = \frac{\alpha_q}{f}, \tag{1.2.8}$$

where α_q has been found in a number of experiments to be of order $(10^{-3}e)^2$ [40, 41, 42, 43, 44].

The *critical current noise* is caused by fluctuations of the Josephson energy E_J. There are a few sources of this noise. First, it might occur due to changes in the ion configurations which lead to opening and closing of the conducting channels of Josephson junctions [45]. Second, it might occur due to electrons trapped in shallow subgap states that can appear at the superconductor-insulator boundary [46, 47]. Phenomenologically, the critical current noise is characterized by $1/f$ spectrum, when f belongs to the range $f = 1$ mHz to 60 Hz:

$$S_{I_0}(f) \approx \frac{\alpha_{I_0}}{f}. \tag{1.2.9}$$

If the area of a junction is 1 μm^2, its temperature is 100 mK, and the critical current is 1 μA, then α_{I_0} can be estimated by $\alpha_{I_0} = 8.2 \cdot 10^{-26} A^2 \cdot Hz^{-1}$ [45, 48].

Flux noise. The source of this noise is fluctuating magnetic fields applied to a quantum bit. Typically, it becomes important, when $E_J \gtrsim E_C$. The qubit's energy levels change, which leads to dephasing. The flux noise is characterized by $1/f$ spectrum, when f belongs to the range $f = 1$ mHz to 10 Hz:

$$S_\Phi(f) = \frac{\alpha_\Phi}{f}, \tag{1.2.10}$$

where $\alpha_\Phi \sim 10^{-12}\ Hz^{-1}$ [49].

Quasiparticles. Even though all real experiments are performed at very low temperatures ($T \ll \Delta$), a small number of quasiparticles might exist. These wandering out-of-equilibrium quasiparticles randomly change the charges of superconducting islands. This effectively resembles the charge noise with very low frequency but very large magnitude.

Finally, *emission of photons and phonons* results in decay of the excited state of a qubit [50, 51, 52]. These processes are similar to the conventional dipolar emission of light by atoms (see Fig. 1.4) and are characterized by the decay rate Γ that strongly depends on the energy gap $\Delta E = \hbar\omega$ between the logical states $|0\rangle$ and $|1\rangle$ [51]:

$$\Gamma \sim \Delta E^4. \tag{1.2.11}$$

As one can see, large energy gaps lead to very short decoherence time[6].

The photon emission can be efficiently suppressed by placing a qubit in a resonator [32, 33, 34, 35], but due to the technological constraints, it is very difficult to avoid coupling of the qubit with substrates and, therefore, to eliminate the phonon emission. This source of decoherence becomes, however, insignificant when the energy gap ΔE separating the logical states of the qubit is small.

It should be clear from this short summary that the most dangerous of all the low frequency noises is the charge noise because of its large magnitude. This noise leads to fast

[6]The main reason why Γ grows so fast as ΔE increases is the following. The particles and quasiparticles that can carry away the energy difference ΔE have a larger density of states at higher energies. The probability of decay $|1\rangle \longrightarrow |0\rangle + \gamma$ is determined by

$$\Gamma \sim \frac{1}{1/\omega} \int \delta\left(\hbar\omega - \Delta E\right) \delta\left(ck - \hbar\omega\right) \frac{d\vec{\mathbf{k}} dw}{(2\pi)^4} \sim \omega^4 \sim \Delta E^4.$$

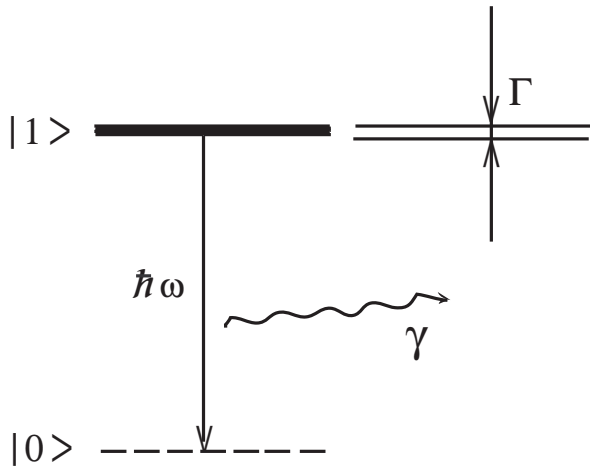

Figure 1.4: The quantum state $|1\rangle$ decays. The energy difference is carried away by a photon or a phonon.

decoherence if it is directly coupled to the energy gap between the logical states. This is a typical situation when $E_C \gg E_J$ because in this regime different states are characterized by different charges and electrostatic potentials. The charge noise dominates in this case and leads to fast dephasing because the difference ΔE_{01} fluctuates (see below).

However, its effects remain large even in the opposite limit of $E_J \gg E_c$, if the phase slips are not excluded. In this case, the energy difference $\Delta E_{01} = E_1 - E_0$ does not fluctuate. What is worse is that the states $|0\rangle$ and $|1\rangle$ change [53]. To explain this, let's return back to the quantum bit described at the beginning of this section. Imagine that the charge of one of the islands of the qubit has increased by δq. In this case the quasiclassical wave functions (1.2.2) rotate:

$$|L\rangle \longrightarrow e^{-i(\pi/3)\delta q}|L\rangle, \qquad |R\rangle \longrightarrow e^{i(\pi/3)\delta q}|R\rangle.$$

As a result, the effective Hamiltonian of the qubit changes:

$$\hat{H}_{eff} = \begin{bmatrix} E_{local} & te^{-i(2\pi/3)\delta q} \\ te^{i(2\pi/3)\delta q} & E_{local} \end{bmatrix},$$

so that the eigenstates (1.2.4) also change:

$$|0\rangle \longrightarrow |0'\rangle = \frac{1}{\sqrt{2}}\left(|L\rangle + e^{i(2\pi/3)\delta q}|R\rangle\right), \qquad E_{0'} = E_{local} - |t|,$$
$$|1\rangle \longrightarrow |1'\rangle = \frac{1}{\sqrt{2}}\left(e^{-i(2\pi/3)\delta q}|L\rangle - |R\rangle\right), \qquad E_{1'} = E_{local} + |t|. \tag{1.2.12}$$

The matrix elements $\langle 1|0'\rangle$ and $\langle 0|1'\rangle$ are not equal to zero. Therefore, the quantum state (1.2.5) can decay. The probability of this event becomes especially large if δq is not a small fluctuation[7]. In section 1.4 we will discuss how one can resolve this problem.

In almost all cases the combined effect of all the noise sources on the qubit states can be described phenomenologically by two parameters that have the dimension of time: the relaxation time τ_r and the pure dephasing time τ_ϕ. In physical literature one can also meet the notations T_1 and T_2 for the quantities[8]

$$T_1 = \tau_r, \qquad T_2^{-1} = \frac{1}{2}\,T_1^{-1} + \tau_\phi^{-1}.$$

Sometimes they are more convenient, because T_1 and T_2 are the quantities that are usually measured in real experiments. However, only τ_r and τ_ϕ make physical sense.

In general, one can distinguish two types of processes that destroy coherence. First, in real systems there are always higher energy levels E_i, $i = 2, 3, ...$ If interaction with the environment is strong, the probabilities of transitions between the quantum state (1.2.5) and the higher energy levels and also between the eigenstates $|0\rangle$ and $|1\rangle$ become large and quantum information is being lost because the magnitudes $|a|$ and $|b|$ change[9]. As a result, if the interaction is very strong, the system cannot be used for quantum calculations. Decay of the coefficients a and b is described by the relaxation time τ_r. This is the typical time that is required for the magnitudes $|a|$ and $|b|$ to decrease to one half of their original value.

---

[7] One can argue that the charges of all the three superconducting islands will increase by the same amount if $E_J \gg E_c$: the additional charge δq will be distributed uniformly over the quantum bit. As a result, the wave functions $|L\rangle$ and $|R\rangle$ should not rotate. However, this will be the case only if all the three islands are absolutely identical. In real life, they are not since there are always some defects caused by non-ideal technological processes. In addition, parasitic charges can be trapped on the islands. As a result, the island potentials are different so that the charge fluctuations are not uniformly distributed and the wave functions do rotate.

[8] The quantity T_2 is called transverse relaxation time.

[9] The stronger the interaction with the environment, the larger the probabilities of transitions and the faster decay of quantum information.

Second, the interaction with the environment can change not only the magnitudes of the coefficients a and b but also their relative phase ϕ. In the ideal case, when there is no decoherence in the system, the time evolution of the state

$$|\psi(0)\rangle = a|0\rangle + b|1\rangle$$

is given by

$$|\psi(t)\rangle = a(t)|0\rangle + b(t)|1\rangle,$$

where

$$a(t) = ae^{-iE_0 t/\hbar}, \qquad b(t) = be^{-iE_1 t/\hbar}.$$

We see that the relative phase of the coefficients evolves as

$$\phi_{ideal}(t) = \log\left(\frac{a(t)}{b(t)}\right) = \phi(0) + \frac{i(E_1 - E_0)t}{\hbar}.$$

In the ideal situation, we know the eigenenergies E_0 and E_1, so that we can take into account this evolution in all our calculations.

However, due to interactions with the environment, the real eigenenergies E_0 and E_1 are not constant quantities. They change unpredictably as time passes so that the time evolution of the relative phase $\phi(t)$ is an extremely complicated stochastic process:

$$\phi_{real}(t) = \phi(0) + \int_0^t \frac{i(E_1(\tau) - E_0(\tau))}{\hbar} d\tau.$$

If the phase error $\Delta\phi = \phi_{real}(t) - \phi_{ideal}(t)$ becomes very large, one can say that all initial quantum information is completely lost.

The typical time that is required for the phase error $\Delta\phi$ to become as large as 1 radian is called the pure dephasing time τ_ϕ. One can calculate it if the spectral densities of all noises are known [40, 41, 45, 48, 49, 54]. To show this, we will assume that fluctuations of the energy difference

$$\delta E(t) = (E_1(t) - E_0(t)) - (E_1 - E_0)$$

are distributed normally. In this case the expected parasitic shift of the relative phase $\phi(t)$

is given by[10] [40, 41]

$$\left\langle e^{i\Delta\phi(\tau)}\right\rangle = \exp\left[-\frac{1}{2}\left\langle\left(\frac{1}{\hbar}\int_0^\tau \delta E(t)dt\right)^2\right\rangle\right] = \exp(-g(\tau)),$$

where

$$g(\tau) = \frac{1}{2\hbar^2}\int_{\omega_m}^{\infty} dw\, S_{\delta E}(w)\left(\frac{\sin(\omega\tau/2)}{\omega/2}\right)^2.$$

Here $\omega_m = 2\pi/t_m$ is the low-frequency cut-off due to the finite duration t_m of all measurements and operations and $S_{\delta E}(\omega)$ is the spectral density of $\delta E(\tau)$. The pure dephasing time can be found from the equation

$$g(\tau_\phi) = 1. \tag{1.2.13}$$

The spectral quantity $S_{\delta E}(\omega)$ can be expressed in terms of the noise spectral density. For example, assuming that the charge noise is a Gaussian noise produced by many fluctuators weakly coupled to a Josephson junction circuit and there are no other noise sources, one can write the equation [40, 41]:

$$S_{\delta E}(\omega) = \left(\frac{4E_c}{e}\right)^2 S_q\left(\frac{\omega}{2\pi}\right),$$

where $S_q(f)$ is given by (1.2.8).

A more detailed analysis of the evolution of the qubit's density matrix reveals that both τ_ϕ and τ_r can be found if the spectral properties of all interactions are known [54, 55]. In addition, such an analysis allows a systematic treatment of different parameter regimes. In particular, the case of relatively high temperatures can be studied.

It is very important to understand that relaxation and dephasing processes lead to very different consequences. Quantum errors caused by relaxation cannot be fixed by error correction algorithms. At the same time, errors caused by dephasing can be fixed if τ_ϕ is not

---

[10] We use the following property of the Brownian motion:

$$\langle e^{iu_t}\rangle = \exp\left(-\frac{\langle u_t^2\rangle}{2}\right).$$

The spectral density $S_x(\omega)$ is defined as:

$$\langle x_\omega x_{\omega'}\rangle = S_x(\omega)\delta(\omega+\omega').$$

Also, we ignore nonzero temperature effects. This can be done if $k_BT \ll \delta E(t)$, $t > 0$.

too short (see below). However, it is much easier to fight with relaxation on physical level than to fight with dephasing, especially with dephasing that occurs due to the charge noise. It is worth emphasizing again that the charge noise is sufficiently different from the rest of the low frequency noises because it leads not only to fluctuations of the energy levels, but also (for some systems) to rotations of the quantum eigenstates $|0\rangle$ and $|1\rangle$. This rotation of the quantum states is a unitary transformation, while the regular noise effects are described by non-unitary operators. The pure dephasing time which characterizes the unitary rotation cannot be calculated from the spectral density of the charge noise, so that one has to use a special probabilistic analysis (see also the discussion earlier in this section)[11].

To complete our brief discussion of noises that affect a Josephson junction quantum bit, we should mention effects of classical impedances in readout circuits. These effects are explained by thermal (Johnson-Nyquist) noise which is the electronic noise that exists regardless of any applied voltage [56]. It can be explained by the thermal agitation of electrons in electric conductors and has approximately white spectrum [57]. The voltage variance (per hertz of bandwidth) is given by

$$\langle V^2(\omega)\rangle = 4k_B T\,\mathrm{Re}[Z(\omega)],$$

where $Z(\omega)$ is the impedance of the outer circuit. The thermal noise leads to very fast dephasing[12] but can be almost completely suppressed by inserting a very small Josephson junction (as shown in Fig.(1.5)). If this additional junction is very small, its capacitance is also very small relative to the capacitance of the quantum bit. As a result, voltage fluctuations do not destroy quantum coherence. In this case, Johnson-Nyquist noise affects only readout current-voltage curves (as explained in detail in Chapter 3).

The lifetime of quantum information is determined by the smallest of the two quantities, τ_r and τ_ϕ. But is it possible to make this lifetime long enough to implement at least the simplest quantum algorithm? In other words, we want to know if there is a limitation on

[11]However, the pure dephasing time which characterizes non-unitary transformations is still given by (1.2.13).

[12]Dephasing is explained by fluctuations of the total charge of a quantum bit (like in the case of the charge noise).

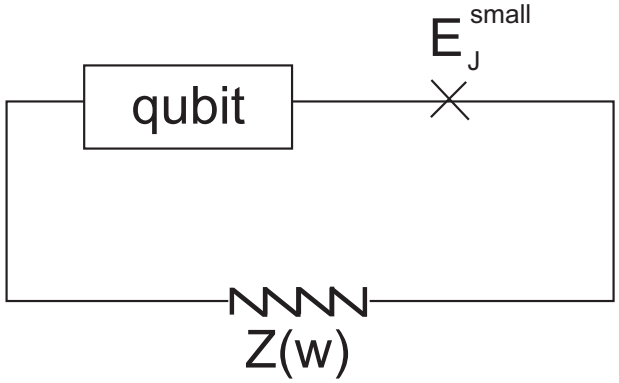

Figure 1.5: A small Josephson junction should be inserted between the qubit and the readout circuit whose impedance $Z(\omega)$ is a source of Johnson-Nyquist noise. The capacitance of the additional Josephson junction is very small relative to the capacitance of the qubit so that voltage fluctuations do not affect the quantum bit and its state.

the decoherence rate and if it is possible to realize Shor's (or any other) error correction scheme (see Appendix (C)). For the error correction scheme to work, the decoherence time should be at least $10^2 - 10^4$ times longer than the greater of the duration of one elementary operation[13] and the typical measurement time[14] [14, 59, 60, 61]. Furthermore, there exist some estimates that show that the required decoherence time can be even longer: $10^6 - 10^8$ times longer than duration of one elementary operation [62].

Unfortunately, all these estimates are distributed too wide and cannot give a clear answer to experimentalists on what they should try to achieve. Also, in practice, our final goal is

[13]Duration of an elementary operation is the typical time required for a quantum logic gate to change a quantum state of a quantum bit. For example, if the quantum bit is represented by an atom, the quantum states $|0\rangle$ and $|1\rangle$ are represented, correspondingly, by the ground and the first excited levels of the atom and the quantum logic gate is represented by a laser beam that induces transitions between the quantum states $|0\rangle$ and $|1\rangle$ then duration of an elementary operation is the laser pulse duration.

In the case of Josephson junction devices, duration of an elementary operation is determined by

$$\tau = \frac{2\pi}{\omega_p} = \frac{\pi\hbar}{\sqrt{E_J E_c}},$$

where ω_p is the plasma frequency of a junction.

If the state $|1\rangle$ is separated from the next excited state by a significant gap ΔE_{12}, then ΔE_{12} sets the scale for duration of all operations because an attempt to change the state of the system faster than for the time $1/\Delta E_{12}$ would excite higher levels. It means that there exists minimal pulse duration that can be used. In practice, it should be at least 10 times longer than $\hbar/\Delta E_{12}$. One should be very cautious comparing the estimates for the decoherence time taken from different papers since this time can be expressed either in terms of logical elementary operations or in terms of ΔE_{12}.

[14]The measurement time is the time taken for the measuring device to reach a signal-to-noise ratio of 1 [58].

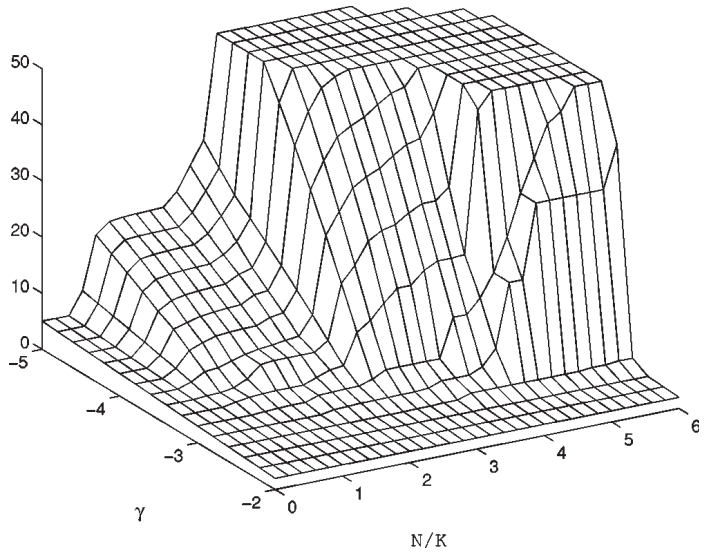

Figure 1.6: This figure has been borrowed from [63]. It shows the dependence of the maximum algorithm size KQ on the gate noise γ and the ratio N/K, at $\varepsilon = \gamma/100$ and $t_m = 25$, where t_m is the time involved in measuring a physical qubit. t_m is expressed in terms of the duration of one elementary operation. All the axes have logarithmic scales, labelled in powers of 10.

doing something more complicated than running the simplest quantum algorithms using a few qubits. Therefore, it is very important to answer a more precise question: given the number of logical qubits K and the number of elementary operations Q needed to complete a quantum algorithm, what is the minimal decoherence time required to run the whole computation and get the right result? This question has been investigated in [63]. The answer is shown in Fig. 1.6. To understand the graph, we will remind here that the error correction scheme requires the actual number of physical qubits N to be much greater than the number of logical qubits K: we have to run a few copies of our computation so that at each step we can fix all errors. Obviously, the more physical copies of a logical qubit we have, the more reliable the error correction scheme is. Therefore, the ratio N/K is an important parameter and shown on one of the horizontal axes of the graph. Another important parameter γ that describes the probability for a physical qubit to get an erroneous state[15] is shown on another horizontal axis. The graph itself shows the dependence of the

[15]There are a few different types of errors: 1) at each step, every freely evolving physical quantum bit has no change in its state with probability $1 - \varepsilon$ but undergoes some random rotation with probability ε; 2) a single-qubit gate can fail with probability γ_1; 3) a two-qubit gate can fail with probability γ_2; 4) each

maximal algorithm size KQ on the probability γ and the ratio N/K. One can see from the graph that large algorithms ($KQ \sim 10^{10}$) are possible for a modest ratio $N/K = 10$, once the probability γ is small enough ($\gamma \leq 10^{-4}$).

Using these results, it is easy to estimate the minimal required decoherence time :

$$\tau_\phi \sim \frac{\tau}{\gamma} = 10^4 \, \tau,$$

where τ is the duration of an elementary operation. Taking into account what we said in Footnote 13, this translates into

$$\tau_\phi \sim 10^5 \, \frac{\hbar}{\Delta E_{12}},$$

where ΔE_{12} is the energy gap between $|1\rangle$ and the first excited level outside the qubit's Hilbert space.

For Josephson junction devices some of the best results were achieved in 2002 [64, 65]. In these experiments the relaxation time was $\tau_r = 1.8\,\mu s$, while the pure dephasing time was as long as $\tau_\phi = 0.5 \ \mu s \approx 8000\tau$, where $\tau = 2\pi\hbar/\Delta E_{01} \sim \pi\hbar/\sqrt{E_J E_c}$. Later these results were significantly improved so that the physical quality factor has reached 25000 [58]. Recently, even better numbers have been received [66]: $T_1 = 11.5 \ ms$, $T_2 = 20 \ ms$.

As we mentioned earlier, the relaxation time strongly depends on the energy gap $\Delta E = \hbar\omega$ between the states $|0\rangle$ and $|1\rangle$, so that it is impossible to increase τ_r without decreasing ΔE. The results [64, 65] cannot be improved neither by using better materials, nor by using better technologies as soon as the gap stays the same. If we substitute the value $\Delta E = 1 \ K$ used in many modern experiments into the formula (1.2.11), we will find that the decoherence time is at least (see Footnote 13)

$$\tau_\phi = 10^4 \, \frac{\hbar}{\Delta E_{12}}.$$

This formula agrees with the experimental result obtained in [64, 65].

---

preparation of a single physical bit in $|0\rangle$ can fail with probability γ_p; 5) every measurement of a single physical qubit can give a wrong result with probability γ_m. All these noise parameters were chosen to be $\gamma_1 = \gamma_2 = \gamma_p = \gamma_m = \gamma$ because as numerical study has shown, the final result depends mostly on γ_2 [63].

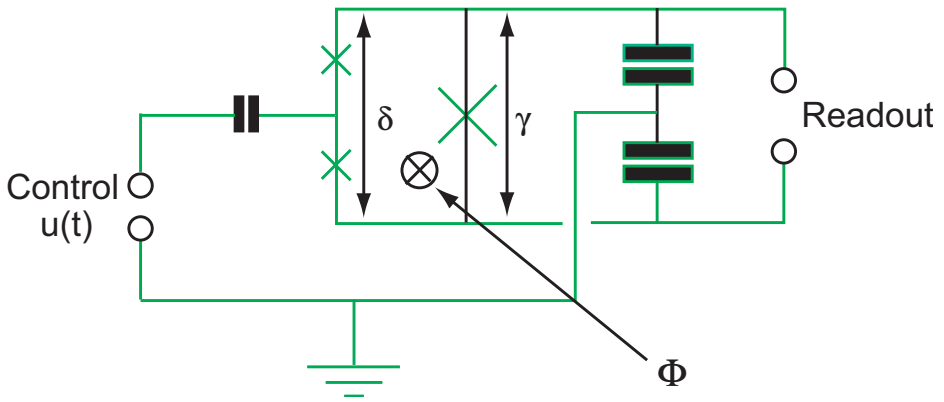

Figure 1.7: Quantronium

1.3 Quantronium and transmon

In this section we will briefly describe some recent experiments that tried to suppress effects of the noises and implement a simple readout scheme. All these experiments built a circuit around a Cooper pair box[16].

The first experiments [64, 67] studied the system called "quantronium" which is a modified version of a Cooper pair box where one Josephson junction (E_J^0, E_C^0) has been replaced by two smaller junctions ($E_J = E_J^0/2$, $C_J = 2C_J^0$) (see Fig. 1.7). If a phase difference δ is the combined phase across the two junctions, the Hamiltonian of the quantronium is given by [67]

$$\hat{H} = -2E_J \cos(\delta/2) \cos\hat{\theta} + E_C(\hat{N} - N_g)^2. \tag{1.3.2}$$

Let $E_C \approx E_J$, where $E_C = (2e)^2/2(C_g + C_J)$. In this case, neither $\hat{N}$ nor $\hat{\theta}$ is a well defined quantum number.

The ground state $|0\rangle$ and the first excited level $|1\rangle$ of the Hamiltonian (1.3.2) form a two-level state space which is separated by a significant gap from the other energy levels

[16]The basic Cooper pair box consists of a superconducting island connected to a superconducting reservoir by a Josephson tunnel junction with capacitance C_J^0 and Josephson energy E_J^0. The junction is biased by voltage V_g applied to the island. The gate capacitance is C_g. Cooper pairs can tunnel to the island from the reservoir and back again. The Hamiltonian of the box is given by [64]

$$\hat{H} = \frac{(2e)^2}{2(C_g + C_J^0)} \left(\hat{N} - N_g\right)^2 - E_J^0 \cos\hat{\theta}, \tag{1.3.1}$$

where $\hat{\theta}$ is the phase of the island and $N_g = C_g V_g/2e$ is the charge of the island induced by the gate voltage V_g.

[67]:

$$E_{0,1} = \mp\sqrt{(E_J \cos(\delta/2))^2 + (E_C(1-2N_g))^2}.$$

The difference $\Delta E_{01} = E_1 - E_0$ is minimal if $N_g = 1/2$. This point is known as the "sweet point" because in this case $\partial E_{0,1}/\partial N_g = 0$, so that the charge noise is suppressed. Also, if $\delta = 0$, we have $\partial E_{0,1}/\partial \delta = 0$, so that the flux and critical current noises are suppressed. As a result, if $N_g = 1/2$ and $\delta = 0$, there is no dephasing in the first order. By applying voltage pulses $V_g(t)$ with frequency $\Omega = \Delta E_{01}/\hbar$ to the gate, one can control the quantum state of the system.

The two states are characterized by currents flowing through the junctions:

$$I_{0,1} = \frac{2e}{\hbar}\left(\frac{\partial E_{0,1}}{\partial \delta}\right).$$

If $\delta \neq 0$, these currents are different. This fact allows us to implement a readout. If one more Josephson junction whose Josephson energy is $E_J^{large} = 20E_J$ is inserted in the circuit (as shown in Fig.1.7), then the phases δ and γ must satisfy the equation $\delta - \gamma = 2e\Phi/\hbar$, where Φ is the external magnetic flux applied to the loop that consists of the three junctions. The maximal total current that can flow through the system depends on the quantum state and is given by

$$I_{total} = I_C^{large}\sin(\gamma) + I_i(\gamma + 2e\Phi/\hbar),$$

where I_i depends on the quantum state of the qubit. If we want to measure the state, we apply a short pulse $I_{read}(t)$:

$$I_{read}(t) = \begin{cases} 0, & t <= 0, \\ I_1, & 0 < t <= T_{read}, \\ 0, & t > T_{read}, \end{cases}$$

where T_{read} is the duration of the pulse and I_1 is slightly lower than I_C^{large}. Because the large junction dominates, the phase γ is very close to $\pi/2$ when the pulse is applied. The current flowing through the large junction is almost equal to I_C^{large}, so that the system can be described by the tilted-washboard model [1, 67]. If $Z(\omega)$ is the impedance and C is the

total capacitance of the circuit, then the damping quality factor is defined as

$$Q_d = \frac{C\omega_p}{\mathrm{Re}\, Z(\omega_p)},$$

where ω_p is the plasma frequency of the large junction. If $Q_d > 1$, then a finite voltage can develop. We assume that the temperature is very low: $k_B T \ll \hbar\omega_p$. In this case, the switching probability is only determined by quantum fluctuations [67]:

$$P = 1 - e^{-\Gamma_i T_{read}}, \qquad \Gamma_i = 52 \sqrt{\frac{\Delta U_i}{\hbar\omega_p}}\, \frac{\omega_p}{2\pi} \exp\left(-7.2\, \frac{\Delta U_i}{\hbar\omega_p}\right),$$

where

$$\Delta U_i = \frac{4\sqrt{2}}{3}\, E_J^{large}(1 - \sin(\gamma_i))^{3/2}.$$

The phase γ_i depends on the quantum state $|i\rangle$, so does the switching probability. This allows us to distinguish the states $|0\rangle$ and $|1\rangle$ and, therefore, read quantum information[17].

The decoherence time has been measured in [64]: $T_1 = 1.8\ \mu s$, $\tau_\phi = 0.5\ \mu s$ (also, see Table 1.1 for the theoretical numbers).

Let's now consider another series of experiments where researchers studied the so-called transmon [32, 33, 34, 35]. This is a superconducting charge qubit derived from the Cooper pair box with minimal sensitivity to $1/f$ noise.

Imagine that we have a one-dimensional transmission line resonator with resonance frequency f_C (see Fig. 1.8). This means that electromagnetic waves with frequencies other than f_C are suppressed inside the resonator, so that we can write the Hamiltonian of the system as

$$\hat{H}_0 = \hbar\omega_C \left(a^\dagger a + \frac{1}{2}\right) + \hat{H}_\kappa, \tag{1.3.3}$$

where $\omega_C = 2\pi f_C$ and $\hat{H}_\kappa$ describes interactions of the resonator with its environment. These interactions lead to decay of the electromagnetic field created in the cavity of the

[17] It is important to note that the pulse current I_1 should be very close to the critical current I_C^{large}. Otherwise, the switching probability for $T_{read} < \tau_\phi$ will be too low and it will be impossible to distinguish the states $|0\rangle$ and $|1\rangle$. However, if the resulting current through the large junction exceeds I_C^{large}, the whole system becomes classical. As a result, quantum states of the qubit decay extremely fast (almost immediately), which does not allow one to distinguish the quantum states. Therefore, I_1 should be small enough, so that the large junction current is less than I_C^{large} for any quantum state of the qubit.

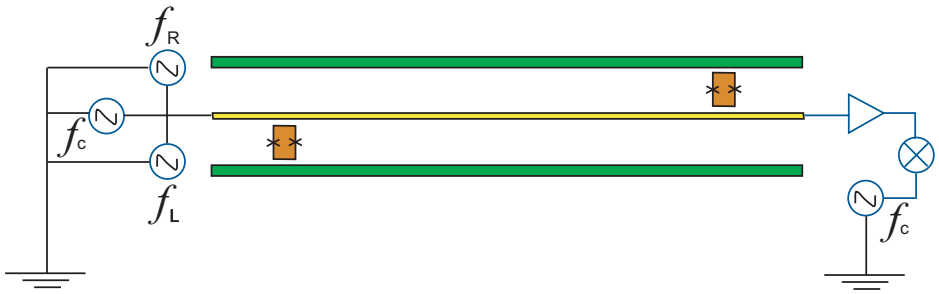

Figure 1.8: The so-called transmon is a Cooper pair box placed in a one-dimensional transmission line resonator. The transmon can be described by the Cavity Quantum Electrodynamics (cQED) equations. Applying microwave pulses at the qubit transition frequencies f_L and f_R, we can control the quantum state of the qubits, while applying pulses at the cavity resonance frequency f_C and measuring the output signal, we can read quantum information. If we have two transmons in the same cavity, they will interact with each other, so that it becomes possible to run quantum computations. The main difference between a transmon and a Copper pair box is that $E_J \gg E_C$ for the transmon, while $E_J \approx E_C$ for the Cooper pair box.

resonator. The quality factor Q of the resonator is high enough $(10^4 - 10^6)$, so that the decay rate $\kappa = \omega_C/Q$ is small (compared to the decoherence rate of the transmon which is discussed below).

Unfortunately, the resonator itself cannot be used as a quantum bit since electromagnetic field applied to it excites all its levels (not just the first one). The reason is that the energy levels of the resonator (which is a linear system) are equidistant[18]. However, we can try to use the high quality factor of the resonator to increase the decorence time of the Cooper pair box. The two lower eigenstates of the box are isolated from the higher levels but depend on the parameters of its environment. The energy levels of the resonator do not depend on these parameters but are not isolated from the higher levels. One can build a system

[18]It is very important to emphasize that any two energy levels that are used as two eigenstates of some qubit should be isolated from all other energy levels. This means that all transitions from these two levels to the others should be energetically forbidden or at least suppressed. In linear systems all levels are equidistant and transitions outside the Hilbert space of the qubit are allowed. Therefore, linear systems cannot be considered as candidates for a quantum bit. The essential parameter that describes how close is the system to being linear is the difference

$$\Delta E = \Delta E_{12} - \Delta E_{01}, \tag{1.3.4}$$

where $\Delta E_{01} = E_1 - E_0$ is the energy splitting of the qubit's levels, and $\Delta E_{12} = E_2 - E_1$ is the gap between the qubit's level $|1\rangle$ and the lowest outer level $|2\rangle$. The energy gap ΔE determines to what extent transitions between the levels $|1\rangle$ and $|2\rangle$ are suppressed and, therefore, the minimal time required to run a quantum algorithm.

Noise source	1/f amplitude	Transmon $E_J/E_C = 100$ $\tau_\phi(\mu s)$	Quantronium $E_J/E_C = 1$ $\tau_\phi(\mu s)$
Charge	$10^{-4} - 10^{-3}e$	24600	1.1
Flux	$10^{-6} - 10^{-5}\Phi_0$	3600	1800
Crit. current	$10^{-7} - 10^{-6}I_0$	35	17

Table 1.1: Comparison of the theoretical contributions to the dephasing time τ_ϕ for the transmon and the Cooper pair box with $\Delta E_{01}/2\pi\hbar = 7$ GHz [34]. In reality, the dephasing time will have an upper limit set by the quality factor of the transmission line that can be as large as $Q \sim 10^6$ [70, 71]. This means that in practice the decoherence time of the transmon cannot exceed $2\pi Q/\omega_r \approx 31\ \mu s$, where $\omega_r/2\pi = 5$ GHz is the typical resonator frequency [32].

that combines the resonator and the Cooper pair box, so that the dependence of the energy levels on the environment parameters is very weak but the gap (1.3.4) is still significant. As a result, the decoherence time increases.

Imagine that a Cooper pair box has been placed into the cavity (1.3.3). This pair interacts with the resonator [68, 69]:

$$\hat{H} = \hbar\omega_C \left(a^\dagger a + \frac{1}{2}\right) + \frac{\hbar\Omega}{2}\sigma^z + \hbar g(a^\dagger\sigma^- + a\sigma^+) + \hat{H}_\kappa + \hat{H}_\gamma, \tag{1.3.5}$$

where $\hat{H}_\gamma$ describes the coupling of the Cooper pair to modes other than the cavity resonance mode (this leads to decay of the state $|1\rangle$). Those modes are suppressed inside the resonator, so that this interaction is much weaker than the interaction with the main mode g. Furthermore, it is obvious that if the frequencies ω_C and $\Omega = \Delta E_{01}/\hbar$ are different, the interaction of the Cooper pair box with the cavity is very weak.

These two observations lead to the conclusion that the probability for the excited state $|1\rangle$ to decay via photon emission is significantly lower than it would be in the case when the Cooper pair box is situated outside the cavity. As a result, the decoherence time increases significantly [34] (see Table 1.1). If the energy gap ΔE_{01} is equal to 7 GHz and $E_J/E_C = 100$ then the dephasing time $\tau_\phi \geq 25$ ms and the decoherence time is only determined by pure relaxation processes. The best experimental result was measured at a flux sweet spot where $T_1 = 1.57 \pm 0.04\ \mu s,\ \ T_2 = 2.94 \pm 0.04\ \mu s$.

We can see that the transmon design has significantly increased the dephasing time τ_ϕ

(great achievement!) but not the relaxation time τ_r. Unfortunately, successful implementation of a quantum computer requires both τ_ϕ and τ_r to be large. The design described in the following section has been developed to solve the problem of small τ_r. If we combine this design with the transmon idea, we will potentially get an ideal quantum bit.

1.4 Josephson junction arrays with non-Abelian symmetry

Another way to resolve the problem described in the second section and eliminate the natural limitation on decoherence time is to build a Josephson junction device whose ground state is degenerate. In this case, there is no relaxation of the quantum state $|1\rangle$ to $|0\rangle$ because their energies are equal, so that the decoherence time τ_r should increase dramatically (it still cannot be infinite).

More formally, the device we want to build should satisfy the following requirements: its ground state should be twofold degenerate[19] and separated from the other states by a significant gap, $\Delta E \sim 1\ K$. This gap sets the scale for the minimal duration of all operations because all attempts to change the state of the system faster than for $\Delta t = 1/\Delta E$ would excite higher levels. Further, the physical noises should have little effect on the ground state splitting.

Very good theoretical progress has been achieved in this field. The natural avenue of research was to study more complicated Josephson junction circuits that are better decoupled from the environment than a simple (consisting of only three junctions) device considered in the previous section. These complicated Josephson junction circuits have a degenerate ground state [72, 73], so that we can use this degenerate low-energy state system as a quantum bit.

The basic idea of some of the recent suggestions for solid-state qubits is to use a small but highly symmetric Josephson junction array [74, 75]. The essential observation is that

[19] Or almost degenerate, that is, the energy gap between the two lower levels must be very small: $\Delta E_{01} \leq 100\ mK$.

a structure with a nonabelian symmetry group naturally has degenerate states that correspond to higher dimensional representations of the group. The simplest structure of this type that contains six junctions has been considered in [74]. Even though it can be implemented as a usual planar circuit, it can be viewed as a tetrahedron made of superconducting wires with one Josephson junction on each edge. The tetrahedron symmetry group is the point group T_d which has two one-dimensional, one two-dimensional and two three-dimensional irreducible representations.

The parameters of the system can be tuned, so that the ground state corresponds to the two-dimensional representation of the symmetry group and, therefore, is twofold degenerate. This degenerate ground state can be used as the Hilbert space of a quantum bit. The degeneracy of the logical states eliminates the problem of decoherence associated with photon and phonon emission. All the other decay processes that involve interaction with the modes characterized by the low density of states at low energies are equally suppressed.

The symmetry of the circuit also significantly suppresses the effects of the charge noise. If the charge induced on one of the islands is different from the others, the tetrahedron symmetry is destroyed. However, the remaining symmetry is described by the point group C_{3v} which has two one-dimensional and one two-dimensional irreducible representations. It is easy to show that the ground state is twofold degenerate and forms the same Hilbert space if the parameters of the system remain the same. This means that the degeneracy is *completely* insensitive to a *local* charge noise: the corresponding coupling is absent in all orders. A simultaneous effect of the charge noise on two different islands would lead to decoherence but this effect is small for uncorrelated noises. It is usually believed that the charge fluctuations on different islands are not correlated, so that decoherence induced by the charge noise in this device should be weak. One can also use this fact to study correlations between the charge noises on different islands.

Unfortunately, the situation is worse for the flux noise and the critical current noise. This is because deviations of the current on one of the edges (or deviations of the magnetic fluxes through one of the faces) destroy the tetrahedron symmetry but the resulting symmetry is

described not by the point group C_{3v} but by the much smaller group C_{2v} (or S_2) which has only one-dimensional irreducible representations. As a result, the degenerate ground state splits and the effects of the critical current noise are not suppressed to the same extent as the effects of the charge noise. However, the decoherence time of the logical states of the tetrahedral qubit is still expected to be much longer than that of a typical unprotected structure because the magnitude of the current and flux noises is usually rather small.

Two questions arise immediately. First, can we improve the noise characteristics of the proposed quantum bits? Second, is it possible to make and manipulate the tetrahedral qubit from an experimental point of view?

To answer the first question we have to study other possible Josephson junction arrays with nonabelian symmetry and calculate the noise magnitude in each of them. The smaller the noise level, the longer the decoherence time.

The second chapter of this thesis is devoted to a modified version of the tetrahedral array that contains 12 identical Josephson junctions (two junctions on each edge). It is shown in Fig. 2.1 and differs from the system described in [74] in the number of Josephson junctions. We show that the twelve-junction tetrahedron has very interesting physical properties:

1. The system's ground state is a doublet.

2. The ground state of the system does not suffer from the classical degeneracy that is inherent to the ground state of the six-junction tetrahedron. This leads to quantitatively smaller effects of the critical current noise. At the same time, the most attractive feature of the six-junction tetrahedron (the absence of linear coupling to the flux and charge noises) still exists. We calculate the coupling strength theoretically.

As a result, we can positively answer the first question and conclude that the twelve-junction tetrahedron is a very perspective candidate for a quantum bit with potentially very long decoherence time. If it is implemented experimentally, it would allow us to study the noises that are not currently known.

The second question is more difficult because experimental techniques available to us will improve in the future. Currently, experimenters cannot make systems containing more

than a few identical Josephson junctions. Also, a variety of different technological problems arise when we want to make very small junctions. Hopefully, these problems will be resolved in the future. However, even now we can propose some experimental methods that can help us to study the properties of the tetrahedral and other symmetric quantum bits.

The third chapter of this thesis proposes and discusses an experimental method that allows to measure spectrums and decoherence times of symmetric circuits. We have chosen a simple pyramidal array to demonstrate the main ideas of our method. Even though the noise resistance and theoretical decoherence time of the pyramidal array are worse than those of the more complex tetrahedral systems, it is much easier to realize the pyramid experimentally. The proposed design can be used with any symmetric Josephson junction circuit.

Chapter 2

A small Josephson junction array with tetrahedral symmetry

This chapter is based on the paper [76] and organized as follows. In section 2.1 we review the system in question. We calculate its spectrum and eigenstates. In section 2.2 we explore the physical properties of the system. Especially we want to know how different physical noises effect the spectrum and the eigenstates. We also find under which physical conditions the system can be used as a quantum bit. In section 2.3 we address the questions of readout and quantum manipulations.

2.1 The system

The system we are going to study is an array that consists of 12 identical Josephson junctions. The symmetries of the system become transparent when it is viewed as a tetrahedron made of superconducting wires with two Josephson junctions on each edge, as shown in Fig. 2.1. This tetrahedron is placed in a magnetic field, so that the magnetic flux through each lateral face equals $\Phi_0/2$ and the magnetic flux through the base face equals $3\Phi_0/2$. Note that any two fluxes that differ by a flux quantum are physically indistinguishable, so that the four faces of the tetrahedron are equivalent.

Each junction is characterized by its Josephson energy $E_J = (\hbar/2e)I_c$ and by its charging energy $E_C = (e^2/2C)$, while the whole system is characterized by the capacitance matrix of the superconducting wires. In principle, the capacitance matrix also contains some contributions of self-capacitances of individual islands, but for a typical physical implementation (see below) these contributions are much smaller than those of the junctions, so that we

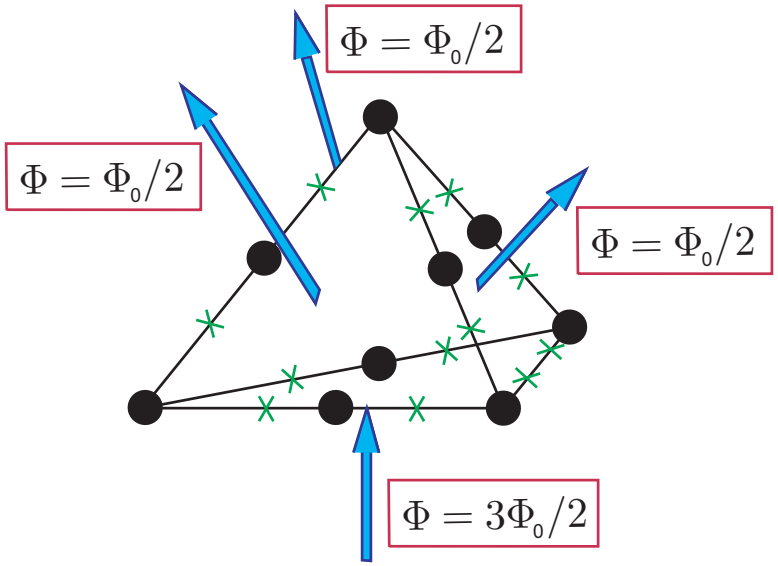

Figure 2.1: The tetrahedral Josephson junction array. Each edge consists of a superconducting wire with two Josephson junctions. The tetrahedron is placed in a uniform magnetic field, so that the fluxes through the lateral faces are $\Phi_0/2$ each, while the flux through the base face is $3\Phi_0/2$.

will neglect them. The whole system is described by the Lagrangian

$$\mathcal{L} = \sum_{i=1}^{12} \frac{1}{16E_c}\dot{\phi}_i^2 + E_J \cos(\phi_i - a_i), \tag{2.1.1}$$

where ϕ_i are the phase differences across the Josephson junctions, and a_i are chosen to produce the correct magnetic fluxes.

In the following analysis it will be more convenient to consider an orthogonal projection of the tetrahedron onto its base (see Fig. 2.2). The planar array that is the result of such a projection is physically equivalent to the three-dimensional tetrahedron but is much simpler from an experimental point of view. To preserve the frustration induced by the magnetic fluxes, we need to place the system in a uniform field, so that the flux through each small triangle is $\Phi_0/2$.

The symmetry group of the system is the point group T_d which is isomorphic to the permutation group S_4. It has two-dimensional representations and, therefore, some of the levels of the tetrahedron can be twofold degenerate. If we want the tetrahedron to perform as a protected quantum bit, we should tune the physical parameters of the system, so that the ground state corresponds to one of these degenerate levels. To find the level structure

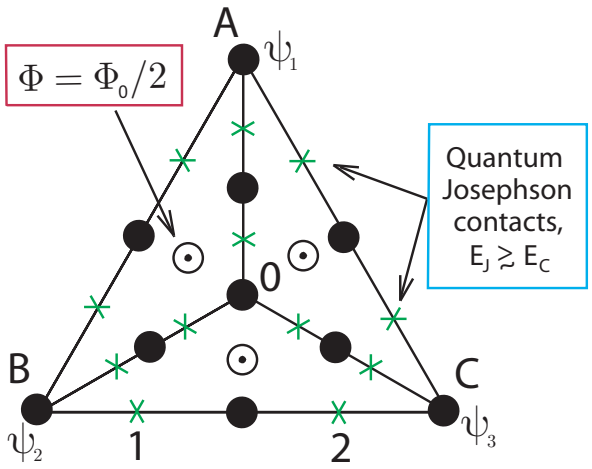

Figure 2.2: The planar array that is obtained by orthogonal projection of the tetrahedron onto its base. An orthogonal magnetic field is applied to the system, so that the flux through each of the small triangles is a half-flux quantum $\Phi_0/2$.

and determine the parameter range that leads to degeneracy of the ground state, we will consider the quasiclassical limit $E_J \gg E_C$, in which all superconducting phases are well-defined quantum variables[1].

The potential energy (2.1.1) is invariant under any gauge transformations, since it depends only on differences of superconducting phases. Let ψ_i, $i = 0, 1, 2, 3$ be the superconducting phases of the vertices of the tetrahedron (as shown in Fig. 2.2). If we choose the gauge, so that $\psi_0 \equiv 0$, then it is easy to show that the potential energy of the system has

[1]The numerical diagonalization that we carried out for the tetrahedron shows that the energy structure stays the same even for very small E_J/E_C.

the following six classical minima:

$$\begin{aligned}
V_1 &: \left(\psi_1 = 0, \psi_2 = -\frac{\pi}{2}, \psi_3 = \frac{\pi}{2}\right), \\
V_2 &: \left(\psi_1 = -\frac{\pi}{2}, \psi_2 = \frac{\pi}{2}, \psi_3 = 0\right), \\
V_3 &: \left(\psi_1 = -\frac{\pi}{2}, \psi_2 = 0, \psi_3 = -\frac{\pi}{2}\right), \\
W_1 &: \left(\psi_1 = 0, \psi_2 = \frac{\pi}{2}, \psi_3 = -\frac{\pi}{2}\right), \\
W_2 &: \left(\psi_1 = \frac{\pi}{2}, \psi_2 = -\frac{\pi}{2}, \psi_3 = 0\right), \\
W_3 &: \left(\psi_1 = -\frac{\pi}{2}, \psi_2 = 0, \psi_3 = \frac{\pi}{2}\right).
\end{aligned} \tag{2.1.2}$$

These minima can be mapped to each other by symmetry transformations.

Even though each minimum represents a whole family of quantum states, we can forget about this in the quasiclassical limit $E_J \gg E_C$ and consider only the lowest level of each family. As a result, we get a sixfold degenerate quasiclassical ground state (all six minima have the same energy). Quantum fluctuations lead to transitions between the minima and, thus, destroy the degeneracy. Taking into account the symmetry, we can write the Hamiltonian:

$$H = \begin{bmatrix}
0 & a & a & b & c & c \\
a & 0 & a & c & b & c \\
a & a & 0 & c & c & b \\
b & c & c & 0 & a & a \\
c & b & c & a & 0 & a \\
c & c & b & a & a & 0
\end{bmatrix}.$$

Here a, b, c are the tunneling amplitudes. The absolute values of a and c are equal because both these amplitudes correspond to rotations around different altitudes of the tetrahedron. However, their signs can be opposite. The amplitude b corresponds to inversion of all currents.

The eigenvalues and the corresponding eigenvectors of the Hamiltonian are given by

$$E_1 = -a + b - c,$$

$$\psi_1 = \frac{1}{2\sqrt{3}}(2V_1 - V_2 - V_3 + 2W_1 - W_2 - W_3),$$

$$\psi_2 = \frac{1}{2}(V_2 - V_3 + W_2 - W_3);$$

$$E_2 = -a - b + c,$$

$$\chi_1 = \frac{1}{2\sqrt{3}}(2V_1 - V_2 - V_3 - 2W_1 + W_2 + W_3),$$

$$\chi_2 = \frac{1}{2}(V_2 - V_3 - W_2 + W_3);$$

$$E_3 = 2a + b + 2c,$$

$$\eta = \frac{1}{\sqrt{6}}(V_1 + V_2 + V_3 + W_1 + W_2 + W_3);$$

$$E_4 = 2a - b - 2c,$$

$$\phi = \frac{1}{\sqrt{6}}(V_1 + V_2 + V_3 - W_1 - W_2 - W_3).$$

One can see that if $c = a$ then the ground state is a singlet, the first excited state is a triplet, and the second excited state is a doublet. But if $c = -a$ and $a > 0$ then the ground state is a doublet, which is what we want (see Fig.2.3). Therefore, the physical parameters of the system should be chosen, so that $c = -a$ and $a > 0$. Of course, such a choice of the parameters should not destroy the tetrahedral symmetry.

Since superconducting phases and charges are conjugate variables, the amplitude t of the process in which the ith phase changes by $\Delta\phi_i$ is given by $t = -|t| \exp(iq_i\Delta\phi_i)$. Here, q_i is the charge of the ith island (in terms of $2e$). Therefore, the sign of each amplitude is

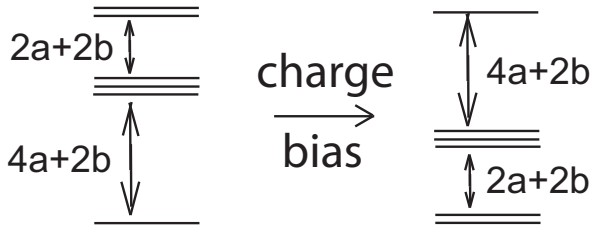

Figure 2.3: The energy spectrum of an isolated tetrahedron.

determined by the exponent $\exp(i\sum q_i\Delta\phi_i)$, where $\Delta\phi_i$ are transformation-specific:

$$a = -|a|\exp(i\sum q_i\Delta\phi_i),$$

$$b = -|b|\exp(i\sum q_i\Delta\phi_i'),$$

$$c = -|c|\exp(i\sum q_i\Delta\phi_i'').$$

The overall sign $(-)$ is explained by the following condition: if the charges of all islands are zero, the quantum state η which is described by the symmetric wave function should have the lowest energy. This means that in this case all the amplitudes a, b, c should be negative.

For a to be positive, the charges of the four tetrahedron vertices should be equal to $1/2$. The charges of the other four islands should be equal to zero. If this is the case, the amplitude b is positive, while c is negative. The ground state is a doublet $E_0 = -2a - b$:

$$\begin{aligned}\chi_1 &= \frac{1}{2\sqrt{3}}(2V_1 - V_2 - V_3 - 2W_1 + W_2 + W_3),\\ \chi_2 &= \frac{1}{2}(V_2 - V_3 - W_2 + W_3).\end{aligned} \tag{2.1.3}$$

The first excited level is a triplet and the second excited level is a singlet. The tetrahedral symmetry survives in this case because the total charge is an integer.

To find the absolute values $|a|$, $|b|$, we need to find the saddle trajectories that correspond to these processes[2] and then use the results to calculate the action of these processes. We

[2]This means that we should numerically look for the solution $\phi_i(t)$ of the Euler-Lagrange equations:

$$\frac{d}{dt}\left(\frac{\partial\mathcal{L}}{\partial\dot{\phi}_i}\right) - \frac{\partial\mathcal{L}}{\partial\phi_i} = 0$$

get:

$$|a| \approx 2E_J^{3/4}E_C^{1/4}\exp(-1.58\sqrt{E_J/E_C}),$$
$$|b| \approx 8E_J^{3/4}E_C^{1/4}\exp(-3.08\sqrt{E_J/E_C}), \tag{2.1.4}$$

that is, $|a| \gg |b|$ in the quasiclassical limit.

2.2 Effects of perturbations

The discussion above assumed that the tetrahedron is completely symmetric. One can see that physical imperfections violate the symmetry of the tetrahedron. Generally, a physical perturbation that reduces the symmetry of the tetrahedron to an abelian group splits the doublet. However, a perturbation applied only to a vertex of the tetrahedron reduces the symmetry to the point group C_{3v} which is nonabelian. Even more, it is easy to show that the doublet forms an irreducible representation of the group C_{3v}. As a result, the perturbation does not split the degeneracy. In particular, electrostatic potential applied to a vertex of the tetrahedron does not affect the degeneracy. This means that the degeneracy is completely insensitive to the local charge noise.

Let's consider effects of the magnetic flux noise. Because the total magnetic flux through the 3D tetrahedron is zero, an increase in flux through a face of the tetrahedron should be accompanied by an increase in flux through another face. Such a perturbation reduces the symmetry to the group S_2, which is abelian. The remaining symmetry itself would not be sufficient to preserve the degeneracy. However, in the case of an integer total charge,

---

with all the magnetic flux constraints on ϕ_i and the boundary conditions

$$\phi_i(0) = \phi_i^{initial\ state}, \qquad \phi_i(1) = \phi_i^{final\ state}$$

and calculate the action along the resulting trajectory (or all trajectories if there are many of them):

$$S = \int_0^1 \mathcal{L}dt.$$

Of course, we should solve dimensionless equations. To get them, we have to replace time t by $t\sqrt{E_J E_C}$.

In the quasiclassical limit, the transition amplitude is determined by the trajectory that has the minimal action S_{min}:

$$amplitude \sim N E_J^{3/4}E_C^{1/4}\exp\left(-S_{min}\right),$$

where N is the number of trajectories along which the action is minimal.

the Hamiltonian has an additional symmetry: the time-reversal symmetry. It ensures that complex one-dimensional representations of S_2 have the same energies. Careful inspection of the doublet (2.1.3) shows that its two states correspond to the symmetric and antisymmetric combinations of the one-dimensional irreducible representations and, therefore, their degeneracy is not affected by the increase in flux through one face. Physically, this means that the matrix elements of the current operator between the states of the doublet are zero and, therefore, the flux noise does not split the ground state in the linear order. Generally, we expect that for small deviations $\delta\Phi$ ($\delta\Phi \ll \Phi_0$), the splitting is given by

$$\varepsilon \sim \left(\frac{\delta\Phi}{\Phi_0}\right)^2 E_J,$$

because in the quasiclassical approximation the tunneling amplitudes a and b do not depend on $\delta\Phi$, but the energies of the six minima of the potential energy change differently. The coefficient in the last formula has to be determined numerically. For example, in the case of an additional flux $\delta\Phi$ through one face and $-\delta\Phi$ through another, we get

$$\varepsilon \approx 40 \left(\frac{\delta\Phi}{\Phi_0}\right)^2 E_J.$$

Let's now consider the situation when all the charges and magnetic fluxes are equal to their ideal values but the junction energies are slightly different. In the general case, the splitting ε depends linearly on variations of Josephson energies δE_J and can be calculated numerically. For example, in the case when the Josephson energies of the junctions 1 and 2 in Fig. 2.2 are different from E_J, the splitting ε is given by $\varepsilon \approx 0.4\, \delta E_J$.

Finally, we need to take into account thermal effects. One can neglect effects of quasiparticles at low temperatures $T \ll \Delta_s$, where Δ_s is the superconducting gap. To be more precise, the number of quasiparticles in each wire should be much smaller than one:

$$W\nu T \exp(-\Delta_s/T) \ll 1.$$

Here W is the volume of the wire, $\nu \sim n_e/\varepsilon_F$ is the density of states, and n_e is the electron density[3]. Note, however, that if this condition is not satisfied, thermally excited quasiparticles would lead to random fluctuations of the charge of each wire, which would affect the

[3] For a typical aluminum wire whose volume is 0.01 μm^3, this condition is satisfied for $T \ll 0.1$ K.

signs of the transition amplitudes a and b and destroy the quantum coherence of the states (2.1.3). Therefore, it is very important to run the quantum bit at low temperatures. For the same reason, measurement processes should not generate quasiparticles. In particular, they should not make the quantum bit switch to the normal state. Even if some junctions used for control and readout do switch to the normal state at some point, these junctions should be isolated from the qubit so that quasiparticles cannot jump to the device. In the following we will assume that this condition is satisfied, and that there are no BCS quasiparticles in the whole system.

In this case the only dangerous modes that can excite the quantum Josephson system are phonons and photons. In a typical setup both phonons and photons are gapless (although one can eliminate photons placing the whole system in a resonator), but the interaction with photons is extremely weak because a typical energy of an excitation is less than 1 K, which corresponds to the photon wavelength of the order of $\lambda \sim 1$ cm or more. The dipole matrix element for the emission or absorption of the photon contains the factor $(L/\lambda)^4$, where L is the typical linear size of the system, so that it is extremely small. The situation is different in the case of phonons [51], because the wavelength λ_s corresponding to excitations is about the size of the system, so that these processes are not rare. Note, however, that transitions between the two states lead to very small energy transfers[4], so that they are suppressed by a factor $(L/\lambda_s)^4$ similar to the one we meet in the case of photon excitations. Therefore, we can conclude that the main temperature effect is photon-mediated excitations of the higher energy levels. The probability of these transitions is determined by the Boltzmann exponent

$$P = \frac{1}{Z} \exp(-\Delta E/T),$$

where Z is the partition function and ΔE is the difference of the initial and the final energies. Taking the energy level structure into account, we find that transitions from the doublet into the triplet play the most important role. In this case, $\Delta E = 2(a + b) \approx 2a$ (since $|b| \ll |a|$) and the temperature T should be much less than $|a|$ ($T \ll |a|$).

[4]The energy splitting is not zero because of small perturbations. However, the gap is very small.

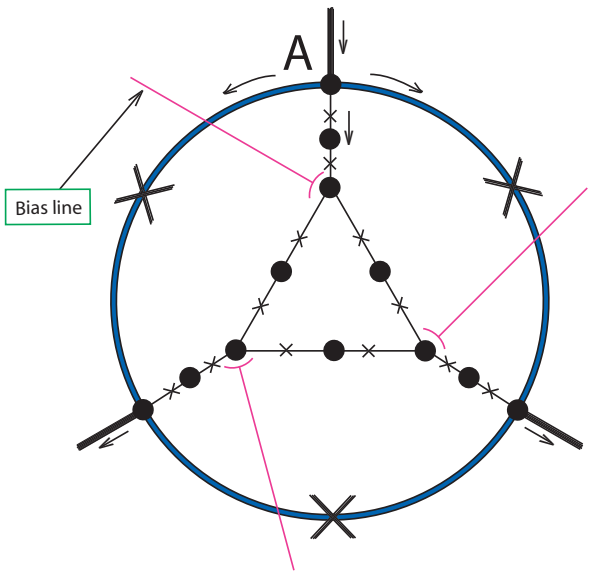

Figure 2.4: Schematic of the experiment. The central island of the tetrahedron is fabricated in the form of three islands. Each pair of these islands is connected by a very large Josephson junction. If external currents across these large Josephson junctions are zeros, then this device is equivalent to the original tetrahedron. The value of the total outside current corresponding to the moment when the large junctions fall into the oscillating regime depends on the state of the tetrahedron.

2.3 Readout and quantum manipulations

Suppose that after some manipulations the system is in a quantum state $\alpha|0\rangle + \beta|1\rangle$, where the logical states $|0\rangle$ and $|1\rangle$ are, correspondingly, χ_1 and χ_2 from (2.1.3). The coefficients α and β are unknown and we want to derive them from the results of some experiment. We will use the main ideas of the quantronium design [67, 64, 77]. A schematic of measurement is shown in Fig. 2.4. One of the islands of the tetrahedron is fabricated in the form of three islands. Each pair of these three islands is connected by a very large Josephson junction. If external currents across these large Josephson junctions are zeros, then the device in Fig. 2.4 is equivalent to the one shown in Fig. 2.2.

We start the measurement process from an initial state in which the external currents are zeros. Then we apply nonzero current to one of the outside wires (for example, the top wire in Fig. 2.4). At point A in Fig. 2.4 the current splits. Most of it flows through the two large junctions but a small part of it flows through the tetrahedron. This small current depends on the state of the tetrahedron. The value of the total outside current corresponding

to the moment when the large junctions fall into the oscillating regime depends on this small current flowing through the tetrahedron and, therefore, depends on the state of the tetrahedron. We can distinguish three possible measurement outcomes: (1) the total current is equal to I_1 for the states V_1, W_1, (2) the total current is equal to I_2 for the states V_2, V_3, and (3) the total current is equal to I_3 for the states W_2, W_3. If we measure the current in the outside chain many times and find the probabilities p_1, p_2, p_3 of these three outcomes, we can determine the absolute values of the coefficients α and β using the following formulas:

$$p_1 = \frac{2}{3}\alpha, \qquad \beta^2 = 1 - \alpha^2.$$

We emphasize that the described effect does not contradict the statement in the last section (which says that effects of the charge noise are absent and effects of the flux noise appear only in the second order) because here we have a nonlinear effect: when the current through the large junctions is close to the critical one, it induces additional phases $\pi/2$ across the corresponding tetrahedron edges. This deforms the quasiclassical states of the tetrahedron and induces significant average currents across each edge of the tetrahedron.

Here, we need to address an important question that arises in any experiment with quantum bits: we should have a procedure that allows us to prepare an initial state $\alpha|0\rangle + \beta|1\rangle$ with given α and β. The solution would be obvious if we had $\Delta E_{01} \neq 0$. For example, in [67, 64] microwave pulses with frequency $\omega = \Delta E_{01}/\hbar$ have been applied to the control gate to prepare any desired initial state. However, in our case $\Delta E_{01} = 0$, so that this method does not work. There is at least one way to resolve the problem. We can intentionally choose the gate potentials, so that ΔE_{01} is very small but nonzero. In this case, the properties of the system are very close to the ideal ones (even though we lose degeneracy) but microwave pulses can be used to prepare the initial state[5].

The described experiment has two potential pitfalls. First, the additional phases induced by the external current across the large Josephson junctions disturb the quantum state of the tetrahedron and might smear the differences between the currents (I_1, I_2, I_3) in

[5]There is a tradeoff here. If the energy gap ΔE_{01} is too large, the noise characteristic of the tetrahedron worsens significantly. If ΔE_{01} is too small, the duration of the control pulse is too long and dephasing processes will not allow to prepare the initial state. Therefore, one should find an optimal value ΔE_{01}.

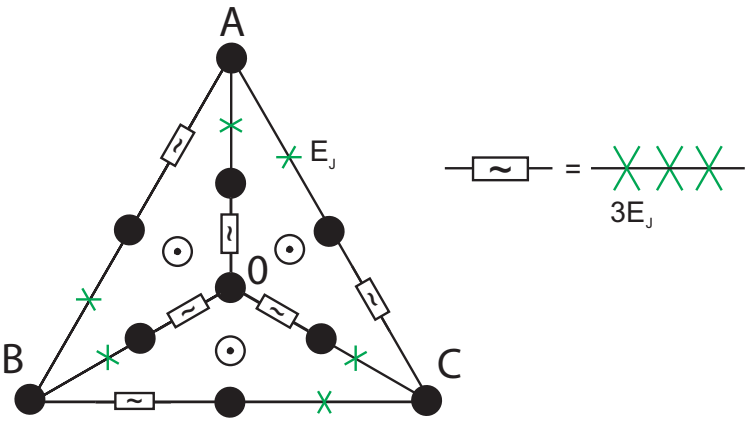

Figure 2.5: If one junction on each edge is replaced by a pseudoinductor, then the charge fluctuations affect only the islands connected to at least two regular junctions. As a result, one needs only three control gates. At the same time, all properties of this modified physical system are very similar to those of the original tetrahedron.

different states. We have solved the classical equations for the minima in the presence of these phases and verified that the quantum states evolve smoothly if external currents characterized by similar values ($\tilde{I}_1$, $\tilde{I}_2$, $\tilde{I}_3$) are applied to the system. We did not find any evidence for abrupt transitions from one state to another. Second, the current operator $\hat{I}$ generally has nondiagonal matrix elements, so that the measurement process itself would excite higher states and would show not the slightly modified values of the currents ($\tilde{I}_1$, $\tilde{I}_2$, $\tilde{I}_3$) corresponding to the six low states, but the values of the current corresponding to these higher states. To estimate this effect, we have calculated numerically matrix elements of $\hat{I}$ between all low-energy states. We have found that all nondiagonal elements are small in the quasiclassical limit, so that the described measurement should be able to distinguish $|0\rangle$ and $|1\rangle$ with probability close to 1.

We see that the tetrahedron is an excellent candidate for a quantum bit from a theoretical point of view. However, it has one very serious drawback: there are 9 superconducting islands whose initial charges are random. As a result, one should have 9 gates to control these charges. Otherwise, the ground state of the system is also random, as we explained in the introduction. In practice, it is very difficult or may be even impossible to control all 9 charges. However, one can modify the design proposed in Fig. 2.1 and consider the system shown in Fig. 2.5, where we replaced one junction on each edge by a pseudoinductor,

that is, a short chain of three larger Josephson junctions whose Josephson energy is $3E_J$. It is easy to show that in this system flux tunneling happens mostly through the weak junctions (not pseudoinductors). Therefore, the charge fluctuations affect only the islands formed by these weak junctions. As a result, one needs only 3 control gates. At the same time, all properties of this modified physical system are very similar to those of the original tetrahedron discussed in this chapter.

Another possible modification of the design avoids complicated elements such as pseudoinductors but uses a different symmetry group. An example is shown in Fig. 3.2 and will be discussed in the next chapter.

Chapter 3

The simplest experiment with nonabelian quantum bits

We have shown in chapter 2 that we can build a physical system with very interesting properties using small Josephson junction arrays. These properties allow us to consider the system as a wonderful candidate for a quantum bit. The most important of them is nonabelity of a symmetry group. Due to this nonabelity, the ground state of the quantum bit can be degenerate (this is the case when the physical parameters of the system which we are able to control have some special values). The degeneracy is important because it eliminates the problem of decoherence associated with the photon and phonon emission. All the other decay processes that involve interaction with the modes characterized by the low density of states at low energies are equally suppressed.

It is important to test the theoretical results obtained experimentally in [74, 76]. This presents two challenges: fabrication of the symmetric systems and tuning their parameters (the differences of the potentials of the islands and the fluxes) to get a degenerate ground state. The latter task is not trivial because of a large number of parameters that one needs to tune (three differences of potentials and three fluxes). This chapter has two goals: it proposes a feasible experimental realization of a symmetric circuit required for significant suppression of all noises and formulates an experimental algorithm that allows one to study the spectrum of the system at the protected point and measure the decoherence time. The system studied is simpler than the tetrahedron qubits but the algorithm can be easily applied to them as well.

3.1 The Josephson circuit and its mathematical model

A significant progress of technologies allows one to produce small Josephson junction arrays with desired properties. However, it is still a difficult engineering task to make an array with geometry of a tetrahedron which was the system studied in [74]. The problem is the following. It is very important for successful implementation of this quantum bit that its six junctions are characterized by identical values of the parameters E_J and E_c and that the geometrical areas of all the superconducting loops are exactly equal to each other. Of these three parameters it is the Josephson coupling E_J that presents the biggest challenge because it depends exponentially on the thickness of a dielectric layer. In contrast, accuracy of producing junction circuits with given geometrical sizes is determined by geometrical reproducibility of a mask which is very good. The charge energy E_c depends on the thickness of a dielectric layer, but to a much lesser extent than E_J does.

The task of producing identical Josephson junctions becomes much simpler if one can rely on the natural symmetries of the technologies used to produce the junctions. For example, the shadow mask litography is symmetric under rotations by 90 degrees. As a result, it might be easier to fabricate a system whose symmetry is given by the point group C_4 than the one associated with the tetrahedron group (see Fig.3.1). In this case, the distribution of the parameters of all Josephson junctions is only determined by the distribution of their geometrical areas and possible locations of defects in the oxide layer.

These considerations imply that the systems characterized by the point group C_4 might be similar in their behavior to the tetrahedral qubits but much simpler to fabricate (see Fig. 3.2). In this paper we are going to focus on a circuit that is made of superconducting wires and has a symmetry of a pyramid. There is one Josephson junction on each edge. The pyramid has almost ideal energy structure. Namely, one can tune the values of its physical parameters so that the ground state of the system becomes almost degenerate, that is, the gap between the ground state (which is still a singlet) and the first excited state (which is a singlet too) turns out to be rather small (in comparison with the gap between the first excited and the second excited levels). This dramatically suppresses the phonon

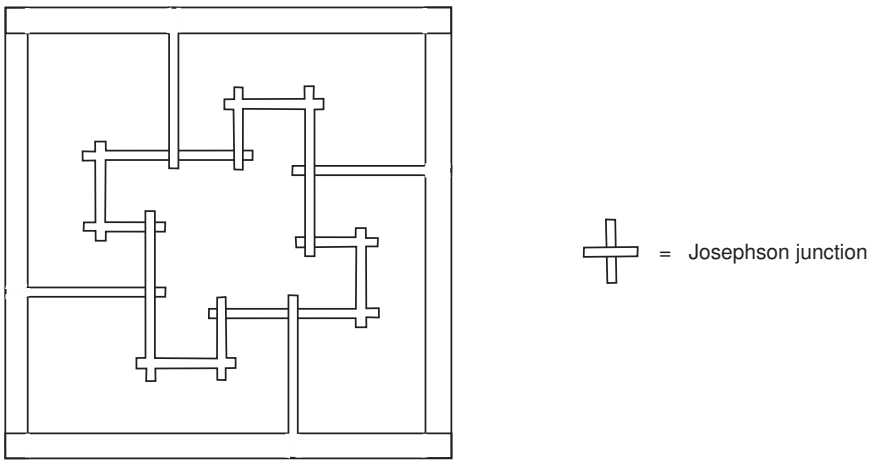

Figure 3.1: The system whose symmetry is given by the point group C_4. One can see that all the Josephson junctions can be made in one process.

and photon emission (1.2.11) whose rate is proportional to the high power of the frequency and significantly decreases the coupling to the local noises.

Each junction is characterized by its Josephson energy, $E_J = (\hbar/2e)I_c$, and by its charging energy, $E_C = (e^2/2C)$, while the system as a whole is characterized by the capacitance matrix of the superconducting wires. Exactly as it was in the case of the tetrahedron, the capacitance matrix contains the contributions from the self-capacitance of individual islands, but in a typical physical implementation these capacitances are much smaller than those of the junctions. The pyramid is placed in a uniform magnetic field, so that the magnetic flux through each small triangle equals $\Phi_0/2$. One of the islands (shown as "0") is grounded, so that its superconducting phase is always zero. The whole system is described by the Lagrangian

$$\mathcal{L} = \sum_{i=1}^{8} \frac{1}{16E_C}\dot{\phi}_i^2 + E_J \cos(\phi_i - a_i),$$

where ϕ_i are the phase differences across the Josephson junctions and a_i are chosen to produce the correct magnetic fluxes.

The spectrum of the system for different values of the Josephson energies of individual junctions can be obtained numerically and is shown in Fig. 3.3. It depends on the potentials of the four islands '1', '2', '3', '4' and the parameters E_J and E_C. We assume that the

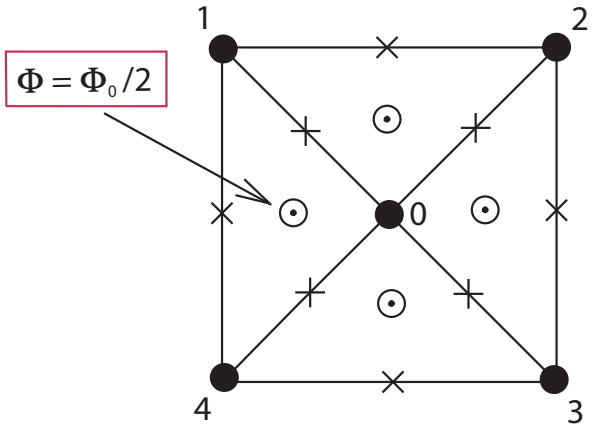

Figure 3.2: A small Josephson junction array with geometry of a pyramid. Each edge consists of a superconducting wire with one Josephson junction. The array is placed in a uniform magnetic field so that the fluxes through each of the smaller triangles is half-flux quanta, $\Phi_0/2$. The Josephson energy is $E_J = E_J^0 = 2$ K and the charge energy is $E_c = E_c^0 = 1$ K.

potentials of all the four islands are equal[1]. In this case, the symmetry group is the pyramid symmetry group D_4.

The ground state of the quantum bit can be described as the state in which the total charge of the system induced by the gates is equal to zero. The four excited states are obtained by adding an additional Cooper pair: each of them can be represented as a quantum superposition of the four basis quantum states (those in which one of the four islands contains an additional Cooper pair).

We are mostly interested in the gap between the ground state and the first excited level. It turns out that the four potentials can be chosen so that the gap is very small (even though it is still nonzero). This happens when the charge induced on each island of the pyramid is approximately equal to $0.11e$ if $E_J/E_C = 1$ and slightly greater for larger E_J/E_C. The gap between two logical levels in these cases is not exactly zero. However, it is very small compared to the distance between the first and the second excited levels. It is very important that at these points the energy gap as a function of the charge has a minimum, so that the linear coupling between the qubit and the charge noise is absent. The

[1]Of course, this is not true in the general case. We have to use a special experimental algorithm to make them equal.

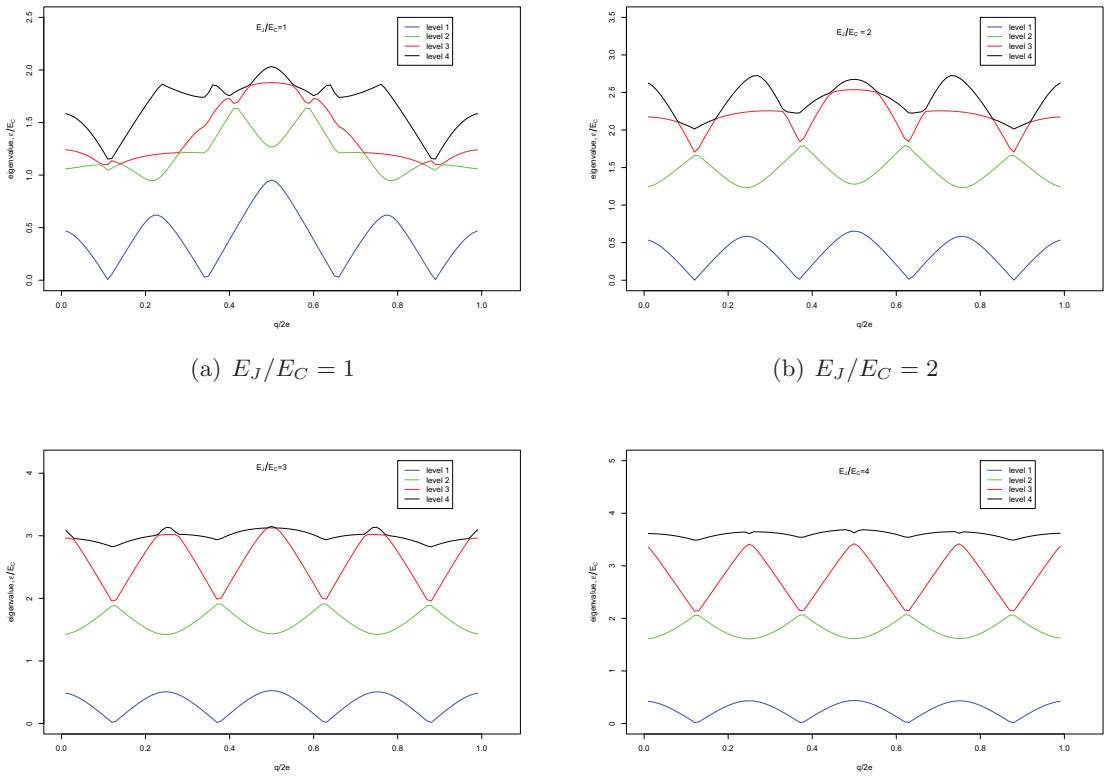

(a) $E_J/E_C = 1$

(b) $E_J/E_C = 2$

(c) $E_J/E_C = 3$

(d) $E_J/E_C = 4$

Figure 3.3: The spectrum of the system obtained numerically. The horizontal axis shows the charge of one island (in terms of $2e$), while the vertical axis shows the energy gap (in terms of E_C) between an excited level and the ground state. We assume that the potentials and charges of all the four islands are the same. The spectrum has been calculated for four different values of the ratio of the parameters E_J and E_C: (a) $E_J/E_C = 1$; (b) $E_J/E_C = 2$; (c) $E_J/E_C = 3$; (d) $E_J/E_C = 4$.

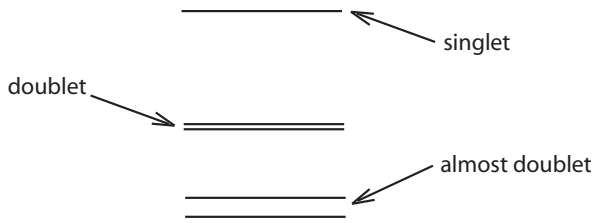

Figure 3.4: The spectrum of the pyramid at the point where the gap between the ground state and the first excited level is minimal.

curvature of this mimimum decreases rapidly as E_J/E_C decreases, so that larger values of this ratio are preferable for the charge noise suppression.

The qualitative understanding of the pyramid is greatly simplified in the charge basis. Furthermore, in the limit of very large charge energies, $E_C \gg E_J$, the qualitative description becomes absolutely correct. However, the circuit also becomes very sensitive to the charge noise in this limit. Therefore, in the following we will mostly discuss the intermediate regime, $E_J \gtrsim E_c$ and give all numerical estimates for $E_J = 2K$ and $E_C = 1K$.

If the potentials of all the islands are equal, the lowest four excited eigenstates of the pyramid can be described in terms of the irreducible representations of the group D_4. If, in addition, the potentials are chosen so that the gap between the ground state and the first excited level is minimal, the second and the third excited levels merge. In this case, the eigenstates are given by (see Fig. 3.4):

$$\begin{aligned}
|\psi_1\rangle &= \frac{1}{2}\left(|1\rangle + |2\rangle + |3\rangle + |4\rangle\right), \\
|\psi_2\rangle &= \frac{1}{\sqrt{2}}\left(|1\rangle - |3\rangle\right), \\
|\psi_3\rangle &= \frac{1}{\sqrt{2}}\left(|2\rangle - |4\rangle\right), \\
|\psi_4\rangle &= \frac{1}{2}\left(|1\rangle + |2\rangle - |3\rangle - |4\rangle\right),
\end{aligned} \tag{3.1.1}$$

where $|\psi_1\rangle$ is the first excited state, $|\psi_2\rangle$ and $|\psi_3\rangle$ form a doublet, and $|\psi_4\rangle$ is a singlet. Here the quantum states $|1\rangle$, $|2\rangle$, $|3\rangle$, $|4\rangle$ have the following physical meaning: the state $|j\rangle$

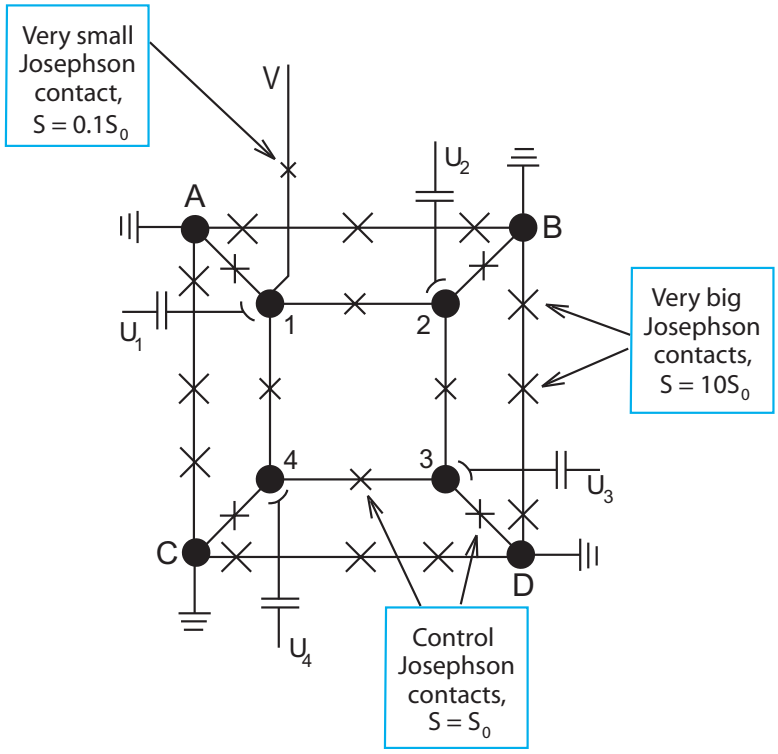

Figure 3.5: Schematic of the measurement. Each Josephson junction belongs to one of the following classes (within each class all junctions are identical): 1) Josephson junctions that constitute the pyramid shown in Fig. 3.2; 2) large Josephson junctions that are situated on the outside edges. Their Josephson energy is $E_J = 10E_J^0$ and their charge energy is $E_c = 0.1E_c^0$; c) one very small junction. Its Josephson energy is $E_J = 0.1E_J^0$ and its charge energy is $E_c = 10E_c^0$. The additional phases of π are created by the current $I = I_c\sqrt{3}/2$ through very big junctions (instead of magnetic fluxes).

($j = 1, 2, 3, 4$) describes the situation when the jth island contains one additional Cooper pair while the others do not.

The schematics of the proposed experiment is shown in Fig. 3.5. It is convenient (as shown in this Figure) to replace the central island '0' by four identical islands 'A', 'B', 'C', and 'D' which are connected by superconducting wires forming an outer closed loop. We do not use magnetic fluxes in our system since it is more difficult to control them independently. To preserve the frustration, we have to insert additional Josephson junctions into the outer loop with currents flowing through them. Doing this, we risk to change the Hamiltonian of the system and destroy the spectrum structure. Therefore, the extra junctions must have large Josephson energy, so that the phase fluctuations in them are negligible. In this case,

their influence is very small. We choose the Josephson energy of the big junctions to be $E_J^{big} = 10E_J^0 = 20\ K$, and their charge energy to be $E_C^{big} = 0.1E_C^0 = 0.1\ K$.

The currents flowing through the outer junctions should be chosen so that they create the phase difference of π between each pair of the four new islands 'A', 'B', 'C', and 'D'. Unfortunately, the corresponding state of a single Josephson junction would be unstable. To overcome this problem each outside edge should contain three identical junctions instead of one (see Fig. 3.5). In this case, the Josephson energy of each junction is equal to $E_J^{big} = 20/3\ K \approx 6.7\ K$, the charge energy is equal to $E_C^{big} = 0.3\ K$, while the phase difference across each junction is equal to $\pi/3$.

We assume that all four leads connecting islands A, B, C and D are electrostatically connected to the ground, so that their electrical potentials are zero. Finally, as shown in Fig. 3.5, the island '1' is connected to the dc current generator. To exclude any influence of the generator on the spectrum and other physical properties, we need to decouple it from the circuit by a very small Josephson junction whose Josephson energy is $E_J = 0.1E_J^0 = 0.2K$ and the charge energy is $E_C = 10E_C^0 = 10K$.

3.2 Proposed measurements

3.2.1 Extracting the spectrum and decoherence rates

The goal of this section is to show that the current-voltage characteristic of the small junction (see Fig. 3.5) gives information on both the spectrum and decoherence rates of the circuit. We begin with the qualitative discussion of the current flow through the system. We apply voltage V to the small junction without changing the potentials of the four islands connected to the ground. The typical current-voltage curve is shown in Fig. 3.6. We see four peaks which correspond to the four excited levels of the pyramid. The positions of the peaks and the distances between each pair of neighbor peaks depend only on the island potentials. Each peak is characterized by its own height I_{max} and width δV.

To understand the origin of the peaks, consider the process depicted schematically in Fig. 3.7 where we have shown the energy structure of the two sides of the small Josephson

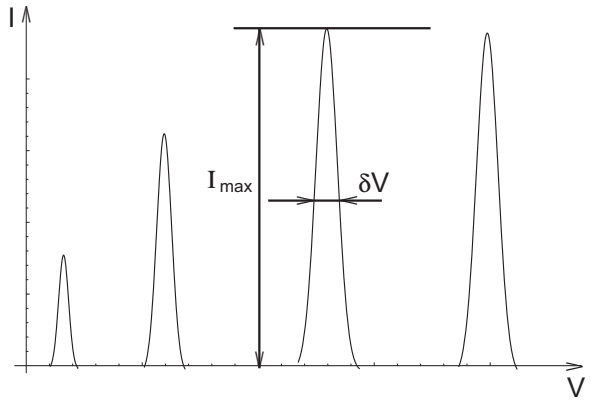

Figure 3.6: The typical current-voltage curve. There are four peaks which correspond to transitions from the four excited levels to the ground state. Each peak is characterized by its own height I_{max} and width δV.

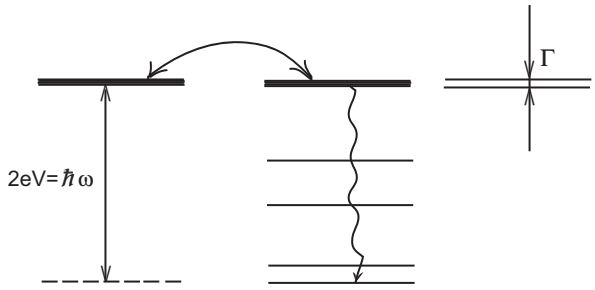

Figure 3.7: The tunneling process. If the chemical potential of the environment matches one of the excited energy level, a Cooper pair can jump from the outside to the quantum bit. As a result, the level gets some finite width $\Gamma_2 = \hbar/\tau_\phi$ determined by the decoherence time τ_ϕ. After the jump, the corresponding excited state decays, with a photon being emitted. This process also contributes to the level width: $\Gamma_1 = \hbar/\tau_r$ determined by the decoherence time τ_r. The total width Γ is obtained as a complex combination of the two values Γ_1 and Γ_2.

junction. Voltage V applied to the small junction implies that a Cooper pair has energy $2eV$ when it tunnels across the junction. If this energy difference matches one of the four excited energy levels, a process in which a Cooper pair jumps into the system from the outside is accompanied by the pyramid excitation.

The lifetime of such an excited quantum state is expected to be short for high energy states. There are two independent processes that destroy it. First, the additional Cooper pair can tunnel back to the left side of the small junction. As a result, the system returns back to the ground state. No current through the system (or, what is the same, the current

in the outside chain) occurs in this case. Second, the pair can tunnel into the ground, that is the quantum state can decay in the usual sense. The current through the system appears, while the excessive energy is carried away by a photon/phonon with the corresponding frequency. As a result, we see the peaks in Fig. 3.6.

These two decay processes compete with each other. If the second process (the additional Cooper pair tunnels to the ground) is very quick (as it is expected for high energy states), the pair does not have time to jump back: as soon as the pair gets on the right, the excited state decays. In this case, the magnitude of the current is only determined by the probability of the initial tunneling of the pair from the left side to the pyramid:

$$I \sim \frac{eE_J^{small}}{\hbar} \exp\left[-\frac{(V-V_0)^2}{2\delta\bar{V}^2}\right], \tag{3.2.2}$$

where we denote the Josephson energy of the small junction by E_J^{small}, while $\delta\bar{V}^2$ is determined by the Johnson–Nyquist formula:

$$\delta\bar{V}^2 = 4k_BT(\mathrm{Re}Z)\Delta f, \tag{3.2.3}$$

where k_B is Boltzmann's constant, Δf is the bandwidth and Z is the impedance of the whole system.

Below we will use the following notations: Z_1 is the impendance of the 8 main Josephson junctions (the junctions shown in Fig. 3.2), Z_s is the impedance of the small junction that connects the pyramid and its environment, and Z_{out} is the impedance of the environment. To compute the impedance we use the equivalent scheme of the pyramid shown in Fig. 3.8 and get

$$Z = Z_{out} + Z_s + \frac{7}{15}Z_1. \tag{3.2.4}$$

The widths of the levels (3.2.2) imposed by the environment become small at low temperatures. They can be further decreased by a proper impedance choice which we discuss below. In this limit, the widths of the levels are dominated by the intrinsic processes responsible for the decoherence in the circuit:

$$\delta V \to \hbar/\tau_\phi$$

In the opposite case, when tunneling of an additional pair to the ground is slow, the pair jumps back and forth through the small junction which strongly suppresses the tunneling current. The magnitude of the current is only determined by the probability of decay:

$$I_r \sim \Gamma_r = \frac{\hbar}{\tau_r}.$$

The width of the peak in this case is given by the sum of decay and dephasing processes:

$$\delta V \to \hbar/\tau_\phi + \hbar/\tau_r.$$

Thus, measuring the current-voltage characteristics of a small junction allows one in principle to determine the spectrum and the decay rate and decoherence time of the excited states.

It should be clear from the above discussion that the possibility of a meaningful measurement depends on the impedance of the environment as seen by a small junction. Let's discuss how we can estimate this impedance. The pyramid and its environment are connected through the small Josephson junction, so that the whole experimental system can be described by the following quantum impedance:

$$Z_{whole}(\omega) = \sum_n \frac{i\omega}{\omega - \omega_0^n + i\Gamma_n} |\langle 0|V^j \hat{q}_j|\psi_n\rangle|^2, \tag{3.2.5}$$

where $\hat{q}_j$, $j = 1, 2, 3, 4$, is the operator of the induced charge of the island j ($\hat{q}_j$ is not necessarily an integer), V^j, $j = 1, 2, 3, 4$, is the potential of the jth island induced by the voltage V, and $|\psi_n\rangle$ is an eigenstate of the system (n runs over all eigenstates below the superconducting gap).

If the quantum state of the system is

$$|\psi_n\rangle = a_1^n|1\rangle + a_2^n|2\rangle + a_3^n|3\rangle + a_4^n|4\rangle,$$

then the decay rate Γ_n in (3.2.5) is given by

$$\Gamma_n = |a_1^n|^2 Re\mathcal{Z}^{(1)} + \left(|a_2^n|^2 + |a_4^n|^2\right) Re\mathcal{Z}^{(2)} + |a_3^n|^2 Re\mathcal{Z}^{(3)},$$

where $\mathcal{Z}^{(1)}$, $Z^{(2)}$, $\mathcal{Z}^{(3)}$ are the effective impedances between the ground and the islands '1', '2', '3' (due to the pyramid symmetry $Z^{(4)} = Z^{(2)}$), correspondingly, and can be described

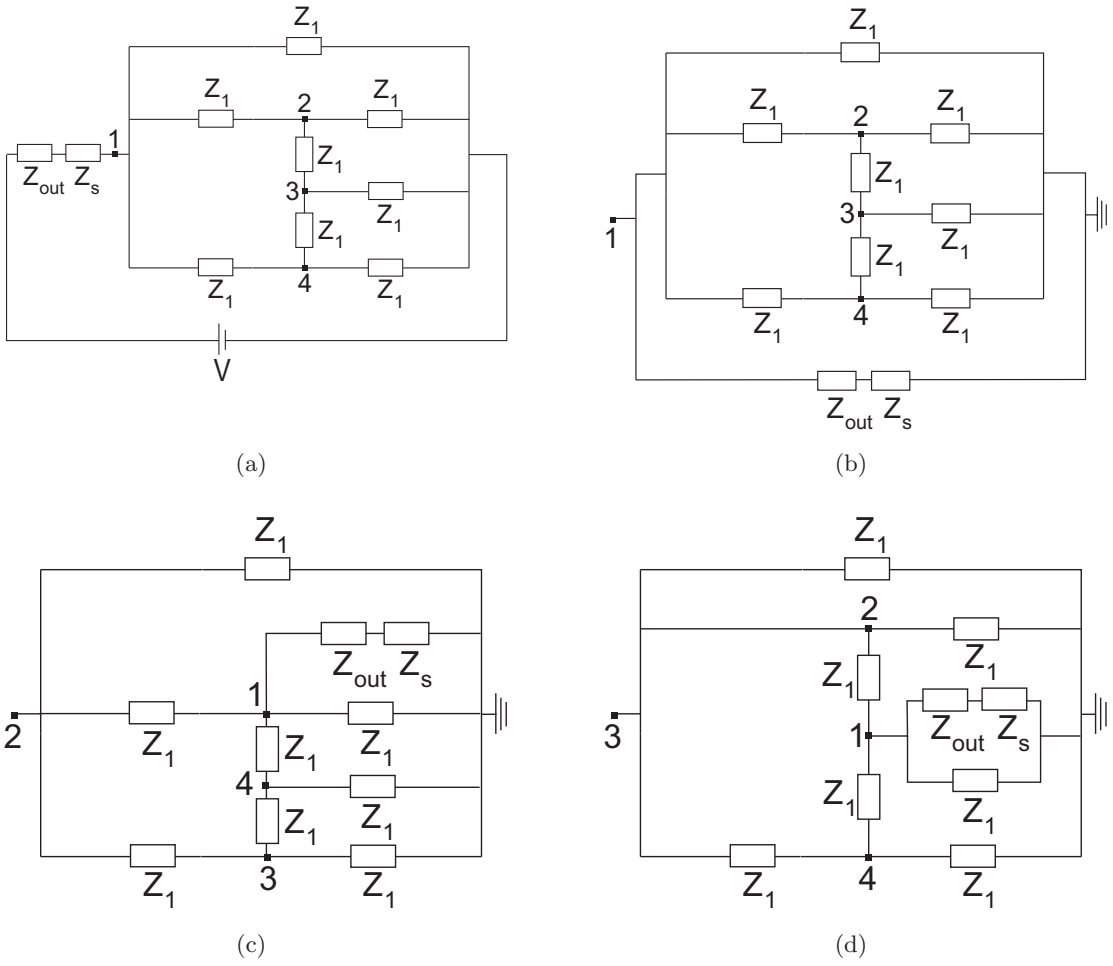

Figure 3.8: **(a)** The equivalent electric scheme of the pyramid and its environment. The islands 1, 2, 3, 4 are shown by the corresponding points of the circuit; **(b)** the equivalent electric circuit of the system describes the impedance $Z^{(1)}$ between the ground and the island '1' and helps to understand decay of a quantum state in which the island '1' contains one additional Cooper pair; **(c)** the equivalent electric circuit of the system describes the impedance $Z^{(2)}$ between the ground and the island '2' and helps to understand decay of a quantum state in which the island '2' contains one additional Cooper pair; **(d)** the equivalent electric circuit of the system describes the impedance $Z^{(3)}$ between the ground and the island '3' and helps to understand decay of a quantum state in which the island '3' contains one additional Cooper pair. We used the following notations: Z_1 is the impendance of the 8 main Josephson junctions (the junctions shown in Fig. 3.2), Z_s is the impedance of the small junction that connects the pyramid and its environment, and Z_{out} is the impedance of the environment.

by the equivalent schemes shown in Fig. 3.8. "Effective" means that these impedances determine the currents that would flow through the system in the classic regime, when some non-zero voltage is applied to the corresponding islands. One can check that the impedances $\mathcal{Z}^{(1)}$, $Z^{(2)}$, $\mathcal{Z}^{(3)}$ are determined by the following formulas:

$$\begin{aligned}
\mathcal{Z}^{(1)} &= \frac{7Z_1(Z_s + Z_{out})}{7Z_1 + 15(Z_s + Z_{out})}, \\
\mathcal{Z}^{(2)} &= \frac{Z_1(8Z_1 + 21Z_s + 21Z_{out})}{21Z_1 + 45Z_s + 45Z_{out}}, \\
\mathcal{Z}^{(3)} &= \frac{Z_1(3Z_1 + 7Z_s + 7Z_{out})}{7Z_1 + 15(Z_s + Z_{out})}.
\end{aligned} \tag{3.2.6}$$

At the point where the gap between the ground state and the first excited level is minimal, we obtain for the quantum states (3.1.1):

$$\begin{aligned}
\Gamma_1 = \Gamma_4 &= \frac{1}{4}\left[Re\mathcal{Z}^{(1)} + 2Re\mathcal{Z}^{(2)} + Re\mathcal{Z}^{(3)}\right], \\
\Gamma_2 &= \frac{1}{2}\left[Re\mathcal{Z}^{(1)} + Re\mathcal{Z}^{(3)}\right], \\
\Gamma_3 &= Re\mathcal{Z}^{(2)}.
\end{aligned} \tag{3.2.7}$$

Taking into account these formulas and technological constraints, we can choose the outside impedance Z_{out}, so that its influence is minimal.

3.2.2 The optimal point of the circuit

One important problem that has to be solved in order for the experiment to be successful is the problem of tuning the parameters of the quantum bit and finding its optimal point. In the case of the pyramid, there are eight such parameters: four charges of the superconducting islands and four currents through the outside edges.

Phases across the outside edges

If there are no magnetic fluxes, the phases across the four outside edges should be equal to π. One does not need to satisfy this condition precisely because small deviations of the

phases lead to the shifts of the energy levels that are quadratic in the phase deviations. In contrast, the deviations from ideality in producing Josephson junctions lead to much stronger distortion of the spectrum (linear in imperfections).

For the phases across the outside edges to be equal to π, some currents should flow through them. The magnitude of the currents is given by

$$I = I_c f(\pi/3),$$

where I_c is the critical current of one large junction, and the function $f(\phi)$ describes the tunneling properties of the junction. If the junctions are characterized by a small transparency, the function $f(\phi)$ can be approximated very well by $f(\theta) = \sin\theta$. The experimental measurement of the critical current in each three-junction chain allows one to determine the I_c and thus to apply the current that produces phase difference $\pi/3$ across each junction.

Parasitic charges of the islands

This problem is much more difficult than the problem discussed in 3.2.2 because we have no *apriori* knowledge about the random charges induced on each island. Fortunately, one still can tune the parameters of the system and find its optimal point. We will use the following algorithm.

We denote the real potentials of the four islands by V_1, V_2, V_3, V_4 (Fig. 3.5). In general, they do not exactly coincide with the potentials of the four gates (we denote the gate potentials by U_1, U_2, U_3, U_4). We can only claim that the island potentials V_i are given by some linear combinations of the gate potentials U_j:

$$V_i = V_i^0 + \sum_{j=1}^{4} C_{ij} U_j, \qquad i = 1, 2, 3, 4, \tag{3.2.8}$$

where the coefficients C_{ij} are some functions of all capacities in the system, and V_i^0 are the terms describing the potentials induced by the initial parasitic charges. Only the real potentials of the islands, V_i, are physically meaningful. However, we can control only the potentials of the gates U_j. Therefore, we need to know the matrix C_{ij}. In 3.2.2, we describe

an algorithm that allows us to determine it, so that in the rest of this subsection we will assume that the coefficients C_{ij} are known.

The expression (3.2.8) also includes linear contributions from the initial parasitic charges of the four islands. These charges are not known, as we mentioned before. Fortunately, we do not need to know these contributions which are static. What is really important for us is that if the island potentials change, the spectrum of the system changes as well. Since the change of the potentials V_1, V_2, V_3, V_4 is uniquely determined by the change of the gate potentials U_1, U_2, U_3, U_4, it follows that we can try to work with the gate potentials and the spectrum only and still be able to tune the system.

At each step of the following algorithm (that we describe in terms of the potentials V_i) we apply the voltage V to the small junction (as shown in Fig. 3.5), while keeping the potentials V_1, V_2, V_3, V_4 of the islands (and, therefore, positions of the peaks) fixed, and measure the current I flowing through the system.

1. Fix the potentials V_2, V_4 and change the potentials V_1, V_3, so that the sum $V_1 + V_3$ stays constant. For each pair of values of the potentials V_1 and V_3 measure the current-voltage characteristic. The positions of two peaks will not change while the other two peaks will move. In particular, the distance between the moving peaks will change. We should choose the potentials V_1 and V_3, so that this distance is minimal. This smallest distance between the two peaks corresponds to the line in the two-dimensional space (V_1, V_3) on which the potentials of the islands '1' and '3' are equal: $V_1 = V_3$. Note that the moving peaks cannot merge because of the perturbation theory splitting.

2. Fix the potentials V_1 and V_3 ($V_1 = V_3$) and change the potentials V_2, V_4, so that the sum $V_2 + V_4$ stays constant. For each pair of values of the potentials V_2 and V_4 measure the current-voltage characteristic. The positions of the two peaks that were motionless in the previous paragraph will change now, while the peaks that were moving will stay fixed. Again, we should choose the potentials V_2, V_4, so that the distance between the corresponding peaks is minimal. This smallest distance between the two peaks corresponds to the line in the two-dimensional space (V_2, V_4) on which

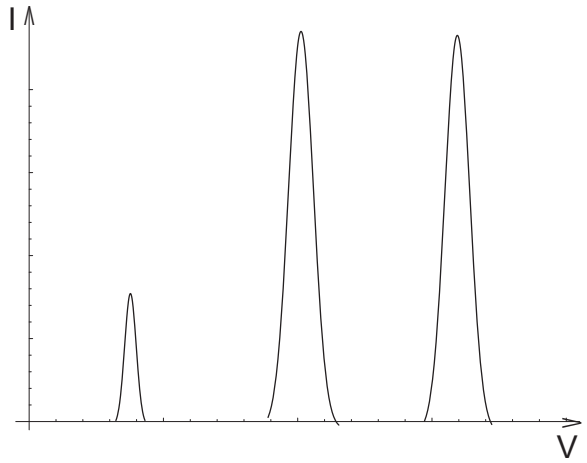

Figure 3.9: The current-voltage curve when the potentials of all the four islands are equal. In this case, there are only three peaks instead of four.

the potentials of the islands '2' and '4' are equal: $V_2 = V_4$.

3. Change the potentials V_1, V_2, V_3, V_4, so that the linear combinations $V_1+V_2+V_3+V_4$, $V_1 - V_3 = 0$, $V_2 - V_4 = 0$ stay constant. This means that the linear combination $V_1-V_2+V_3-V_4$ can change its value. The positions of all the four peaks will change. When any two of the four peaks merge (see Fig. 3.9), we can say that the potentials of all islands are equal: $V_1 = V_2 = V_3 = V_4$.

4. Change the potentials V_1, V_2, V_3, V_4 so that the linear combinations $V_1-V_2+V_3-V_4 = 0$, $V_1 - V_3 = 0$, $V_2 - V_4 = 0$ stay constant. This means that the linear combination $V_1 + V_2 + V_3 + V_4$ can change its value. All peaks will move, while at least one of them will move to the left. Its height and width decrease as the peak moves. When the peak that was received as a result of the merge of two original peaks reaches the origin or disappears, the qubit is tuned.

Spectrum distortion caused by the small Josephson junction

The procedure described in the previous section allows us to tune the system assuming that the potential V applied to the small junction does not cause any spectrum distortions. This

would be true if the junction had infinitely small capacitance which is not realistic. A non-zero value of its capacitance implies that the potentials of the four islands vary proportional to V.

In order to compensate for this effect, we have to take into account the additional potentials δV_i, $i = 1, 2, 3, 4$. Using the notations of Fig. 3.8, we get

$$\delta V_1 = \frac{7Z_1}{7Z_1 + 15Z_s} V,$$

$$\delta V_{2,4} = \frac{3Z_1}{7Z_1 + 15Z_s} V, \tag{3.2.9}$$

$$\delta V_3 = \frac{2Z_1}{7Z_1 + 15Z_s} V.$$

One can see that the variations δV_i are very small if $|Z_s| \gg |Z_1|$ which is true for the system we study. Therefore, in the following discussion we will assume that the additional potentials δV_i can be treated as small corrections. This implies that even though the elements of the matrix C_{ij} do depend on δV_i (see the next section), we can neglect this dependence.

We now describe the algorithm that allows one to compensate for these additional potentials. As we discussed earlier, we cannot directly control the potentials of the four islands. Therefore, we should use a method similar to those described in the previous section. First, we fix the potentials of the islands '2' and '4'. We choose the potential of the island '3', so that the corresponding peak on the current-voltage curve is very close to the origin (this means that the corresponding energy is very small). Using the algorithm described in the previous subsection, we choose the potential of the island '1', so that the distance between the peaks '1' and '3' is minimal. At this point, the potentials V_1 and V_3 are equal. Since the peaks are close to the origin, the voltage V that should be applied to the pyramid to produce the peaks is very small and the additional potentials are even smaller: $V_1 = V_3 \approx 0$, $\delta V_1 = \delta V_3 \approx 0$.

We now increase the potential of the island '3' by a small amount and repeat all the steps from the previous paragraph. That is, we find the gate voltages that correspond to the minimal distance between the peaks '1' and '3'. At this point, we can assume again that the potentials of the two islands are equal. However, this time the total potential of

each island is the sum of two contributions: $V_i^{total} = V_i + \delta V_i$, where the variations δV_i are determined by (3.2.9). Since the voltage V is not zero, $\delta V_1 \neq \delta V_3$. Therefore, $V_1 \neq V_3$, that is, the gate potentials should be changed by different amounts if we want the peaks to coincide. We know the exact changes of the gate potentials required to move the peaks '1' and '3'. Their difference corresponds to the difference $\delta V_1 - \delta V_3$. Using this information and the fact that all dependencies are linear, we can always determine the necessary corrections in terms of the gate potentials.

If it is needed, we can repeat the same procedure for the islands '2' or '4' and, thus, find the corrections for the potentials of these islands. One can also use (3.2.9).

Matrix C

As we mentioned before, the only physical quantities that have real physical meaning, are the potentials V_i, $i = 1, ..., 4$, of the four islands. But at the same time we are able to control only the potentials U_j, $j = 1, ..., 4$, of the four gates. In other words, we need to know the 4×4 matrix C_{ij} from (3.2.8) which binds the two sets, V_i and U_j. To find this matrix we can use one very simple property of the pyramid.

Imagine that we can control the potentials of the islands V_i. We start increasing the potential V_1 of the island '1'. At the same time, the potentials of the other islands should be kept constant. As the potential V_1 increases, the current-voltage curve changes. Namely, one of the peaks moves.

Apparently, when the potential V_1 becomes large enough, an additional Cooper pair will tunnel from the outside onto the island '1'. If we continue to increase V_1, at some point we will obtain the current-voltage curve that is identical to the initial one. In other words, the properties of the system depend on V_1 periodically, with the period being determined by all capacities. The same arguments can be used for the other potentials V_i, $i = 2, 3, 4$. It is evident that all the periods are the same due to the pyramid symmetry.

We now use the linear dependence (3.2.8). It implies that the current-voltage curve is periodical in the gate voltages U_j, $j = 1, ..., 4$, or, to be more precise, in the four linear

combinations of U_js. For example, when the potential of the first island, V_1, changes by one period (with the potentials of the other islands being fixed), the gate voltages change in the following way:

$$\begin{aligned} \Delta U_1 &= (C^{-1})_{11}\Delta V_T, \\ \Delta U_2 &= (C^{-1})_{21}\Delta V_T, \\ \Delta U_3 &= (C^{-1})_{31}\Delta V_T, \\ \Delta U_4 &= (C^{-1})_{41}\Delta V_T, \end{aligned} \tag{3.2.10}$$

where ΔV_T is the period in V_1. Let us start with some values of the potentials and corresponding positions of the peaks on the current-voltage curve. As the gate potentials change, the peaks move. For the change corresponding to (3.2.10), the positions of the peaks exactly match their initial positions.

If we repeat all the arguments for the potentials V_i, $i = 2, 3, 4$, we will find the other twelve equations that give us the dependence between the change of U_js and the change of V_is. As a result, we have 16 equations and 17 unknowns (16 elements of the inverse matrix C^{-1} and the period ΔV_T). From the 16 equations, we can easily express 15 coefficients $(C^{-1})_{ij}$ in terms of the coefficient $(C^{-1})_{11}$. Thus, we know the matrix C^{-1} up to an unknown common prefactor. But we do not need to know this prefactor because the period ΔV_T (which is determined by the prefactor) is not important for us.

Inverting the matrix C^{-1}, we find how the potentials of the islands change when the gate potentials change (again, up to an unknown common factor):

$$\Delta V_i = C_{ij}\Delta U_j. \tag{3.2.11}$$

Experimental search for different periods in the gate voltage space U_j might be performed in the following way. One scans the four-dimensional voltage space using some square grid, measures current-voltage characteristics at each node and compares them to each other. Because of a large space dimensionality (4D) the straightforward implementation of this procedure would require scanning of a large number of nodes. The problem can be made significantly easier by using the approximate values of the capacitance matrix that corresponds to the simplified circuit shown in Fig. 3.5. In this approximation the matrix

C^{-1} relating the applied and induced potentials is given by

$$\hat{C}^{-1}_{full} = C_g^{-1} \begin{pmatrix} C_g + 3C_0 & -C_0 & 0 & -C_0 \\ -C_0 & C_g + 3C_0 & -C_0 & 0 \\ 0 & -C_0 & C_g + 3C_0 & -C_0 \\ -C_0 & 0 & -C_0 & C_g + 3C_0 \end{pmatrix},$$

where C_0 is the capacitance of the individual Josephson junctions constituting the pyramid and C_g is the gate capacitance. From here one can derive the approximate values of the gate voltages that correspond to one charge period. Measuring current-voltage characteristics around this point, one can locate the values of the potentials that correspond to exactly one period after a small number of steps.

Chapter 4

Implementation of large protected Hilbert spaces

4.1 Higher symmetry systems

As we showed in the second chapter, the Josephson junction circuit with tetrahedral symmetry has a double-degenerate ground state protected from external noises and is a good candidate for a quantum bit. A few such quantum bits connected by tunable elements form a circuit that is in principle can be used for quantum computations. However, the tunable elements break the symmetry of the individual qubits and destroy the protection. Thus, it is worth asking if it is possible to construct more complex systems with much larger protected space which can serve as a *combined* Hilbert space of two or more qubits.

The degeneracy required for existence of the protected subspace can be only realized in highly symmetric qubits. From an experimental point of view, the simplest nontrivial symmetry group is the pyramid group C_{nv} which contains rotations and reflections. It can be implemented, for instance, as a long chain of identical junctions, or as a chain in which all nodes are connected to the central island by a junction (see Fig.4.1).

Unfortunately, the pyramid groups have only one- and two-dimensional irreducible representations (which are not protected), so that, they cannot be used for creating high-dimensional protected spaces. Furthermore, a perturbation acting on any physical element of such circuits (a junction or an island) destroys the symmetry completely. As a result, the degenerate ground level splits, with the energy gap being proportional to the strength of the perturbation. Therefore, in order to get higher dimensional Hilbert spaces with built-in protection, one needs more complex symmetry groups such as the tetrahedron group which

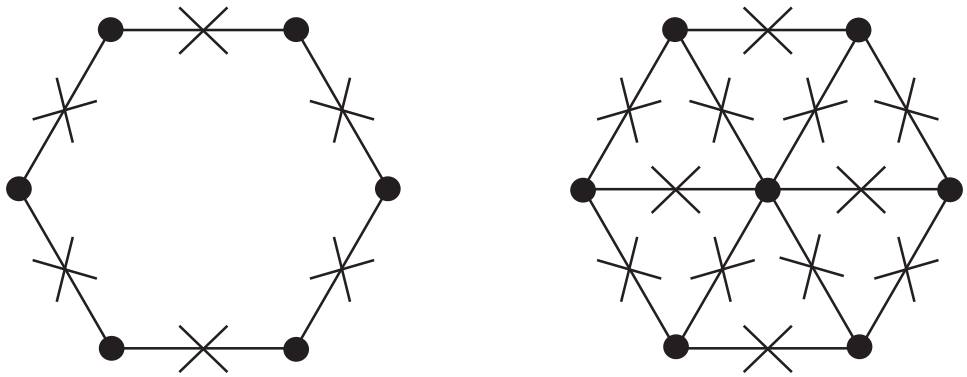

Figure 4.1: The simplest Josephson junction arrays whose symmetry group is C_{nv}, $n = 6$: a) a closed loop with 6 junctions and b) a similar loop in which all islands are connected to the central island.

is isomorphic to the permutation group S_4 and was discussed earlier.

In this chapter we explore a natural generalization of the tetrahedral quantum bit and consider devices whose symmetry can be described by one of the higher order permutation groups S_n which have remarkable mathematical properties[1].

We consider the level structure and associated built-in protection of some conceptually simple circuits. They are probably not the best candidates for a real experimental system but the discussion allows us to demonstrate the most interesting properties of higher-symmetry circuits. In these devices each pair of superconducting islands is connected by a junction, while the fluxes through the basic loops[2] are all equal to $\Phi_0/2$. The Josephson energy of each junction is given by

$$V_{i,j} = -E_J \cos(\varphi_i - \varphi_j - \pi) = E_J \cos(\varphi_i - \varphi_j), \tag{4.1.1}$$

where we chose the gauge so that at each link there exists an additional phase difference π (mod 2π) and φ_i is the phase of the ith island[3]. This formula can be rewritten using the spin representation, in which the state of each superconducting island is characterized by

[1]Unfortunately, they also have a big drawback: it is very difficult (in most cases, impossible) to project the corresponding Josephson junction circuit to a plane if $n > 4$. This means that their experimental implementation might require bridges.

[2]The loops that cannot be represented as a sum of two smaller loops.

[3]One can easily show that both conditions and the gauge choice are realistic for all the specific systems discussed below in this chapter.

the complex classical unit vector $z = (\cos\varphi_i, i\sin\varphi_i)$ called a pseudospin. The Josephson energy is given by the sum of antiferromagnetic interactions between the pseudospins:

$$V = \frac{1}{2}E_J\sum_{i,j} z_i^* z_j = \frac{1}{2}E_J\left|\sum_j z_j\right|^2 . \qquad (4.1.2)$$

Everywhere in this chapter we will assume that $E_J/E_C \gg 1$. Repeating all the steps done in [74] for the tetrahedron, we find the classical minima of the potential energy (4.1.2) and then the tunneling amplitudes between these minima[4]. Similar to the tetrahedron case, the level structure of the high-symmetry system described by the potential energy (4.1.2) is peculiar because the classical ground state is infinitely degenerate: all states satisfying the complex condition $\sum_j z_j = 0$ have exactly zero energy. This means that if the system has n islands then the classical energy is equal to zero on a $(n-3)$-dimensional hypersurface in the $(n-1)$-dimensional space of the superconducting phases $\{\varphi_i\}$ (note that one degree of freedom corresponds to the global phase and, therefore, is always irrelevant)[5]. The classical degeneracy is destroyed by quantum fluctuations, so that there are some special points on this hypersurface, where the energy is lowest. To proceed further we should find these points and discuss the quantum transitions between them. For simplicity, we consider the particular cases $n = 5$ and $n = 6$ for which our calculations can be done explicitly.

4.1.1 Pentagram

We begin with a five-node system that can be viewed as a pentagram and can be implemented as a star or a square with two diagonals connected to the ground (see Fig.4.2). Its symmetry group is isomorphic to the permutation group S_5. Note that there is no any electric contact (including Josephson junctions) between the diagonal wires of the pentagram. As was mentioned before, this presents an implementation problem because a bridge is required.

Now we need to take the steps discussed earlier. First, we should choose the fluxes that

---

[4] These tunneling amplitudes depend on the charging energy E_C and the Josephson energy E_J.

[5] In the case of the tetrahedron, the hypersurface is a line in the 3-dimensional space [74].

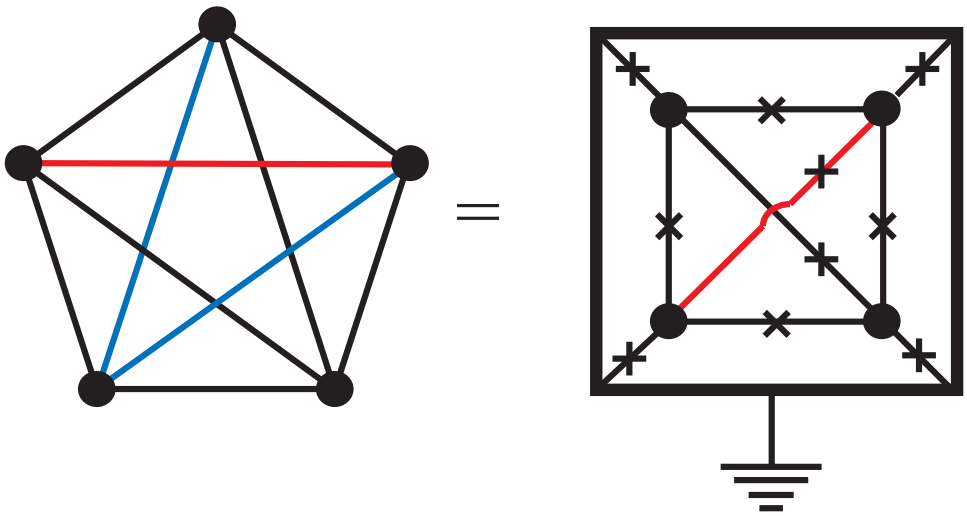

Figure 4.2: Schematics of the pentagonal Josephson circuit whose symmetry group is isomorphic to the permutation group S_5 . Here all lines represent Josephson couplings, black circles represent superconducting islands. Different colors represent different physical layers of the structure, so that there is no contact between the wires of different colors when they cross. The right pane shows an equivalent representation that involves only one bridge crossing: in this representation one of the islands is replaced by a circuit shown as a large outer square. All phases are measured with respect to this island.

result in the antiferromagnetic signs of Josephson couplings. To do this, we consider the square representation of the pentagram (the right pane in Fig.4.2) and apply an external magnetic field, so that the flux through the inner square is Φ_0. We can also choose the size of all contours in such a way that the flux through the outer square is $3\Phi_0$ (i.e. the area of the outer square should be 3 times greater than the area of the inner square). In this case, the fluxes through all the basic loops are equal to $\Phi_0/2$. This is exactly what we required when we wrote the expression (4.1.1).

As we mentioned above, the classical ground state is infinitely degenerate. The manifold of these degenerate states is a surface described by the equation $\sum_{j=1}^{5} z_j = 0$. We can always fix one phase (for example, set $z_5 = 1$) and consider the remaining four phases as independent variables. The real and imaginary parts of the complex equation $\sum_{j=1}^{4} z_j = -1$ reduce the four-dimensional space to the two-dimensional surface. Therefore, the manifold that describes infinitely degenerate states is a two-dimensional surface in the four-dimensional phase space. The degeneracy is destroyed by quantum fluctuations. In the limit of large

E_J/E_C quantum fluctuations orthogonal to the surface are small. Therefore, one can replace the potential $V(\varphi)$ by its harmonic approximation. For a simple (diagonal) mass term the quantum system moving in a harmonic potential has energy

$$E = \frac{1}{2\sqrt{m}} \sum_a \sqrt{\lambda_a},$$

where λ_a are eigenvalues of the quadratic form that approximates the harmonic potential. This energy describes quantum fluctuations orthogonal to the surface and provides an effective potential for the motion on the surface. This can be symbolically written as

$$V_{eff} = \frac{1}{2\sqrt{m}} \operatorname{Tr} \sqrt{\frac{\partial^2 V}{\partial x_i \partial x_j}},$$

where x are the coordinates normal to the surface defined by the equation $V(\varphi)$=0. More explicitly,

$$\begin{aligned} V &= \cos(\varphi_1) + \cos(\varphi_2) + \cos(\varphi_3) + \cos(\varphi_4) \\ &+ \cos(\varphi_1 - \varphi_2) + \cos(\varphi_1 - \varphi_3) + \cos(\varphi_1 - \varphi_4) \\ &+ \cos(\varphi_2 - \varphi_3) + \cos(\varphi_2 - \varphi_4) + \cos(\varphi_3 - \varphi_4) \end{aligned}$$

The surface is defined by the following two equations:

$$\begin{aligned} f_1(\varphi) &= 1 + \cos(\varphi_1) + \cos(\varphi_2) + \cos(\varphi_3) + \cos(\varphi_4) = 0 \\ f_2(\varphi) &= \sin(\varphi_1) + \sin(\varphi_2) + \sin(\varphi_3) + \sin(\varphi_4) = 0. \end{aligned} \tag{4.1.3}$$

From these equations we can find two non-orthogonal (and non-unitary) vectors $u_1 = \nabla f_1(\varphi)$ and $u_2 = \nabla f_2(\varphi)$ which form the basis of the subspace orthogonal to the surface.

Fortunately, we do not need to work explicitly with the coordinates x_i, because the potential energy is constant on the surface, so that $\frac{\partial^2 V}{\partial y_i \partial y_j} = 0$ for the coordinates on the surface y_i. As a result, the trace in V_{eff} would not change if we calculate it for the whole space. Since the trace is invariant under unitary transformations, the effective energy can be written as

$$\begin{aligned} V_{eff} &= \frac{1}{2\sqrt{m}} \operatorname{Tr} \sqrt{\widehat{V}}, \\ V_{ij} &= \frac{\partial^2 V}{\partial \varphi_i \partial \varphi_j}. \end{aligned}$$

The arguments above can be used only if we assume that φ_i are canonical variables, that is, if the kinetic energy is proportional to a unit matrix. If this is not correct (and this is not correct in the realistic case when the charging energy is mostly determined by the capacitances of the Josephson contacts), the result becomes slightly more complex. In the general case, the kinetic energy is

$$T = \frac{1}{16E_c} \sum_{i,j} \left(\frac{\partial \varphi_i}{\partial t} \right) C_{ij} \left(\frac{\partial \varphi_j}{\partial t} \right), \tag{4.1.4}$$

where C_{ij} is the dimensionless capacitance matrix.

Let's assume that the capacitances of the Josephson junctions in Fig.4.2 are much larger than the capacitances of the superconducting islands. In this case, the kinetic energy is given by the formula (4.1.4) with the capacitance matrix

$$\widehat{C} = \begin{pmatrix} 4 & -1 & -1 & -1 \\ -1 & 4 & -1 & -1 \\ -1 & -1 & 4 & -1 \\ -1 & -1 & -1 & 4 \end{pmatrix}. \tag{4.1.5}$$

The effective potential energy is given by

$$V_{eff} = \mathrm{Tr} \sqrt{8E_c \widehat{C}^{-1/2} \widehat{V} \widehat{C}^{-1/2}}.$$

It is easy to show that the square root of $\widehat{C}$ is given by

$$\widehat{C}^{-1/2} = \frac{1}{\sqrt{5}} \widehat{1} + \frac{1}{4} \left(1 - \frac{1}{\sqrt{5}} \right) \widehat{I},$$

where all elements of the matrix $\widehat{I}$ are equal to 1: $I_{ij} = 1$. If we consider V_{eff} as a function of two phases φ_1, φ_2 (one phase $\varphi_0 = 0$ is fixed and two other phases φ_3 and φ_4 can be expressed in terms of φ_1 and φ_2 using (4.1.3)), we will find that the energy is minimal at very special points. For example,

$$\begin{aligned} z_0 &= 1, \\ z_{1,2} &= z_+ \equiv -\tfrac{1}{4} + \tfrac{\sqrt{15}}{4} i, \\ z_{3,4} &= z_- \equiv -\tfrac{1}{4} - \tfrac{\sqrt{15}}{4} i. \end{aligned} \tag{4.1.6}$$

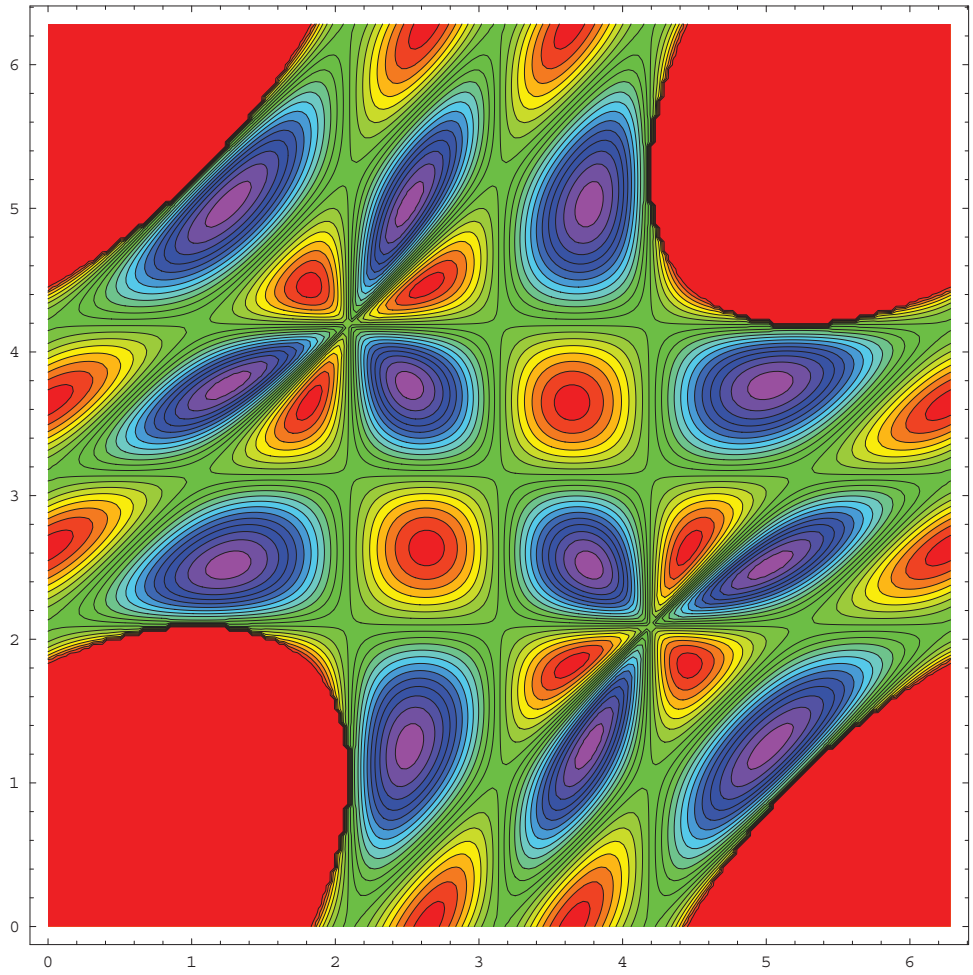

Figure 4.3: The quasiclassical energy as a function of two independent phases (φ_1, φ_2). The phase φ_0 is fixed and equal to 0, while the values (φ_3, φ_4) are determined from (4.1.3). The energy minima (red) are given by the solution (4.1.6) and its mappings.

The plot of $V_{eff}(\varphi_1, \varphi_2)$ is shown in Fig. 4.3. Notice that the gauge choice $\varphi_0 = 0$ which is convenient for numerical calculations breaks the symmetry of the pentagram. This makes interpretation of the figure more difficult. The close inspection of the plot reveals 30 energy minima: 1) 12 different points (φ_1^0, φ_2^0) for which there exist two different sets (φ_3^0, φ_4^0) and 6 points (φ_1^0, φ_2^0) for which there exists only one set (φ_3^0, φ_4^0). All these minima can be obtained from (4.1.6) by simple mappings.

To further discuss the quasiclassical minima and quantum transitions between them, we will work in the symmetric gauge in which the phase φ_0 is not fixed, so that the pentagram symmetry is not broken. Different quasiclassical states can be obtained from (4.1.6) by

permutations. To describe these states, we will denote the three possible values of each phase by 0 , $+\kappa$, and $-\kappa$, where $\kappa = \arccos(-1/4) \approx 1.82$. We will also drop the letter κ to make our notations compact. Thus, the state ($\varphi_1 = 0$, $\varphi_{2,3} = \kappa$, $\varphi_{4,5} = -\kappa$) corresponds to $(0 + + - -)$. There are 30 different states[6]: we need to choose an island with $z = 1$ (five alternatives) and then choose two islands with $z = -\frac{1}{4} + \frac{\sqrt{15}}{4}$ (6 alternatives). The states can be obtained from each other by different symmetry transformations and form a basis of the 30-dimensional Hilbert space.

We can use the general methods of the group representation theory to describe how quantum tunneling makes these 30 degenerate quasiclassical states split. Let's consider the representation of the pentagram symmetry group in the 30-dimensional Hilbert space spanned by these states. The corresponding characters of the group elements are given in the following table:

n_P	1	10	15	20	20	30	24
P	1^5	$(2,1^3)$	$(2^2,1)$	$(3,1^2)$	$(3,2)$	$(4,1)$	(5)
χ	30	6	2	0	0	0	0

Here we use the following conventional notations: P denotes a permutation that consists of a few cycles of the given lengths $n_1, n_2, n_3, ...$ (for example, $(2,1^3)$ is a permutation that exchanges any two islands and does not move the others) and n_P is the number of such permutations. To calculate the characters χ of our 30-dimensional representation, we notice that the matrix element $\langle\psi|P|\psi\rangle$, where $|\psi\rangle$ is one of the basis states, is not equal to zero only if the state $|\psi\rangle$ is invariant under P. For a permutation of the type $(2,1^3)$ the invariant states are those in which the phases that are exchanged both correspond to z_+ (or z_-). One of the remaining three phases corresponds to z_0 and the other two correspond to z_- (or z_+). The total number of such states (and, therefore, the character of this group element) is 6 (as shown in the table). For a permutation of the type $(2^2,1)$ there are only two invariant states: the first two phases that are exchanged correspond to either

[6]In each state one of the phases is zero, two of the phases are $+\kappa$, and the other two phases are $-\kappa$. However, it is important to remember that two states correspond to the same physical state if all five phases are shifted by the same amount. For example, the states (0, $2\pi - 2\kappa$, $2\pi - 2\kappa$, 0, $-\kappa$) and (κ, $2\pi - \kappa$, $2\pi - \kappa$, κ, 0) are equivalent because they both correspond to $(+ - - + 0)$.

$z = -\frac{1}{4} + \frac{\sqrt{15}}{4}$ or $z = -\frac{1}{4} - \frac{\sqrt{15}}{4}$. Using the characters of the irreducible representations of S_5, one can find that our 30-dimensional representation is a product of the following irreducible representations:

$$30 = 1 \oplus 4 \oplus 4 \oplus 5 \oplus 5 \oplus 5_A \oplus 6.$$

This means that if quantum fluctuations are taken into account, the 30-fold degenerate quasiclassical ground state splits into one non-degenerate, two four-fold degenerate, three five-fold degenerate, and one six-fold degenerate states.

For the system to be a promising candidate for a qubit, the ground state should be highly degenerate. Thus, our next goal is to find the leading-order quantum processes that determine the energies of our 30 states and, therefore, conditions under which the ground state is degenerate. The tunneling amplitudes between quasiclassical minima depend exponentially on E_J/E_c: $t \propto \exp[-c(E_J/E_c)^{1/4}]$ (similar to what we had for the tetrahedron). The numerical coefficient c in this formula depends on the distance between the states[7]. Because of the exponent the only important quantum processes are those connecting the nearest states, so that we will deal only with them. Of course, the set of tunneling processes that we consider should be invariant under the full group of symmetry transformations.

Let's now discuss the structure of the phase space and find the nearest neighbors of a given state. Consider the classical state $A = \{0, 2\pi - 2\kappa, 2\pi - 2\kappa, 0, -\kappa\}$ which is equivalent (after overall shift by κ) to the state $(+--+0)$. The four states closest to it in the phase space (see Fig.4.3) are

$$(+--+0) \rightarrow \begin{array}{l} \{0, 2\kappa, 2\kappa, \kappa, 0\} = (-++0-) \\ \{0, 2\kappa, \kappa, 0, 2\kappa\} = (-+0-+) \\ \{0, \kappa, 2\kappa, 0, 2\kappa\} = (-0+-+) \\ \{0, \kappa, \kappa, -\kappa, -\kappa\} = (0++--) \end{array}$$

Using the short-hand notations introduced above, these transitions can be described by the following recipe: *Swap zero and one of the pluses (or minuses) and then change all*

[7]The distance is defined as the action $S = \int \mathcal{L}dt$ corresponding to the quasiclassical path in the phase space.

signs. For example, we have for the first transition:

$$(+--+0) \Rightarrow (+--0+) \Rightarrow (-++0-).$$

As a result, the phases φ_1, φ_2 change from $2\pi - 2\kappa, 2\pi - 2\kappa$ to $(2\kappa, 2\kappa)$, while the phases φ_3, φ_4 increase by κ.

These transitions impose a peculiar structure in the space of the 30 states: direct inspection shows that the shortest cycles consist of five or six transitions, i.e. these states form a graph with the branching number exactly equal to 4 and with loops having periods of 5 or 6. An example of a 6-cycle is provided by the following chain of transitions:

$$(0++--) \to (-0-++) \to (++0--) \to$$
$$(0--++) \to (+0+--) \to (--0++) \to (0++--)$$

An example of a 5-cycle is given by

$$(0++--) \to (-0-++) \to (+-+0-) \to$$
$$(-+0-+) \to (+---+0) \to (0++--)$$

The tunneling amplitudes t of all these transitions should be identical due to the symmetry constraints imposed by the permutation group. In order to find the resulting energy spectra, we need to compute the eigenvalues of the tunneling matrix. The numerical diagonalization of this matrix gives the following spectrum:

$$E = -t \begin{pmatrix} 4^{(1)} \\ 2^{(11)} \\ 0^{(5)} \\ -1^{(4)} \\ -2^{(5)} \\ -3^{(4)} \end{pmatrix}.$$

Here the upper subscript shows the degeneracy of each level. Thus, if the sign of t is negative, the ground state is four-fold degenerate. Note that the spectrum is not symmetric

due to the presence of odd cycles. Also, the eleven-fold degeneracy of the fifth level is coincidental: if we take into account smaller transition amplitudes, the level splits into 5- and 6-fold degenerate states. Apart from this coincidence, the spectrum is exactly what we expected to find from the general symmetry arguments.

The sign of the transition amplitude t depends on the charges induced on the islands by the control gates. To evaluate t, it is convenient to use the gauge that does not violate the symmetry of the pentagram. Physically, this means that the total charge of the whole system is fixed and the charges of the five islands are equal. We expect that in this case the tunneling amplitudes of all transitions are identical. Let's consider the transition we discussed earlier:

$$(+--+0) \to (-++0-)$$

The shortest path between the states (in the phase space) is given by

$$\delta\varphi = \{2\pi - 2\kappa, 2\kappa - 2\pi, 2\kappa - 2\pi, -\kappa, -\kappa\}$$

Each of these transitions results in Berry's phase

$$\exp\left(\sum_j iQ\delta\varphi_j\right),$$

where Q is the charge of each island (in terms of $2e$). The total charge of an isolated system must be an integer number n. This means that the charge of each island is $n/5$, so that the full amplitude of the transition is $t \propto \exp(-\frac{2\pi i n}{5})$. Appropriately choosing n, we can make the real part of t negative and its imaginary part small. As a result, the ground state of the pentagram will be four-fold degenerate. Note that the complex value of t implies that the states can be partitioned into two groups. Alternatively, one should be able to assign arrows to all transitions. This classification should be compatible with the global symmetry group.

In order to check the above conclusions, we numerically diagonalize the Hamiltonian

$$H = \sum_{i=1}^{4} n_i^2 + \left(\sum_{i=1}^{4} n_i\right)^2 + \frac{E_J}{2}\left(\sum_{i,j} b_i^\dagger b_j + \sum_i \left(b_i^\dagger + b_i\right)\right),$$

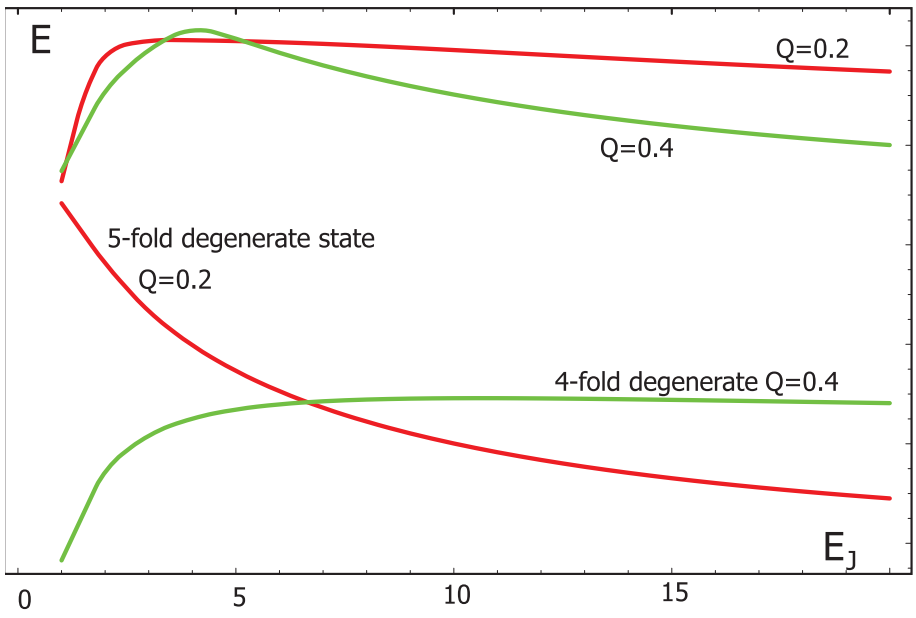

Figure 4.4: The gaps between the ground state and first two excited energy levels of the pentagram as functions of E_J. The red lines correspond to the bias charge $Q = 0.2$, the 4-fold degenerate ground state, and the 5-fold degenerate first excited state, while the green lines correspond to the bias charge $Q = 0.4$, the 5-fold degenerate ground state, and the 4-fold degenerate first excited state.

where $n_i = b_i^\dagger b_i - Q$ and the values of n_i are restricted and belong to the interval $(-K, K)$, while Q is the charge bias. We choose the charging energy coefficient to be 1. This corresponds to the charging energy of the individual junctions $E_C = 5/4$. The system is equivalent to the closed pentagram if $Q = n/5$, where n is an integer. The numerical results shown in Fig. 4.4 indicate that in this case the ground state degeneracy coincides with the one we get from the symmetry arguments. One can also check that for other values of Q (for example, $Q = 0.5$) the ground state degeneracy is lower.

In more detail, the results of the numerical diagonalization are the following. The ground state is a quadruplet for $Q = 1/5$ and a quintuplet for $Q = 2/5$. In both cases, the gap between the ground state and the next energy level changes slowly. In Fig. 4.4, we show the gap as a function of E_J. The red lines correspond to the bias charge $Q = 0.2$, the 4-fold degenerate ground state, and the 5-fold degenerate first excited state, while the green lines correspond to the bias charge $Q = 0.4$, the 5-fold degenerate ground state, and the 4-fold degenerate first excited state.

We can conclude that the Josephson junction circuit that contains five superconducting islands connected as shown in Fig. 4.2 displays high degeneracy of the ground state (depending on the gate potential, it is 4- or 5-fold degenerate). All decay processes in this system are naturally eliminated. Therefore, one can expect that the system will display very long decay times. Unfortunately, effects of the low frequency noises on its energy levels are probably strong: there are not any symmetry reasons why the matrix elements of the noise should be small. To suppress the noises, one needs to add a few additional superconducting islands and Josephson junctions to the system. This makes it too complicated. In this respect, the situation is similar to the one realized in a simple chain of three junctions frustrated by the flux $\Phi_0/2$. If the charge bias is $Q = n/3$, the ground state level is degenerate. However, this degeneracy is destroyed by perturbations even in the linear order.

4.1.2 The Star of David

To achieve protection, we should find an array whose symmetry group contains many more elements than it is needed for degeneracy, so that a local perturbation that violates some symmetries of the group does not destroy the degeneracy completely. One can formulate a criterion more precisely. Degenerate levels of a qubit correspond to irreducible representations of the symmetry group. A local perturbation makes one or more islands or junctions different from the others, destroying some part of the symmetry. The action of the remaining subgroup of the full symmetry group on the degenerate ground state of the qubit generates a representation of this subgroup. If this representation is irreducible, then the ground state remains degenerate and the qubit is protected.

It is a non-trivial task to design a circuit that satisfy the requirement outlined above. In this subsection we show that it can be resolved for a pentagram-like circuit: we should build a system whose symmetry is the permutation group S_6. Physically, such a circuit can be implemented in the form of the Star of David shown in Fig. 4.5.

A uniform magnetic field corresponding to the total flux $3\Phi_0$ is applied to the star. Some links should be deformed to guarantee that the fluxes through all the basic triangles (those

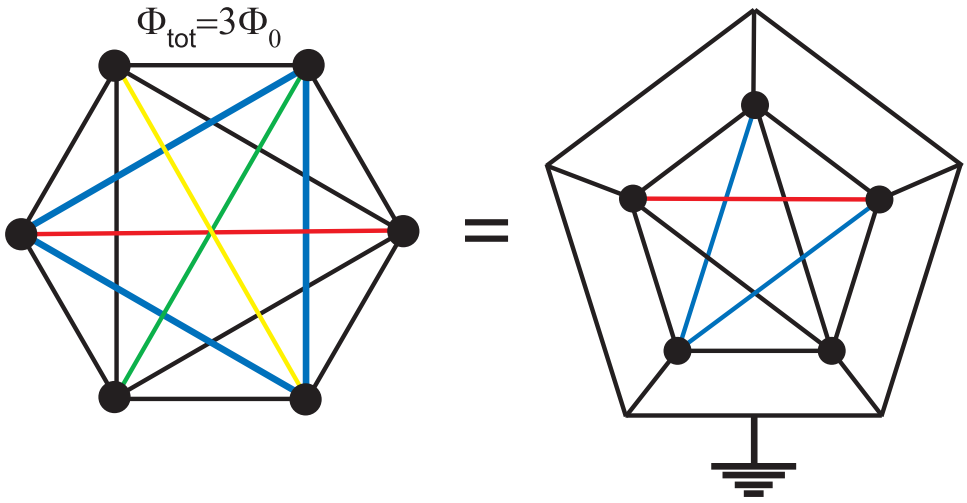

Figure 4.5: The Josephson junction circuit whose symmetry is the permutation group S_6. The circles represent superconducting islands. The lines represent Josephson junctions connecting the islands. Different colors represent different layers, so that if two lines intersect, they do not contact with each other. The left-hand diagram shows the star itself. The right-hand diagram shows an equivalent circuit in which one island is implemented as the ground.

formed by any three islands) are equal to either $\Phi_0/2$ or $3\Phi_0/2$ (it would be enough to deform only the red, yellow and green links). These fluxes can be described by a gauge field that induces an additional phase $a = \frac{2e}{c}\int Adl = \pi$ across all the junctions. As a result, the nodes of the star effectively interact with each other. The interaction is antiferromagnetic.

We will assume that this system is in the quasiclassical regime, that is, $E_J \gg E_C$. Exactly as it was for the tetrahedron and the pentagram, quantum fluctuations select the states for which the effective potential V_{eff} is minimal[8], while quantum transitions between the minima split the degenerate ground state.

If the star is in one of the minima realized in the quasiclassical regime, then three superconducting islands have phases 0 and the other three islands have phases π. In total, there are 20 such states. However, the states that can be obtained from each other by simultaneous shift of all phases by π are physically identical, so that one can write down

[8]The fluctuations are strongest if all the spins $z_j = \exp(i\phi_j)$ are collinear because in this case the complex equation $\sum_j z_j = 0$ reduces to two simple conditions: the linear equation $\sum \delta\phi_i = 0$ and the quadratic equation $\sum \pm\delta\phi_i^2 = 0$, while in the generic case of non-collinear spins we receive two linear equations for the phase deviations.

the following ten minima (0 corresponds to 0 and 1 corresponds to π):

$$
\begin{array}{ll}
1 & (111000) \leftrightarrow (000111) \\
2 & (110100) \leftrightarrow (001011) \\
3 & (110010) \leftrightarrow (001101) \\
4 & (110001) \leftrightarrow (001110) \\
5 & (101100) \leftrightarrow (010011) \\
6 & (101010) \leftrightarrow (010101) \\
7 & (101001) \leftrightarrow (010110) \\
8 & (100110) \leftrightarrow (011001) \\
9 & (100101) \leftrightarrow (011010) \\
10 & (100011) \leftrightarrow (011100)
\end{array}
$$

The amplitudes of transitions between these states are invariant under the symmetry transformations. In particular, they should be equal for all processes in which two phases 0 and π swap. Such processes transform a basis state either to another basis state (for instance, $(111000) \rightarrow (110100)$) or to a state that is physically equivalent to another basis state (for instance, $(111000) \rightarrow (011100) \leftrightarrow (100011)$). For each basis state there exist six transformations of the first type and three transformations of the second type. In general case, their amplitudes might be different because simultaneous shift of all the six phases by π results in Berry's phase $e^{i\pi n}$, where n is the total charge (in terms of $2e$) induced in the circuit by

control gates. For odd values of n we have the following Hamiltonian:

$$H = -t \begin{pmatrix} 0 & 1 & 1 & 1 & 1 & 1 & 1 & -1 & -1 & -1 \\ 1 & 0 & 1 & 1 & 1 & -1 & -1 & 1 & 1 & -1 \\ 1 & 1 & 0 & 1 & -1 & 1 & -1 & 1 & -1 & 1 \\ 1 & 1 & 1 & 0 & -1 & -1 & 1 & -1 & 1 & 1 \\ 1 & 1 & -1 & -1 & 0 & 1 & 1 & 1 & 1 & -1 \\ 1 & -1 & 1 & -1 & 1 & 0 & 1 & 1 & -1 & 1 \\ 1 & -1 & -1 & 1 & 1 & 1 & 0 & -1 & 1 & 1 \\ -1 & 1 & 1 & -1 & 1 & 1 & -1 & 0 & 1 & 1 \\ -1 & 1 & -1 & 1 & 1 & -1 & 1 & 1 & 0 & 1 \\ -1 & -1 & 1 & 1 & -1 & 1 & 1 & 1 & 1 & 0 \end{pmatrix}.$$

Diagonalizing it, we get two quintuplets $E = \pm 3t$. They form a basis of two different irreducible representations of the permutation group S_6.

If one of the elements of the star (an island or a junction) is different from the others, the symmetry S_6 reduces to S_5. In this case, one of the 5-dimensional representations of S_6 reduces to a product $4 \otimes 1$ (where the four-dimensional and one-dimensional representations of S_5 are irreducible), while the other 5-dimensional representation of S_6 becomes an irreducible representation of S_5. Physically, this means that one of the quintuplets splits into a quadruplet and a singlet, while the other one is stable under local perturbations. If the second quintuplet is the ground state, then the quantum bit is protected.

In conclusion, we have shown that symmetric Josephson junction arrays that consist of a small number ($N \leq 6$) of identical superconducting islands possess many remarkable properties. In particular, their ground state can be highly degenerate and stable with respect to perturbations that violate the symmetry of the circuit. Unfortunately, both designs we studied require a large number of identical Josephson junctions connecting the islands. Therefore, experimental realization of these symmetric arrays is a non-trivial task.

4.2 Systems less sensitive to induced charges

4.2.1 Pseudoinductors

The main problem of the highly symmetric qubits discussed in this thesis is that one needs to adjust the charges of superconducting islands which are not ideal because of different noises and impurities. This can be done by applying proper electrostatic potentials to the islands. We mentioned in the previous chapters that the distribution of the charges induced by control gates should have a symmetry that is compatible with the symmetry of the whole system. For example, implementation of the tetrahedron in which one of the islands is connected to the ground requires three control gates. They should induce charges $n/4$ (in terms of $2e$) on each non-grounded island. Only in this case the resulting symmetry is tetrahedral. Any other distribution of the induced charges breaks the symmetry of the system. In particular, it breaks the symmetry between the grounded island and the other three islands.

Similarly, the more symmetric qubit with four (or five) non-grounded islands requires four (or five) control gates. The gates should induce charges $n/5$ (or $n/6$) on each non-grounded island, because only in this case the symmetry of the system given by the permutation group S_5 (or S_6) does not break. Since it is very difficult to tune the gate potentials so precisely, producing such a symmetric charge distribution seems to be a very non-trivial task.

In this section we will discuss an alternative approach that might be used to design different highly symmetric systems that are not sensitive to the charge noise. The main idea of this new approach is replacing all the Josephson junctions in Fig. 4.1, 4.2, 4.5 by pseudoinductors whose Josephson energy is a periodic function of the phase difference ϕ:

$$\varepsilon(\varphi) = \frac{1}{2} E_L(\varphi - 2\pi n)^2. \tag{4.2.7}$$

Here n is an integer (see Fig. 4.6). Different n correspond to different branches of the Josephson energy. Such pseudoinductors are characterized by very small (but non-zero!) amplitudes of transitions between the branches corresponding to different n. We will use

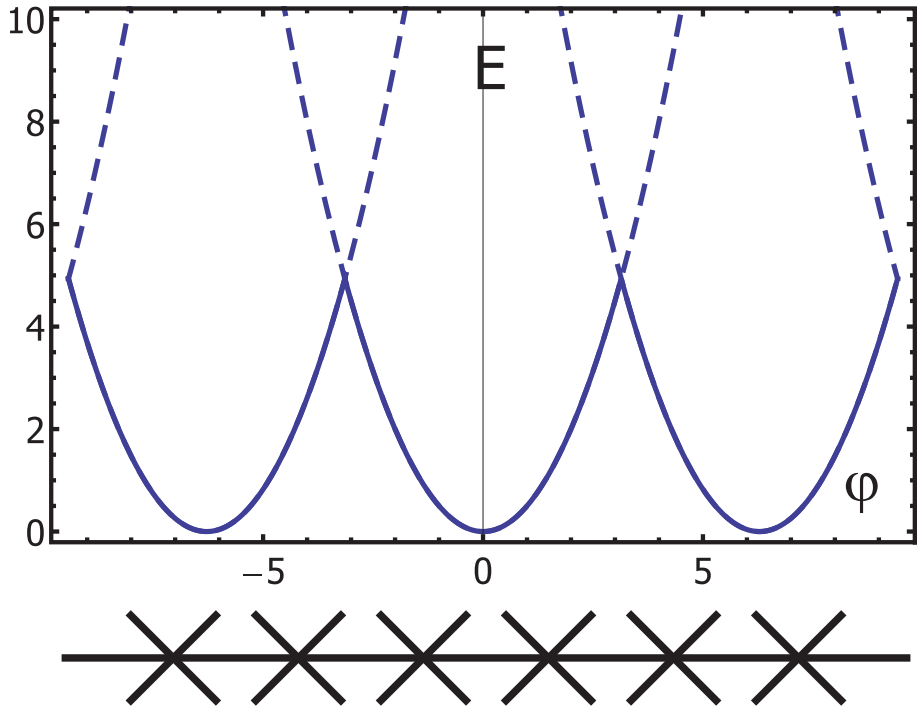

Figure 4.6: The Josephson energy of a pseudoinductor, for which the amplitudes of transitions between different branches are small (but non-zero). Such a pseudoinductor can be implemented as a long chain of large Josephson junctions.

the notation $\tilde{t}$ for these amplitudes and discuss the lower bounds on their magnitude later in this subsection.

A pseudoinductor can be implemented as a very thin superconducting wire with large kinetic inductance or as a long chain of N large Josephson junctions (see Fig.4.6). Such a chain is characterized by the effective Josephson energy $E_L = E_J/N$, where E_J is the Josephson energy of each junction. The amplitude of transitions between different branches is exponentially small if $E_J/E_c^{(J)} \gg 1$ [78, 79]:

$$\tilde{t} = \left(\frac{16}{\sqrt{\pi}}\sqrt[4]{\frac{E_J}{2E_c^{(J)}}}\right)\sqrt{E_J E_c^{(J)}}N\exp\left(-\sqrt{\frac{8E_J}{E_c^{(J)}}}\right)$$

We show below that the optimal regime of the whole circuit is realized when the parameters characterizing the pseudoinductor satisfy the condition $E_L/E_c \gtrsim 1$. When the phase difference across the pseudoinductor changes by $O(\pi)$, the phase difference across each junction changes by a small amount $O(\pi/N)$. This allows us to use the Gaussian approximation. In this approximation, the phase difference across the pseudoinductor is

described by the same classical equation of motion as the phase differences across the individual junctions and is characterized by the same plasma frequency $\omega_p = \sqrt{8E_J E_c^{(J)}}$ as the individual junctions. Thus, the effective charging energy of the pseudoinductor is given by $E_c = NE_c^{(J)}$. In terms of the parameters characterizing the pseudoinductor, the tunneling amplitude is

$$\tilde{t} = \left(\frac{4\sqrt{2N}}{\sqrt{\pi}} \sqrt[4]{\frac{E_L}{2E_c}} \right) N\omega_p \exp\left(-N\sqrt{\frac{8E_L}{E_c}} \right) \tag{4.2.8}$$

For reasonable values of the ratio $E_L/E_c \sim 2$, the formula (4.2.8) implies that the tunneling amplitude has the order of $\tilde{t} \sim 10^{-9}\omega_p$ for chains that contain six individual junctions and $\tilde{t} \sim 10^{-5}\omega_p$ for chains that contain four individual junctions.

In the limit of small tunneling amplitudes, effects of the charges on the energy spectrum of a Josephson device can be estimated using quasiclassical arguments. Since the charge of an island is a conjugate to the phase of this island, in the regime when $E_J \gg E_c$, the dynamics of the circuit can depend on the charge only because of Berry's phase in the action:

$$L_{Berry} = i\dot{\varphi}q,$$

where q is measured in terms of $2e$. The only effect of the charge is due to the process in which the phase of the island changes by 2π and the physical state does not change. This is possible in a circuit that consists of pseudoinductors only if the phase differences across *all* the links connected to the island change by 2π. The amplitude of the phase rotation in the case when there is only one pseudoinductor is equal to $\tilde{t}$. Simultaneous rotation of phases across $n-1$ pseudoinductors connected to the island is a higher order process. Assuming that the energies of all intermediate states are of the same order $\sim E_L$, we can estimate the energy splitting of the degenerate quasiclassical ground state caused by the charge noise:

$$\Delta E \sim \left(\frac{\tilde{t}}{E_L} \right)^{n-1} \tilde{t}.$$

Thus, we expect that if the tunneling amplitude $\tilde{t}$ is smaller than the inductive energy ε_L, effects of random charges of islands on a single quantum phase rotation process quickly become insignificant as the symmetry of the system increases.

The discussion above assumes that the energies of all intermediate states in which the system finds itself in the process of phase rotation have the same order of magnitude ($\sim E_L$). Therefore, these intermediate states are not classically allowed. We will return to this important question below.

4.2.2 Highly symmetric systems made of pseudoinductors

In this section we discuss the most important properties of symmetric qubits made of pseudoinductors. The pseudounductors are characterized by the effective Josephson energy (4.2.7) and small transition amplitude $\tilde{t}$. In the quasiclassical approximation $E_L/E_c \gg 1$, we should find the minima of the inductive energy

$$V = \frac{1}{4}\sum_{i,j} E_L(\varphi_i - \varphi_j - a_{ij})^2, \tag{4.2.9}$$

where a_{ij} are the phase differences induced by external magnetic fields. As we discussed before, the symmetry of the magnetic fields (and, therefore, the symmetry of the corresponding fluxes) should not be lower than the symmetry of a quantum bit. In addition, the flux through any closed surface should be a multiple of 2π. Only two sets of parameters a_{ij} satisfy these two conditions. The first set corresponds to $a_{ij} = 0$ across all links, while all a_{ij} from the second set are equal to π. The first case is trivial, because it leads to the quasiclassical minimum $\phi_j = 0$ on all islands[9], and, therefore, is not interesting.

We will assume below that $a_{ij} = \pi$ across all links. Physically, this means that all the magnetic fluxes through basic triangles are equal to $\Phi_0/2$. Minimizing the Josephson energy of the tetrahedron, the pentagram, and the star of David, we find that in all these cases the quasiclassical minima are given by

$$\varphi_k = 2\pi(i[k]/n),\ k = 0, \ldots, n-1,$$

where $i[k]$ is an arbitrary permutation of the indices $(0, \ldots, n-1)$. Similarly, for the systems, in which one island is grounded, the quasiclassical minima are given by

$$\varphi_k = 2\pi(i[k]/n),\ k = 1, \ldots, n-1,$$

[9]We would get the same result for symmetric circuits with usual Josephson junctions.

where $i[k]$ is an arbitrary permutation of the indices $(1, \ldots, n-1)$. The space spanned by these quasiclassical states forms $(n-1)!$-dimensional representation of the symmetry group. The corresponding energy level is $(n-1)!$-fold degenerate[10].

Quantum tunneling destroys this classical degeneracy (similar to the case of the Josephson junction devices discussed in the previous sections): the leading-order process swaps the phases φ_i and φ_j of the islands $\{i, j\}$. Furthermore, in the quasiclassical approximation $E_L/E_c \gg 1$ which we consider here, the amplitude of such a process depends exponentially on the phase difference between the swapped phases $\delta\varphi = \varphi_i - \varphi_j$. This allows us to focus on the leading process that corresponds to a swap of the phases characterized by the smallest possible phase difference $\delta\varphi = \varphi_i - \varphi_j = 2\pi/n$. This process changes the sign of the phase difference between phases on these two islands whereas all other phase differences retain their signs. This means that the inductive energy $\varepsilon(\varphi_k - \varphi_l - \pi)$ changes its branch only for the pair i,j in which the phases are swapped. This leading-order quantum process involves only one tunneling, so that its amplitude t is approximately equal to the tunneling amplitude $\tilde{t}$:

$$t \sim \tilde{t}.$$

Ignoring other quantum processes for which two or more phase differences change their sign or a given phase difference changes by more than $2\pi/n$, we get a Hamiltonian in the quasiclassical approximation. For example, in the case of the tetrahedron and one grounded island (whose phase is 0), the classical minima are described by the phases $\varphi = k\pi/2$, $k = 1, 2, 3$ of the three non-grounded islands. We denote these states by $|123\rangle, |213\rangle, |132\rangle, |231\rangle, |312\rangle, |321\rangle$ and consider them as a basis of the Hilbert space.

[10] For the star of David, the level is 120-fold degenerate!

In this basis the Hamiltonian has the explicit form

$$H = -t \begin{pmatrix} 0 & 1 & 1 & 1 & 1 & 0 \\ 1 & 0 & 1 & 1 & 0 & 1 \\ 1 & 1 & 0 & 0 & 1 & 1 \\ 1 & 1 & 0 & 0 & 1 & 1 \\ 1 & 0 & 1 & 1 & 0 & 1 \\ 0 & 1 & 1 & 1 & 1 & 0 \end{pmatrix}.$$

Its diagonalization determines the lower energy levels of the tetrahedron:

$$E_4 = t \begin{pmatrix} 2^{(2)} \\ 0^{(3)} \\ -4 \end{pmatrix}, \tag{4.2.10}$$

where the upper subscript shows the degeneracy of the corresponding level.

Note that the spectrum is not symmetric. This means that the spectrum depends on the sign of the tunneling amplitude which is in turn depends on the charges of the islands. To understand this result, note that each tunneling process changes the phase difference across one of the links by π. It follows from here that cycles such as

$$|123\rangle \to |213\rangle \to |312\rangle \to |123\rangle \tag{4.2.11}$$

are possible. Note that in the symmetric gauge the last transition shifts the phases of *all* islands by $\pi/2$: $|312\rangle = |0312\rangle \to |3012\rangle \overset{+\pi/2}{=} |0123\rangle$. Thus, it acquires Berry's phase $e^{\pi i Q/2}$ that depends on the charge. In the case of the three island circuit with a ground wire, the process (4.2.11) changes the superconducting phase of the first island by 2π and results in Berry's phase $e^{2\pi i q_1}$, where q_1 is the charge induced on this island. These phases coincide in the case of the symmetric system with $q_1 = Q/4$.

We can say that in the case of the tetrahedron, the cycles described in the previous section are sensitive to the charges of the islands, so that the charge noise is not completely eliminated.

We now turn to the higher symmetry devices. Repeating what we have just done for the tetrahedron, we get the spectrum of the pentagram:

$$E_5 = t \begin{pmatrix} 5^{(1)} \\ \sqrt{5}^{(6)} \\ 1^{(5)} \\ -1^{(5)} \\ -\sqrt{5}^{(6)} \\ -5^{(1)} \end{pmatrix}, \tag{4.2.12}$$

which is obviously symmetric. This indicates that the spectrum does not depend on the sign of the tunneling amplitude. This can be better understood if we note that the sequence of tunneling processes that forms a closed cycle similar to (4.2.11):

$$|1234\rangle \to |2134\rangle \to |3124\rangle \to |1234\rangle \tag{4.2.13}$$

contains an even number of tunnelings, so that only even powers of the amplitude are present. Similar to (4.2.11), in the symmetric gauge the last process in this sequence shifts the phases of all the islands by $2\pi/5$. This induces Berry's phase $e^{2\pi i Q/5}$, where Q is the total induced charge of all the islands. In the four-island configuration the loop (4.2.13) can be thought of as vortex motion around the first island that induces Berry's phase $e^{2\pi i q_1}$. The two phases coincide in the case of the symmetric system with $q_1 = Q/5$.

Finally, we consider the star of David. The energy levels are given by

$$E_6 = t \begin{pmatrix} (1+\sqrt{13})^{(5)} \\ 4^{(9)} \\ 2^{(25)} \\ (-1+\sqrt{5})^{(9)} \\ 0^{(15)} \\ -1^{(32)} \\ (1-\sqrt{13})^{(5)} \\ (-1-\sqrt{5})^{(9)} \\ -4^{(10)} \\ -6^{(1)} \end{pmatrix} \tag{4.2.14}$$

Similar to the case of the tetrahedron, the energy spectrum is not symmetric relative to the sign of t. This asymmetry can be explained by odd-cycles responsible for flips of the phase of individual islands. Berry's phase obtained as a result of a simple process in which a vortex goes around an individual island is again $e^{2\pi iq}$, where q is the charge of this island induced by impurities and control gates.

The most interesting situation is realized when the transition amplitude is negative and the lowest energy level is five-fold degenerate. The representation of S_6 corresponding to this level is an irreducible representation of S_5, so that the quantum bit is protected from all local external noises.

Thus, we conclude that symmetric quantum bits in which regular Josephson junctions are replaced by pseudoinductors have very interesting properties. In particular, their ground state is degenerate and protected (in the lowest order) from local noises. Unfortunately, circuits of this type remain sensitive to charges induced by control gates. This is a serious implementation problem and requires further investigation.

Chapter 5

Conclusion

In this thesis we have positively answered the first question stated in Section 1.3: can we improve the noise characteristics of the tetrahedral quantum bit proposed in [74]?

We have studied a small Josephson junction device whose ground state is twofold degenerate and which is well protected from different noises. This device contains twelve identical Josephson junctions and is a modified version of the simple six-junction quantum bit studied in [74].

We have shown that interactions of this twelve-junction circuit with the charge and magnetic noises destroy the ground-state degeneracy. However, this splitting is very small because the linear coupling is completely absent. The only known source of physical noise that remains linearly coupled to the ground-state doublet is the critical current noise but the corresponding coupling constant is rather small (smaller than it is for the simpler six-junction qubit in [74]). This makes the twelve-junction tetrahedron very attractive as a candidate for a quantum bit with very long decoherence time.

However, our tetrahedron has one very serious drawback. It is a very complicated system from an experimental point of view because modern technologies do not allow to produce many identical Josephson junctions with sufficient accuracy.

In the future we would like to find a simple system in which the linear coupling with all three types of noise (electric potential noise, magnetic noise, and critical current noise) are suppressed. Also, it should contain as few Josephson junctions as possible. This can be done by using arrays whose symmetry group is different from the tetrahedron symmetry group T_d. In fact, existence of other nonabelian arrays whose ground state is twofold degenerate is an open question. Even though almost all symmetry groups do have multi-dimensional

irreducible representations, only a few of them have two-dimensional ones.

We have studied some highly symmetric Josephson junction circuits and shown that they have many very interesting properties. In particular, their ground state can be manifold degenerate and stable with respect to perturbations violating the symmetry. Unfortunately, experimental implementation of these highly symmetric systems requires a large number of identical Josephson junctions and, therefore, is not a trivial task.

In this thesis we have also proposed an experimental method that can facilitate answering the second question stated in Section 1.3: is it possible to make any of the proposed nonabelian quantum bits from an experimental point of view? Our method can be used for initial characterization of Josephson junction quantum bits by measuring their spectrums and decoherence times. We have also addressed the questions of readout and quantum manipulations.

We focused on a simple pyramidal array to demonstrate the main ideas of our method. However, it can be easily generalized and used for studying spectrums of any reasonable Josephson junction arrays.

Appendix A

The RSA algorithm

The algorithm RSA which is one of the best known algorithms for data encryption was invented by R.Rivest, A.Shamir, and L.Adleman in 1977 and, therefore, is named after them [80]. The idea that underlies the algorithm is very simple [81]. It is based on the mathematical properties of prime numbers. We will describe the RSA algorithm in the general case and then give a numerical example.

Imagine that we have two prime numbers p and q. In practice, these numbers should be very large. We calculate the number $n = pq$ and the so-called totient function $\phi(n)$ which is defined as the number of positive integers less than or equal to n and comprime to n. It can be easily shown that in our case,

$$\phi(n) = (p-1)(q-1).$$

The next step is to find an integer e that satisfies two conditions: (i) $e > 1$; (ii) the largest common divisor of the cotient $\phi(n)$ and e is equal to 1. The number e is called the *public key exponent*[1].

We will also need the *private key exponent* d which is defined as

$$de = k\phi(n) + 1,$$

where k is an integer.

The *public key* consists of the modulus n and the public exponent e. It can be known to the general public. The *private key* consists of the modulus and the private exponent d. It should be kept in secret.

---

[1] A popular choice for the public exponent is $e = 2^{16} + 1 = 65537$

Imagine now that we have a text symbol m that must be encrypted. To do this, we compute:

$$c = m^e \mod n.$$

We should use the symbol c in our conversations.

We can decrypt the symbol c if the private key d is known:

$$m = c^d \mod n.$$

We see that the larger the numbers p and q, the more difficult to decipher our code for an outsider.

To understand the RSA algorithm better, we consider one numerical example. We choose the prime numbers p and q to be $p = 83$ and $q = 47$. As a result, we find $n = pq = 3901$ and $\phi(n) = (p-1)(q-1) = 3772$. We set the public key exponent: $e = 19$. The private key exponent is given by

$$de = 17 * 3772 + 1 = 19 * 3775,$$

so that, $d = 3775$.

The encryption function is

$$c = m^e \mod n = m^{19} \mod 3901,$$

while the decryption function is

$$m = c^d \mod n = c^{3775} \mod 3901.$$

Appendix B

Shor's algorithm

Shor's algorithm is an algorithm for factoring large numbers on a quantum computer. It was invented by Peter Shor in 1994 [10]. In 2001, Shor's algorithm was successfully implemented by a research group from IBM [19, 38]. Using 7 quantum bits, they could factor the number 15 into 3 and 5.

While it has not been proven that factoring large numbers cannot be achieved on a classical computer in polynomial time, one of the fastest known algorithms for factoring a large number N (whose representation has $\lceil \log N \rceil$ bits) requires $O\left(e^{c(\log N)^{1/3} * (\log\log N)^{2/3}}\right)$ basic operations, or time that is exponentially large in N (see Appendix A). In contrast, Shor's algorithm requires $O\left((\log N)^2 * \log\log N\right)$ basic operations on a quantum computer, and then must perform $O(\log N)$ steps of post processing on a classical computer. Overall then this time is polynomial. Of course, one quantum basic operation can be much slower than one classical basic operation. However, if we speak about very large numbers N, the quantum computer seems to be much more efficient.[1]

It is generally accepted to separate classical and quantum parts of Shor's algorithm. The classical part can be implemented on a classical computer. What is really important and makes the algorithm so efficient is its quantum part.

To describe Shor's algorithm in detail we need to prove a simple lemma.

Lemma. *Let (N, a) be a pair of integer numbers and assume that $a < N$. If r is the period*

[1] Shor's algorithm is not the only useful algorithm that seems to run faster on a quantum computer. Approximately at the same time when Peter Shor invented his algorithm, L.K.Grover developed a quantum algorithm to find an item in an unsorted array of N elements in $O(N^{1/2})$ basic operations [8]. No classical algorithm can guarantee finding the item in less than N operations, even though some of the known classical algorithms can be very efficient for special types of sorted arrays.

of the function

$$f(x) = a^x \mod N \tag{II.1}$$

and r is an even number such that $a^{r/2} \neq -1 \mod N$, then the number N is composite and the factors of N are given by $gcd(a^{r/2} \pm 1, N)$, where $gcd(x, y)$ is the greatest common divisor of x and y.

Proof.

We have ($f(x + r) = f(x)$ since r is the period of $f(x)$)

$$f(0) = 1 \mod N = 1 \qquad \Longrightarrow \qquad f(r) = a^r \mod N = 1.$$

Therefore,

$$a^r - 1 = (a^{r/2} - 1)(a^{r/2} + 1) = 0 \mod N = pN, \tag{II.2}$$

where p is an integer number. The last equation can be satisfied in three cases: (a) N divides $\xi = (a^{r/2} - 1)$ but does not have any nontrivial common factors with $\eta = (a^{r/2} + 1)$; (b) N divides η but does not have any nontrivial common factors with ξ; (c) N has a nontrivial common factor with each of ξ and η.

We consider all these cases. The number N cannot divide ξ because r is the smallest positive integer such that $a^r = 1 \mod N$. Therefore, (a) cannot be true. The case (b) cannot be true either because $a^{r/2} \neq -1 \mod N$.

Imagine now that $gcd(\xi, N) = 1$. In this case, it should be also $gcd(\eta, N) = 1$ as we have shown above. We have

$$k\xi = mN + 1 \qquad \Longrightarrow \qquad k\xi\eta = m\eta N + \eta,$$

where k and m are some integers. We obtain from (II.2):

$$kpN = m\eta N + \eta,$$

that is, the integers N and η must have nontrivial common factors. But $gcd(\eta, N) = 1$ and we get a contradiction. Therefore, the greatest common factor of N and ξ (as well as the greatest common factor of N and η) cannot be equal to 1.

We see that the integers $gcd(\xi, N)$ and $gcd(\eta, N)$ are divisors of N. If they are prime numbers, there is only one factorization of N:

$$N = gcd(a^{r/2} + 1, N) \cdot gcd(a^{r/2} - 1, N).$$

□

We can know describe Shor's algorithm which is based on the lemma. The classical part of the algorithm is very simple. Imagine that we want to factorize the large number N. First, choose a number $a < N$ and calculate the greatest common divisor $gcd(a, N)$[2]. If $gcd(a, N) \neq 1$ then the problem can be reduced to much simpler problem of factorizing the numbers $gcd(a, N)$ and $N/gcd(a, N)$ which can be solved using either Shor's algorithm or any classical algorithm.

If $gcd(a, N) = 1$, we need to compute the period of the function (II.1). If r is an odd number or $a^{r/2} = -1 \mod N$, we have to start from the very beginning and choose another number $a < N$. Otherwise, we use the lemma and obtain the factors of N which are given by $gcd(a^{r/2} \pm 1, N)$.

As one can see, the key step of the classical part is computation of the period r. Classical computers can do this but all known classical algorithms are extremely slow. Shor was the first to realize that quantum computers can help here. The quantum part of Shor's algorithm calculates the period r of the function (II.1).

Imagine that we have two independent systems, with each of them containing $n = \lceil \log_2 N \rceil$ quantum bits. Also imagine that we managed to prepare the initial state $|\psi_0\rangle$ given by

$$|\psi_0\rangle = \left(\frac{1}{\sqrt{N}} \sum_{x=0}^{N-1} |x\rangle \right) \otimes |0\rangle = \frac{1}{\sqrt{N}} \sum_{x=0}^{N-1} |x\rangle \otimes |0\rangle.$$

We apply the quantum function (II.1) to the state $|\psi_0\rangle$:

$$|\psi\rangle = U_f |\psi_0\rangle = (1 \otimes f(x))|\psi_0\rangle = \frac{1}{\sqrt{N}} \sum_{x=0}^{N-1} |x\rangle \otimes |f(x)\rangle$$

[2]The most efficient algorithm for doing this is Euclid's algorithm [81, 82].

The calculation by itself is done. Now we need to extract the information from the quantum computer. This is not so trivial because we destroy the quantum information when we perform our measurement. We have to repeat our calculation and measurement many times and find probabilities of all possible different outputs. Analysis of these probabilities will give us the answer.

Peter Shor have found a way to minimize the number of repetitions[3]. He used the inverse Quantum Fourier Transform:

$$U_{qf}|x\rangle = \frac{1}{\sqrt{N}} \sum_{y=0}^{N-1} e^{2\pi i x y/N} |y\rangle$$

Upon application the unitary transformation U_{qf} to $|\psi\rangle$, we obtain

$$|\psi_{qf}\rangle = (U_{qf} \otimes 1)|\psi\rangle = \frac{1}{N} \sum_{x=0}^{N-1} \sum_{y=0}^{N-1} e^{2\pi i x y/N} |y\rangle \otimes |f(x)\rangle.$$

Now we perform measurements in the basis of $|y\rangle \otimes |f(x)\rangle$ and compute the probabilities of all possible outputs[4]. The probability of obtaining the state $|y_0\rangle \otimes |f(x_0)\rangle$ is equal to

$$P(x_0, y_0) = |\langle y_0 \otimes f(x_0)|\psi_{qf}\rangle|^2 = \frac{1}{N^2} \left| \sum_b e^{2\pi i (x_0 + rb) y_0/N} \right|^2 = \frac{1}{N^2} \left| \sum_b e^{2\pi i r b y_0/N} \right|^2 .$$

Let's find all extremal points of $P(x_0, y_0)$. We have

$$N^2 P(x_0, y_0) = \phi(\alpha) = \sum_b \sum_{b'} e^{2\pi i \alpha (b - b')},$$

---

[3]Generally, Shor's algorithm requires up to 30 repetitions.

[4]We should not forget that the function (II.1) has a period r, so that, for any x,

$$|f(x + r)\rangle = |f(x)\rangle.$$

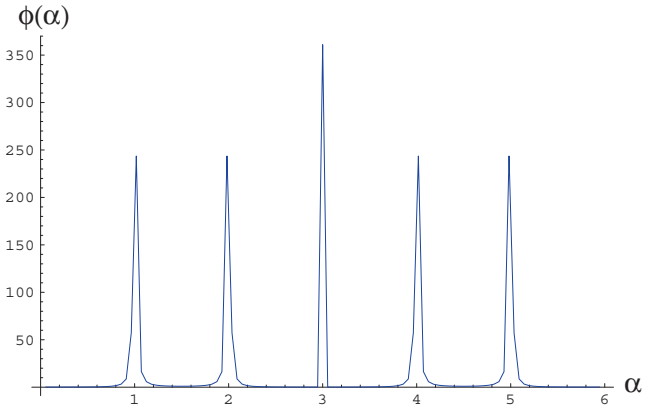

Figure B.1: The dependence $\phi(\alpha)$ in the case where $N = 112$, $a = 17$, $r = 6$. One can see that the probability of the corresponding output is extremely small everywhere except for the points where α is close to an integer.

where $\alpha = y_0 r/N$. The maximum of $\phi(\alpha)$ is observed at the point $\alpha = \alpha_0$ where

$$\begin{aligned} 0 = \frac{d\phi}{d\alpha} &= \sum_b \sum_{b'} 2\pi i (b' - b) e^{2\pi i \alpha (b'-b)} = \\ &= 2\pi i \left[\sum_{b'} b' e^{2\pi i \alpha b'} \sum_b e^{-2\pi i \alpha b} - \sum_b b e^{-2\pi i \alpha b} \sum_{b'} e^{2\pi i \alpha b'} \right] = \\ &= 2\pi i \sum_b b e^{2\pi i \alpha b} \sum_{b'} \left(e^{2\pi i \alpha b'} + e^{-2\pi i \alpha b'} \right) = \\ &= 4\pi i \sum_b b e^{2\pi i \alpha b} \sum_{b'} \cos(2\pi \alpha b') = 0. \end{aligned}$$

This expression can be equal to zero if and only if

$$\sum_b b e^{2\pi i \alpha b} = 2i \sum_{b=1}^{b_{max}} b \sin(2\pi \alpha b) = 0. \tag{II.3}$$

The series converges only if α is an integer. It follows from (II.3) that the probability of obtaining the state $|\psi_{y_0,x_0}\rangle = |y_0\rangle \otimes |f(x_0)\rangle$ is large only if $y_0 r/N$ is very close to some integer value (see Fig. B.1). Therefore, if we repeat our experiment many times, we can assume that the value y_0 that is shown by our measurement in each of these repetitions is almost always corresponds to the case where $\alpha = y_0 r/N$ is an integer (or very close to an integer). Since in each measurement we know y_0 and $f(x_0)$, we can calculate y_0/N and

extract $r = r(\alpha)$ for all possible values of α:

$$r(\alpha) = \frac{\alpha}{y_0/N}, \qquad \alpha = 1, 2, ..., \qquad \alpha \leq \frac{(N-1)^2}{N}.$$

Now for each value $r = r(\alpha)$ we can check if it is really the period of $f(x)$:

$$f(x + r(\alpha)) = f(x). \tag{II.4}$$

If (II.4) is satisfied for some α then the period of the function $f(x)$ is found and we are done. If for any α, (II.4) is not satisfied, we have to repeat our measurement and our calculation with another y_0.

As soon as the period r is known, it can be used in further calculations of the classical part of the algorithm.

Appendix C

Quantum error correction

One of the five most important criteria that any industrial quantum computer must satisfy [13] says that the level of noise affecting quantum bits and logical gates should be low enough (correspondingly, the decoherence time should be long) to make implementation of at least the simplest quantum algorithms possible.

However, it is extremely difficult to build a system that is scalable and whose decoherence time is long. Therefore, another approach has been invented. In 1994, Peter Shor proposed the so-called quantum error correcting code [83].

The main idea used in Shor's quantum error correcting code, redundancy, has been borrowed from the classical theory of computational errors. In this theory, if we have a classical bit that must be protected against accidental errors and a sequence of classical logical gates that must be applied to the bit, we can make a few exact copies of the bit, apply the sequence of the logical gates to each copy and compare the states of all the bits after each operation. If some of them disagree with the majority, we can assume that an error occured and fix the state of the renegades. One can see that we need to have at least three bits to implement this error correction scheme.

Of course, there is a non-zero probability that more than half of the bits flip due to the error. However, this probability is extremely small. The more bits we have, the less probability of missing the error is.

Similarly, Shor notices that if we have a quantum bit that contains some quantum information, we can make a few copies of the quantum bit in the same quantum state[1].

[1]Of course, the so-called no-cloning theorem forbids creation of perfectly identical copies [84, 85]. However, it is still possible to produce imperfect copies [86, 87].

If after a unitary transformation, the quantum states of some of them are different from the quantum states of the majority, we can conclude that these qubits's states have been corrupted and apply suitable one-qubit unitary transformations to fix the errors.

The main problem here is that in the quantum case, we can potentially destroy quantum information if we try to compare the quantum states of the qubits because we have to use some measurement for comparison. Shor's main invention is the so-called syndrome measurement which can determine if a qubit's state has been corrupted but does not tell us anything about the quantum state itself. This measurement does not destroy the quantum information and allows us to fix all errors.

Shor's quantum error correcting code requires at least 9 qubits per one logical qubit for its implementation because in the quantum case there are two different types of errors: flips and phase errors.

However, there exist a few more complicated quantum error correcting codes which use a smaller number of quantum bits. First of all, this is Andrew Steane's error correcting code which requires only 7 qubits [88]. A generalization of Shor's and Steane's concepts are the CSS codes named after A.R.Calderbank, P. Shor, and A.Steane [88, 89, 90]. The CSS codes require at least 5 physical qubits per one logical qubit for their implementation. A more general class of codes (encompassing the former) are the stabilizer codes of Daniel Gottesman [91].

A new very interesting family of error correcting codes was invented in 2006 [92]. It was noticed that the noise in physical qubits is strongly asymmetric: phase errors occur much more frequently than bit flips[2]. One can take an advantage of this asymmetry and implement error correcting codes that require only 2 to 3 physical qubits per one logical qubit.

In practice, each unitary transformation U can differ from the intended transformation

[2]For example, in a typical NMR device $T_1 \sim 10 - 100\ s$, $T_2 \sim 1\ s$ [19]; in superconducting phase qubits $T_1 \sim 10\ \mu s$, $T_2 \sim 100\ ns$ [50]; in superconducting charge qubits $T_1 \sim 100\ ns$, $T_2 \sim 1\ ns$ [40]; in spin dot qubits $T_1 \sim 1\ \mu s$, $T_2 \sim 10\ ns$ [93, 94]

U_0 by some small amount of order ε:

$$U = U_0(1 + O(\varepsilon)).$$

After about $1/\varepsilon$ unitary transformations are applied, these errors accumulate and induce a serious failure. We can avoid the failure using some error correcting code. However, if a sequence of unitary transformations is long enough and the typical magnitude of errors ε is large enough, even error correcting codes will not be able to help. Provided that we have the necessary number of physical qubits per one logical qubit (the number depends on the error correcting code we choose to use), we can correct all errors in quantum computation of arbitrary length as soon as the magnitude of these errors is less than some small predetermined threshold ε [95]. There are different estimates of this threshold [14, 59, 60, 62].

Some of the quantum error correcting codes have been implemented experimentally [96, 97].

In 1997, Alexey Kitaev proposed an idea of the so-called topological quantum codes [98]. Even though the mathematical tools used by Kitaev are rather complicated, his basic ideas can be easily understood from a physical point of view.

Kitaev notices that classical computers do not require any error correction schemes even though they do interact with the environment. It becomes possible due to the remarkable physical properties of magnetic materials that are used to make classical memory. Magnetism exists due to interaction of quantum spins of electrons within a material. The ferromagnetism is defined as the state when the electron spins all point in the same direction. Each spin in a ferromagnetic classical bit interacts with the environment and with the other spins. The latter interaction is much stronger than the interaction with the environment. If one of the spins flips at some moment, the interaction with the other spins immediately makes it flip back. We can say that the classical magnetic bit corrects itself if an error occurs.

A natural question arises: can we make a quantum bit that will correct itself? Kitaev gives a positive answer but emphasizes that the task is rather difficult. He considers a very special Hamiltonian with local interactions and shows that quantum computation can be

implemented if quantum bits are represented by the so-called non-Abelian anyons, that is, excitations of this Hamiltonian which undergo a nontrivial unitary transformation when one excitation moves around the other.

At the present time, we know a variety of two-dimensional physical systems that have such excitations (for example, the fractional Quantum Hall Effect and sheets of graphite[3]).

The anyon approach has been further developed in [75, 99, 100, 101, 102, 103].

[3]It's very easy for electrons in graphite to move within a plane, while jumps between different planes are strongly suppressed.

References

[1] M. Tinkham, *Introduction to Superconductivity*. Dover Publications, Inc., second ed., 2004.

[2] D. Averin and V. Aleshkin *Pisma ZhETF*, vol. 50, p. 331, 1989.

[3] Y. Nakamura, C. Chen, and J. Tsai *Nature (London)*, vol. 398, p. 786, 1999.

[4] Y. Nakamura, C. Chen, and J. Tsai *Phys. Rev. Lett*, vol. 79, p. 2328, 1997.

[5] E. Bibow, P. Lafarge, and L. Lévy *Phys. Rev. Lett.*, vol. 88, p. 017003, 2002.

[6] D. Deutsch and R. Jozsa *Proc. Roy. Soc.*, vol. A439, p. 553, 1992.

[7] M. Nielsen and I. Chuang, *Quantum Computation and Quantum Information*. Cambridge University Press, 2000.

[8] L. Grover *Proceedings, 28th Annual ACM Symposium on the Theory of Computing*, p. 212, 1996.

[9] C. Bennett, E. Bernstein, G. Brassard, and U. Vazirani *SIAM Journal on Computing*, vol. 26(5), pp. 1510–1523, 1997.

[10] P. Shor *SIAM J.Sci.Statist.Comput.*, vol. 26, p. 1484, 1997.

[11] R. Feynman *Internat.J.Theoret.Phys.*, vol. 21, pp. 467–488, 1982.

[12] R. Feynman *Found.Phys.*, vol. 16, pp. 507–531, 1986.

[13] D. DiVincenzo *Fort.Phys.*, vol. 48, pp. 771–783, 2000.

[14] J. Preskill *Proc. R. Soc. London, Ser.A*, vol. 454, p. 385, 1998.

[15] J. Cirac and P. Zoller *Phys. Rev. Lett.*, vol. 74, p. 4091, 1995.

[16] C. Monroe, D. Meekhof, B. King, W. Itano, and D. Wineland *Phys. Rev. Lett.*, vol. 75, p. 4714, 1995.

[17] N. Gershenfeld and I. Chuang *Science*, vol. 275, p. 350, 1997.

[18] M. Steffen, W. van Dam, T. Hogg, G. Breyta, and I. Chuang *Phys.Rev.Lett.*, vol. 90, p. 067903, 2003.

[19] L. Vandersypen, M. Steffen, G. Breyta, C. Yannoni, M. Sherwood, and I. Chuang *Nature*, vol. 414, pp. 883–887, 2001.

[20] Q. Turchette, C. Hood, W. Lange, H. Mabushi, and H. Kimble *Phys. Rev. Lett.*, vol. 75, p. 4710, 1995.

[21] C. Yang, S. Chu, and S. Han *Phys.Rev.A*, vol. 67, p. 042311, 2003.

[22] B. Kane *Nature (London)*, vol. 393, p. 133, 1998.

[23] A. Shnirman and Y. Makhlin *JETP Lett.*, vol. 78, p. 447, 2003.

[24] Y. Makhlin, G. Schon, and A. Shnirman *Nature (London)*, vol. 398, p. 305, 1999.

[25] M. Bocko, A. Herr, and M. Feldman *IEEE Trans. Appl. Supercond.*, vol. 7, p. 3638, 1997.

[26] L. Ioffe, V. Geshkenbein, M. Feigel'man, A. Fauchère, and G. Blatter *Nature (London)*, vol. 398, p. 679, 1999.

[27] J. Mooij, T. Orlando, L. Levitov, L. Tian, C. van der Wal, and S. Lloyd *Science*, vol. 285, p. 1036, 1999.

[28] T. Orlando, J. Mooij, L. Tian, C. van der Wal, L. Levitov, S. Lloyd, and J. Mazo *Phys.Rev.B*, vol. 60, p. 15398, 1999.

[29] Y. Pashkin, T. Yamamoto, O. Astafiev, Y. Nakamura, D. Averin, and J. Tsai *Nature*, vol. 421, p. 823, 2003.

[30] T. Yamamoto, Y. Pashkin, O. Astafiev, D. Nakamura, and J. Tsai *Nature*, vol. 425, p. 944, 2003.

[31] J. Martinis, S. Nam, J. Aumentado, and C. Urbina *Phys.Rev.Lett.*, vol. 89, p. 117901, 2002.

[32] A. Blais, R.-S. Huang, A. Wallraff, S. Girvin, and R. Schoelkopf *Phys.Rev.A*, vol. 69, p. 062320, 2004.

[33] L. DiCarlo, J. Chow, J. Gambetta, L. Bishop, B. Johnson, D. Schuster, J. Majer, A. Blais, L. Frunzio, S. Girvin, and R. Schoelkopf *Nature*, vol. 460, pp. 240–244, 2009.

[34] A. Houck, J. Koch, M. Devoret, S. Girvin, and R. Schoelkopf *Quant.Inc.Proc.*, vol. 8, p. 105, 2009.

[35] J. Koch, T. Yu, J. Gambetta, A. Houck, D. Schuster, J. Majer, M. Devoret, S. Girvin, and R. Schoelkopf *Phys.Rev.A*, vol. 76, p. 042319, 2007.

[36] D. Loss and D. DiVincenzo *Phys. Rev. A*, vol. 57, p. 120, 1998.

[37] C. van der Wiel, S. De Franceschi, J. Elzerman, T. Fujisawa, S. Tarucha, and L. Kouwenhoven *Rev.Mod.Phys.*, vol. 75, p. 1, 2003.

[38] D. Beckman, A. Chari, S. Devabhaktuni, and J. Preskill *Phys.Rev.A.*, vol. 54, pp. 1034–1063, 1996.

[39] V. Bouchiat, D. Vion, P. Joyez, D. Esteve, and M. Devoret *Phys. Scr.*, vol. T76, p. 165, 1998.

[40] O. Astafiev, Y. Pashkin, Y. Nakamura, T. Yamamoto, and J. Tsai *Phys.Rev.Lett.*, vol. 93, p. 267007, 2004.

[41] Y. Nakamura, Y. Pashkin, T. Yamamoto, and J. Tsai *Phys.Rev.Lett.*, vol. 88, p. 047901, 2002.

[42] G. Zimmerli, T. Eiles, R. Kautz, and J. Martinis *Appl.Phys.Lett.*, vol. 61, p. 237, 1992.

[43] S. Verbrugh, M. Benhamadi, E. Visscher, and J. Mooij *J.Appl.Phys.*, vol. 78, p. 2830, 1995.

[44] H. Wolf, F. Ahlers, J. Niemeyer, H. Scherer, T. Weimann, A. Zorin, V. Krupenin, S. Lotkhov, and D. Presnov *IEEE Trans.Instr.Meas.*, vol. 46, p. 303, 1997.

[45] D. Van Harlingen, T. Robertson, B. Plourde, P. Reichardt, T. Crane, and J. Clarke *Phys.Rev.B*, vol. 70, p. 064517, 2004.

[46] L. Faoro and L. Ioffe *Phys.Rev.Lett.*, vol. 94, p. 047001, 2006.

[47] L. Faoro and L. Ioffe *Phys.Rev.B*, vol. 75(13), p. 132505, 2007.

[48] J. Eroms, L. van Schaarenburg, E. Driessen, J. Plantenberg, C. Huizinga, R. Schouten, A. Verbruggen, C. Harmans, and J. Mooij *Appl.Phys.Lett.*, vol. 89, p. 122516, 2006.

[49] F. Yoshihara, K. Harrabi, A. Niskanen, Y. Nakamura, and J. Tsai *Phys.Rev.Lett.*, vol. 97(16), p. 167001, 2006.

[50] P. Bertet, I. Chiorescu, G. Burkard, K. Semba, C. Harmans, D. DiVincenzo, and J. Mooij *Phys.Rev.Lett.*, vol. 95, p. 257002, 2005.

[51] L. Ioffe, V. Geshkenbein, C. Helm, and G. Blatter *Phys. Rev. Lett.*, vol. 93, p. 057001, 2004.

[52] R. Lutchyn, L. Glazman, and A. Larkin *Phys.Rev.B*, vol. 74, p. 064515, 2006.

[53] D. Ivanov, L. Ioffe, V. Geshkenbein, and G. Blatter *Phys.Rev.B*, vol. 65, p. 024509, 2002.

[54] Y. Makhlin, G. Schon, and A. Shnirman *Rev.Mod.Phys.*, vol. 73, pp. 357–400, 2001.

[55] A. Shnirman, Y. Makhlin, and G. Schon *Physica Scripta*, vol. T102, pp. 147–154, 2002.

[56] J. Johnson *Phys. Rev.*, vol. 32, p. 97, 1928.

[57] H. Nyquist *Phys. Rev.*, vol. 32, p. 110, 1928.

[58] M. Devoret, A. Wallraff, and J. Martinis cond-mat/0411174.

[59] C. Zalka quant-ph/9612028.

[60] E. Knill, R. Laflamme, and W. Zurek quant-ph/9610011.

[61] E. Knill quant-ph/0410199.

[62] E. Knill and R. Laflamme quant-ph/9608012.

[63] A. Steane *Phys.Rev.A*, vol. 68, p. 042322, 2003.

[64] D. Vion, A. Aassime, A. Cottet, P. Joyez, H. Pothier, C. Urbina, D. Esteve, and M. Devoret *Science*, vol. 296, pp. 886–889, 2002.

[65] D. Vion, A. Aassime, A. Cottet, P. Joyez, H. Pothier, C. Urbina, D. Esteve, and M. Devoret *Proceedings, Quantum Interferometry IV, Trieste, March 2002*, cond-mat/0209315.

[66] J. Simon, A. Gustafson, W. Oliver, Y. Nakamura, and J. Tsai *to be published*.

[67] A. Cottet, D. Vion, A. Aassime, P. Joyez, D. Esteve, and M. Devoret *Physica C*, vol. 367, pp. 197–203, 2002.

[68] D. Walls and G. Milburn, *Quantum optics*. Springer-Verlag, Berlin, 1994.

[69] J. Gambetta, A. Blais, D. Schuster, A. Wallraff, L. Frunzio, J. Majer, M. Devoret, S. Girvin, and R. Schoelkopf *Phys.Rev.A*, vol. 74, p. 042318, 2006.

[70] L. Frunzio, A. Wallraff, D. Schuster, J. Majer, and R. Schoelkopf *IEEE Transactions on Applied Superconductivity Proceedings of Applied Superconductivity Conference, Jacksonville, FL*, vol. 15, p. 860, 2004.

[71] P. Day, H. LeDuc, B. Mazin, A. Vayonakis, and J. Zmuidzinas *Nature*, vol. 425, p. 817, 2003.

[72] L. Ioffe and M. Feigelman *Phys. Rev. B*, vol. 66, p. 224503, 2002.

[73] B. Doucot, M. Feigelman, and L. Ioffe *Phys. Rev. Lett.*, vol. 90, p. 107003, 2003.

[74] M. Feigelman, L. Ioffe, V. Geshkenbein, P. Dayal, and G. Blatter *Phys.Rev.Lett.*, vol. 92(9), p. 098301, 2004.

[75] B. Doucot, L. Ioffe, and G. Vidal *Phys. Rev. B*, vol. 69, p. 214501, 2004.

[76] R. Usmanov and L. Ioffe *Phys. Rev. B*, vol. 69, p. 214513, 2004.

[77] C. van der Wal, F. Wilhelm, C. Harmans, and J. Mooij *Eur.Phys.J. B*, vol. 31, p. 111, 2003.

[78] K. Likharev and A. Zorin *J.Low Temp. Phys.*, vol. 59, p. 347, 1985.

[79] D. Averin, A. Zorin, and K. Likharev *Sov.Phys.JETP*, vol. 61, p. 407, 1985.

[80] R. Rivest, A. Shamir, and L. Adleman *Communications of the ACM*, vol. 21(2), pp. 120–126, 1978.

[81] T. Cormen, C. Leiserson, R. Rivest, and C. Stein. MIT Press and McGraw-Hill, second ed., 2001.

[82] D. Knuth, *The Art of Computer Programming*. Addison-Wesley, third ed., 1997.

[83] P. Shor *Phys.Rev.*, vol. A52, p. 2493, 1995.

[84] W. Wootters and W. Zurek *Nature*, vol. 299, pp. 802–803, 1982.

[85] D. Dieks *Phys.Lett.A*, vol. 92(6), pp. 271–272, 1982.

[86] K. Fujii quant-ph/0207178.

[87] V. Buzek and M. Hillery *Physics World*, vol. 14(11), pp. 25–29, 2001.

[88] A. Steane *Proc. Roy. Soc.*, vol. A452, p. 2551, 1996.

[89] A. Steane *Phys.Rev.Lett.*, vol. 77, p. 793, 1996.

[90] A. Calderbank and P. Shor *Phys.Rev.A*, vol. 54, p. 1098, 1996.

[91] D. Gottesman *PhD thesis, California Institute of Technology, Pasadena, CA*, 1997, quant-ph/9705052.

[92] L. Ioffe and M. Mezard quant-ph/0606107.

[93] J. Elzerman, R. Hanson, L. Willems van Beveren, B. Witkamp, L. Vandersypen, and L. Kouwenhoven *Nature*, vol. 430, p. 431, 2004.

[94] Y. Kato, R. Myers, A. Gossard, and D. Awschalom *Nature*, vol. 427, p. 50, 2004.

[95] D. Aharonov and M. Ben-Or *Proceedings, the 29th Annual ACM Symposium on the Theory of Computation (STOC)*, pp. 176–188, 1996.

[96] A. Calderbank, E. Rains, S. P.W., and N. Sloane *IEEE Trans. Inform. Theory*, vol. 44, p. 1369, 1998.

[97] E. Dennis, A. Kitaev, A. Landahl, and J. Preskill *J.Math.Phys.*, vol. 43, p. 4452, 2002.

[98] A. Kitaev *Annals Phys.*, vol. 303, pp. 2–30, 2003.

[99] B. Doucot and L. Ioffe *New.J.Phys.*, vol. 7, p. 187, 2005.

[100] B. Doucot and L. Ioffe *Phys.Rev.A*, vol. 72, p. 032303, 2005.

[101] J. Preskill quant-ph/9712048.

[102] C. Mochon *Phys.Rev.A*, vol. 67, p. 022315, 2003.

[103] C. Mochon *Phys.Rev.A*, vol. 69, p. 032306, 2004.

Vita

Ruslan A. Usmanov

2000 Bachelor of Science, Department of General and Applied Physics, Moscow Institute of Physics and Technology, Russia.

2002 Master of Science, Department of General and Applied Physics, Moscow Institute of Physics and Technology, Russia.

2005 Master of Science, Department of Physics and Astronomy, Rutgers, The State University of New Jersey.

2010 Doctor of Philosophy, Department of Physics and Astronomy, Rutgers, The State University of New Jersey.

Publications

1. R. A. Usmanov and L. B. Ioffe, "Theoretical investigation of a protected quantum bit in a small Josephson junction array with tetrahedral symmetry", Phys.Rev.B **69**, 214513, 2004

2. R. A. Usmanov, L. B. Ioffe, and S. Pereverzev, "On a simple experiment with a non-abelian quantum bit", to be published

3. R. A. Usmanov, L. B. Ioffe, "Nonabelian protected quantum bits", to be published

4. A. A. Belavin and R. A. Usmanov, "New relations in the algebra of the Baxter Q-operators", Theor.Math.Phys. **126**, 48, 2002

5. A. A. Belavin, A. G. Kulakov, and R. A. Usmanov, "Lectures in Theoretical Physics", MCNMO, Moscow, 2001

6. F. C. Alcaraz, A. A. Belavin, and R. A. Usmanov, "Correspondence between the XXZ model in roots of unity and the one-dimensional quantum Ising chain with different boundary conditions", J.Phys.A **34**, 211, 2001

7. R. A. Usmanov, in "Integrable structures of exactly solvable two-dimensional models of quantum field theory : [Proceedings of the NATO advanced research workshop on dynamical symmetries of integrable quantum field theories and lattice models, Kiev, Sept. 25-30, 2000]", ed. by S. Pakuliak, G. von Gehlen (NATO science series)